



**Strategies to Obtain Tumor-reactive Cells for Cancer Immunotherapy by
Cell Sorting and Genetic Modifications of T Lymphocytes**

**Zellsortierung und genetische Modifikation von T-Lymphozyten zur
Gewinnung tumorreaktiver Zellen für die Krebsimmuntherapie**

Thesis for a doctoral degree at the
Julius-Maximilians-University Würzburg
and University of Seville

Submitted by

Estefanía García Guerrero

from

Seville-Spain

Würzburg, 2017

Submitted on:

Office stamp

Members of the PhD thesis committee:

Chairperson: Dean Prof. Thomas Rudel

Primary Supervisor: Prof. Dr. José Antonio Pérez Simón

Supervisor (Second): Dr. Michael Hudecek

Supervisor (Third): Prof. Dr. Hermann Einsele

Supervisor (Fourth): Dr. Alois Palmetshofer

Date of Public Defense:

Date of Receipt of Certificates:

Affidativ

I hereby declare that my thesis entitled: "Strategies to Obtain Tumor-reactive Cells for Cancer Immunotherapy by Cell Sorting and Genetic Modifications of T Lymphocytes" is the result of my own work.

I did not receive any help or support from commercial consultants. All sources and / or materials applied are listed and specified in the thesis.

Furthermore, I verify that the thesis has not been submitted as part of another examination process neither in identical nor in similar form.

Place, date

Signature

Dedication

To Jose Carlos.

To my mum and my brother

ACKNOWLEDGMENTS

I would like to express my sincere gratitude and appreciation to my first supervisor, Prof. Jose Antonio Pérez Simón for his guidance, encouragement and constructive criticisms, which brought to the completion of this thesis.

I would like to thank my second PhD supervisor, Dr. Michael Hudecek for hosting me in his lab during the second part of my thesis, and giving me the opportunity to work freely as just another lab member. I would like to express my sincere gratitude and appreciation to him.

I would also like to sincerely thank Prof. Dr. Hermann Einsele and Prof. Dr. Alois Palmetshofer for their valuable comments and advices during the progress of this project.

I am truly thankful to Dean Prof. Thomas Rudel, who kindly accepted to be my chairperson.

I also want to thank Dr. Antonio Díaz Quintana and Prof. Dr. Miguel Angel de la Cruz for hosting me in the first part of my thesis.

I owe my deepest gratitude to my Spanish labmates: Nacho, Paoli, Ana, Teresa, Jorge, Cristina, Pedro, Concha, Reme, Ángela, Olaya, Palmira y Gracia, Paco de Paula, Antonio, Piru, Cuca, Iván, Mayte, Bejarano, Clara. M^a J. Castro and Rocío.

I am truly thankful to my labmates and friends, Tea and Razieh, for your care, support and love. Without you, I could not have done it. I

will never forget neither of you. I owe my deepest gratitude to Katrin, for your support during one of the worst periods here! Also to Hardik, I really like to tease you! I would also like to thank my other labmates: Sophia, Julia, Sabrina, Markus, Lars, Julian, Silke, Elke, Andreas, Thomas, for their kind helps.

Extremely huge thanks to Fanni, Dragana, Anthony and Ivan, for their care, love, help and for being my international family when I was alone. Fanni, I will miss your Carbonara Spaguettis!!

Finally, I want to thank my family.

To my grandfathers, Fidela and Manuel, I hope you are proud of me. It's a shame I cannot share this moment of my life with you.

I would like to thank my mother-in-law, Isa, for being a second mother to me. I also want to thank my brother-in-law, Daniel, always ready to help.

To my Mother, for being the best mother in the world. I am very fortunate to have your unconditional support and love. I want to thank my brother, for being my little boy, for being my joy. I am so grateful to have you as my brother.

And now to you, my Jose Carlos, my everything. Thank you for trusting me when I needed you, thank you for loving me so much.

You are my half, my person. Together we're invincible.

ABBREVIATIONS.....	17
ABSTRACT.....	21
ZUSAMMENFASSUNG (German).....	23
INTRODUCTION.....	25
1. Adoptive T Cell Immunotherapy for Cancer.....	27
2. Cytotoxic T Cells: Recognition of Tumor Antigens.....	32
3. Conventional Methods for Obtaining Tumor-Specific Cytotoxic T Cells.....	35
4. The T Cell-Tumor Cell Interaction.....	38
5. Tumor-Infiltrating Lymphocyte Therapy.....	41
6. Gene-Modified T Cell Therapy.....	45
7. CAR Design and Mode of Action.....	48
8. CAR Clinical Trials.....	54
HYPOTHESIS.....	55
OBJECTIVES.....	59
MATERIAL AND METHODS.....	63
1. Biological Material.....	65
1.1. Healthy Human Samples.....	65
1.2. Tumor Human Samples.....	65
1.2.1. Acute myeloid leukemia (AML).....	65
1.2.2. Multiple myeloma (MM).....	66
1.3. Tumor Cell Lines.....	66
1.3.1. Multiple myeloma cell lines.....	66
1.3.2. Other cell lines.....	67
2. Non-Biological Material.....	69

2.1. <i>Equipment and Consumables</i>	69
2.2. <i>Software</i>	71
2.3. <i>Chemicals and Reagents</i>	71
2.3.1. <i>Molecular biology</i>	71
2.3.2. <i>Cell culture and immunology</i>	72
2.4. <i>Media and Buffers</i>	74
2.5. <i>Commercial Kits</i>	76
2.6. <i>Antibodies</i>	76
2.6.1. <i>Flow cytometry</i>	76
2.6.2. <i>Western blot</i>	78
3. <i>Molecular Dynamics</i>	79
4. <i>Doublet Cell Culture and Functional Tests</i>	81
4.1. <i>PBMC Purification</i>	81
4.2. <i>CD3 Depletion and Irradiation</i>	81
4.3. <i>Primary Co-Culture</i>	82
4.4. <i>FACS-Based Cell Sorting</i>	83
4.5. <i>Immunophenotype</i>	84
4.6. <i>Secondary Co-Cultures</i>	85
4.6.1. <i>Cytotoxicity assay</i>	85
4.6.2. <i>Suppression assay</i>	85
4.6.3. <i>Activation assay</i>	86
5. <i>CAR Manufacturing and Functional Tests</i>	88
5.1. <i>Preparation of BCMA CAR-Encoding Plasmids</i>	88
5.2. <i>Preparation of Viral Vectors</i>	89
5.3. <i>Titration of Lentivirus</i>	90
5.4. <i>Isolation of Human T Cell Subsets</i>	91
5.5. <i>Lentiviral Transduction of T Cells</i>	92
5.6. <i>Enrichment of CAR+ T Cells</i>	92
5.7. <i>Antigen Dependent Expansion</i>	93
5.8. <i>Immunological and Functional Tests</i>	93

5.8.1. Immunophenotype.....	93
5.8.2. Cytotoxicity assay.....	94
5.8.3. Cytokine secretion assay and ELISA.....	94
5.8.4. CFSE proliferation assay.....	95
5.9. <i>Functional Tests in The Presence of Soluble BCMA</i>	95
5.9.1. Cytotoxicity assay.....	95
5.9.2. Activation assay.....	96
6. Western Blotting.....	97
7. Preclinical <i>in vivo</i> Experiments.....	99
7.1. <i>Multiple Myeloma Xenograft Model</i>	99
7.2. <i>Adoptive Transfer of T Cells and Analysis of Antitumor Efficacy</i>	99
8. Statistical Analysis.....	100
RESULTS	101
PART I: “DOUBLET TECHNOLOGY” TO OBTAIN TUMOR REACTIVE T CELLS	
1. Reactivity of pMHC Complexes Correlates with The Strength of pMHC-TCR Interaction.....	105
1.1. <i>Model system</i>	105
1.2. <i>Stability of computational simulations</i>	106
1.3. <i>Effect of the peptide in HLA structure</i>	109
1.4. <i>Effects of TCR binding on pHLA dynamics</i>	112
1.5. <i>Salt-bridge patterns and electrostatics</i>	114
2. The Basics of “Doublet Technology”: Co-Culture, Incubation Time and FACS-Based Cell Sorting.....	122
2.1. <i>Co-culture conditions</i>	122
2.2. <i>Incubation time</i>	125

2.3. <i>FACS-based cell sorting</i>	126
3. Doublet T Cells Show Higher Percentage of Effector Cells and Specific Cytotoxic Activity as Compared to Non-Doublet T Cells.....	128
3.1. <i>Immunophenotype</i>	128
3.2. <i>Cytotoxic activity</i>	132
4. A Subset of Non-Doublet T Cells Have Immuno-Suppressive Function.....	135
4.1. <i>Immunophenotype</i>	135
4.2. <i>Immuno-suppressive function</i>	135
5. Clinical Application: Doublet T Cells from AML Patients Have Specific Cytotoxic Activity against Primary Blast Cells.....	138
5.1. <i>Patient samples</i>	138
5.2. <i>Cytotoxic activity of doublet T cells against blast cells</i>	139
6. Interim Conclusion for “Doublet Technology”	143

PART II: CAR TECHNOLOGY TO GENERATE TUMOR REACTIVE T CELLS

1. Substantial Expression of BCMA on Myeloma Cells and Generation of BCMA CAR T Cells.....	147
1.1. <i>BCMA expression on myeloma cells</i>	147
1.2. <i>BCMA expression on non-myeloma cells</i>	148
1.3. <i>CAR design: 2^o generation CAR with 4-1BB domain</i>	149
1.4. <i>Transduction of T cells by lentiviral gene transfer</i>	152
2. BCMA CAR Design Affects Anti-Myeloma Function.....	156
3. BCMA CAR T Cells Eliminate Myeloma Cells <i>in Vitro</i>	157
3.1. <i>Cytotoxic activity of BCMA CAR T cells</i>	157
3.2. <i>Cytokine production of BCMA CAR T cells</i>	158

3.3. Proliferation of BCMA CAR T cells.....	159
4. The Serum of Multiple Myeloma Patients Contains a Soluble Form of BCMA Which Is Correlated with Disease Status.....	161
5. Soluble BCMA Does Not Abrogate the Efficacy of BCMA CAR T Cells.....	163
5.1. Cytotoxic activity in the presence of sBCMA.....	163
5.2. Activation in the presence of sBCMA.....	164
5.3. sBCMA protein detection.....	165
6. BCMA CAR T Cells Eradicate Tumor <i>in Vivo</i>	167
7. Interim Conclusion for CAR Technology.....	167
DISCUSSION.....	171
1. “Doublet Technology” to Obtain Tumor-reactive T Cells from Acute Myeloid Leukemia Patients.....	173
2. CAR Technology to Generate Tumor-reactive T Cells from Multiple Myeloma Patients.....	178
3. Clinical Translation.....	183
4. Final remarks and Further Work.....	186
CONCLUSIONS.....	187
REFERENCES.....	191
CURRICULUM VITAE.....	205

ABBREVIATIONS

7-AAD	7-aminoactinomycin D
ACT	Adoptive T cell therapy
AML	Acute myeloid leukemia
APC	Antigen presenting cells
APRIL	Proliferation-inducing ligand
BAFF	B-cell activating factor
BCMA	B-cell maturation antigen
BM	Bone marrow
bp	Base pair
CAIX	Carboxyl anhydrase IX
CAR	Chimeric antigen receptor
CD	Cluster of differentiation
CEA	Carcinoembryonic antigen
CFSE	Carboxyfluorescein succinimidyl ester
CML	Chronic myelogenous leukaemia
CR	Complete remission
CTLs	Cytotoxic T lymphocytes
DC	Dendritic cells
DMSO	Dimethyl sulfoxide
DNA	Deoxyribonucleic acid
EDTA	Ethylenediaminetetraacetic acid

EGFRt	Human truncated epidermal growth factor receptor
ELISA	Enzyme-linked immunosorbent assay
FACS	Fluorescence-activated cell sorting
FCS	Fetal calf serum
Ffluc	Firefly luciferase
GFP	Green fluorescent protein
GM-CSF	Granulocyte-macrophage colony-stimulating factor
HSC	Hematopoietic stem cells
HSCT	Hematopoietic stem cell transplantation
HTLV-1	Human T cell lymphotropic virus
ICOS	Inducible T cell co-stimulator
IFN-γ	Interferon gamma
IgG	Immunoglobulin G
IL-2	Interleukin-2
ITAMs	Immunoreceptor tyrosine-based activation motifs
kbp	Kilobase pairs
K_d	Dissociation constant
LB	Luria-bertani
LCK	Leukocyte C terminal SRC kinase
mAb	Monoclonal antibody
MACS	Magnetic-activated cell sorting
mBCMA	Membrane B-cell maturation antigen
MD	Molecular dynamics

MDSCs	Myeloid-derived suppressor cells
MFI	Mean fluorescence intensity
MHC-I	Class I major histocompatibility complex
MHC-II	Class II major histocompatibility complex
MILs	Marrow-infiltrating lymphocytes
MIP-1β	Macrophage inflammatory protein 1 β
MM	Multiple myeloma
MOI	Multiplicity of infection
NCI	National Cancer Institute
NK cells	Natural killer Cells
ORR	Objective response rates
PBMC	Peripheral blood mononuclear cells
PBS	Phosphate-buffered saline
pHLA	Peptide- human leukocyte antigen
pHLA-TCR	Peptide-human leukocyte antigen-T cell receptor
PMA	Phorbol-12-myristat-13-acetate
pMHC	Peptide-major histocompatibility
pMHC-TCR	Peptide- major histocompatibility -T cell receptor
PMSA	Prostate-specific membrane antigen
RECIST	Response Evaluation Criteria In Solid Tumors
R_G	Radii of gyration
RMSD	Root mean-squared deviation

RMSFs	Root mean square fluctuations
sBCMA	Soluble B-cell maturation antigen
scFv	Single-chain variable fragment
TCM	T cell medium
TCR	T cell receptor
TILs	Tumor infiltrating lymphocytes
TM	Transmembrane domain
Tregs	Regulatory T cells
WT	Wild type
XRD	X-ray Diffraction

ABSTRACT

Recent advances in the field of cancer immunotherapy have enabled this therapeutic approach to enter the mainstream of modern cancer treatment. In particular, adoptive T cell therapy (ACT) is a potentially powerful immunotherapy approach that relies on the administration of tumor-specific T cells into the patient. There are several strategies to obtain tumor-reactive cytotoxic T lymphocytes (CTLs), which have already been shown to induce remarkable responses in the clinical setting. However, there are concerns and limitations regarding the conventional approaches to obtain tumor-reactive T cells, such as accuracy of the procedure and reproducibility. Therefore, we aimed to develop two approaches to improve the precision and efficacy of tumor-reactive T cells therapy. These two techniques could constitute effective, safe and broadly applicable alternatives to the conventional methods for obtaining tumor-specific CTLs.

The first approach of this study is the so called “Doublet Technology”. Here, we demonstrate that peptide-human leukocyte antigen-T cell receptor (pHLA-TCR) interactions that involve immune reactive peptides are stable and strong. Therefore, the CTLs that are bound by their TCR to tumor cells can be selected and isolated through FACS-based cell sorting taking advantage of

this stable interaction between the CTLs and the target cells. The CTLs from acute myeloid leukemia (AML) patients obtained with this technique show cytolytic activity against blast cells suggesting a potential clinical use of these CTLs. “Doublet Technology” offers a personalized therapy in which there is no need for a priori knowledge of the exact tumor antigen.

The second approach of this study is the Chimeric Antigen Receptor (CAR) Technology. We design several CARs targeting the B-Cell Maturation Antigen (BCMA). BCMA CAR T cells show antigen-specific cytolytic activity, production of cytokines including IFN- γ and IL-2, as well as productive proliferation. Although we confirm the presence of soluble BCMA in serum of multiple myeloma (MM) patients, we demonstrate that the presence of soluble protein does not abrogate the efficacy of BCMA CAR T cells suggesting that BCMA CAR T cells can be used in the clinical setting to treat MM patients. The high antigen specificity of CAR T cells allows efficient tumor cell eradication and makes CAR Technology attractive for broadly applicable therapies.

ZUSAMMENFASSUNG

Durch jüngste Fortschritte auf dem Gebiet der Krebsimmuntherapie konnte dieser therapeutische Ansatz in der Mitte moderner Krebsbehandlungen ankommen. Insbesondere die adoptive T-Zelltherapie (ACT), die auf der Verabreichung tumorspezifischer T-Zellen an den Patienten beruht, stellt einen potentiell schlagkräftigen immuntherapeutischen Ansatz dar. Es existieren bereits verschiedene Strategien um tumorreaktive zytotoxische T-Lymphozyten (CTL) herzustellen, von denen bereits gezeigt wurde, dass sie klinisch bemerkenswerte Antworten hervorrufen. Dennoch gibt es Bedenken und Grenzen bezüglich dieser konventionellen Ansätze zur Herstellung tumorreaktiver T-Zellen, wie zum Beispiel die Genauigkeit und Reproduzierbarkeit des Verfahrens. Daher arbeiteten wir an der Entwicklung zweier Ansätze um die Präzision und Effizienz der tumorreaktiven T-Zelltherapie zu verbessern. Diese beiden Techniken könnten effektive, sichere und breit anwendbare Alternativen zu den konventionellen Methoden der tumorspezifischen CTL-Gewinnung darstellen. Der erste Ansatz dieser Studie wird als „Doublet Technology“ bezeichnet. Hierbei zeigen wir, dass die Interaktionen zwischen Peptid/MHC-Komplex und T-Zellrezeptor (pHLA-TCR), die immunreaktive Peptide involvieren, stabil und solide sind. Außerdem zeigen wir, dass

CTLs, die über ihren TCR an Tumorzellen gebunden sind, selektioniert und durch FACS-basierte Zellsortierung isoliert werden können. Hierbei wird die Stabilität der Interaktion von CTLs und Zielzellen genutzt. Die CTLs von Patienten mit Akuter Myeloischer Leukämie (AML), die auf diese Weise gewonnen werden, zeigen zytolytische Aktivität gegenüber Blasten, was auf einen potentiellen klinischen Nutzen dieser CTLs hinweisen könnte. Die „Doublet Technology“ bietet eine personalisierte Therapie, die kein vorheriges Wissen über ein exaktes Tumorantigen erfordert. Der zweite Ansatz dieser Studie ist die Chimere Antigenrezeptor (CAR) Technologie. Wir entwickeln verschiedene CARs gegen das B-Zellmaturationsantigen (BCMA). BCMA-CAR T-Zellen zeigen antigenspezifische zytolytische Aktivität, Produktion der Zytokine IFN- γ und IL-2 sowie produktive Proliferation. Obwohl wir bestätigen, dass lösliches BCMA im Serum von Multiplen Myelompatienten zu finden ist, zeigen wir auch, dass dieses lösliche Protein nicht die Effizienz von BCMA-CAR T-Zellen beeinträchtigt und somit BCMA-CAR T-Zellen zur Behandlung von Multiplen Myelompatienten klinisch genutzt werden können. Die hohe Antigenspezifität der CAR-T-Zellen erlaubt eine effiziente Vernichtung von Tumorzellen und macht die CAR-Technologie attraktiv für breit einsetzbare Therapien.

INTRODUCTION

1. Adoptive T Cell Immunotherapy for Cancer

Cancer remains the major devastating disease throughout the world, with approximately 14 million new cases and 8.2 million cancer related deaths in 2012. The number of new cases is expected to rise by about 70% over the next 2 decades. Globally, nearly 1 in 6 deaths is due to cancer (McGuire, 2016).

Historically, there have been three pillars of cancer treatment: surgery, chemotherapy, and radiotherapy. Although these conventional therapies are often active in eliminating tumor cells, they are associated with toxic side effects and require extensive care and extended treatments. In recent years, immunotherapy has emerged as a possible fourth pillar, targeting cancer not by its anatomic location or propensity to divide, but by utilization of the inherent mechanisms used by the immune system to distinguish between healthy and pathologic tissue (Perica *et al.*, 2015). Immunotherapy approaches include the use of immune modulators, immune checkpoint blockade antibodies and cancer vaccines capable to boost the immune system and T cells. However, variable tumor regression is achieved in the majority of cancers (Rosenberg *et al.*, 2008). Adoptive T cell therapy (ACT) is a potentially powerful immunotherapeutic approach to cancer

treatment that relies on the infusion of tumor-specific T cells into the patient. From a theoretical standpoint, cancer immunotherapy using T cells has long been recognized as a promising approach. The ability of the immune system to recognize and eradicate cancer is well established (Kolb *et al.*, 1995; Kolb, 2008). Adaptive immunity has numerous beneficial properties that make it amenable for cancer treatment: 1) T cell responses are specific, and can thus potentially distinguish between healthy and cancerous tissue; 2) T cells responses are robust, undergoing up to 1,000-fold clonal expansion after activation; 3) T cells can traffic to the site of antigen presentation, suggesting a mechanism for eradication of distant metastases; and 4) T cell responses have memory, maintaining therapeutic effect for many years after initial treatment (Perica *et al.*, 2015).

While the mechanism of action was not initially understood, allogeneic hematopoietic stem cell transplantation (HSCT) for hematological malignancies represents the earliest adoptive transfer of T cells with anti-cancer activity (Welniak *et al.*, 2007). Rather than simply replacing leukemic bone marrow with a healthy transplant, donor cells mediate a graft-versus-tumor effect against allogeneic antigens present on leukemic cells (Fabre, 2001), which reduces tumor burden and recurrence (Kolb *et al.*, 1995).

Unfortunately, lack of specificity in the allogeneic responses makes it challenging to separate the graft effect on tumor from the graft effect on host. Nowadays, the advanced knowledge of immunology, genetic engineering and cell culture has made it possible to enhance anti-tumor specificity and functionality of T cells.

The most avant-garde approaches to obtain tumor-reactive T cells are harvesting and expanding tumor infiltrating lymphocytes (TILs) with endogenous tumor associated antigen T cell receptor (TCR) specificity, and genetic modification of T cells with either an engineered TCR, or a chimeric antigen receptor (CAR) (Figure 1) (Smith *et al.*, 2014; Papaioannou *et al.*, 2016).

Cancer immunotherapy with tumor-reactive T cells has shown remarkable responses in patients (Rosenberg *et al.*, 2008; Turtle *et al.*, 2016). Although each type of ex-vivo modification of T cells has its different strengths and limitations (Figure 2), a single infusion might be sufficient to not only confer therapeutic anti-tumor effects, but also to cause life-long protection from relapse, even in patients where conventional treatment has failed or is no longer effective (Rosenberg *et al.*, 2008; Curran *et al.*, 2012).

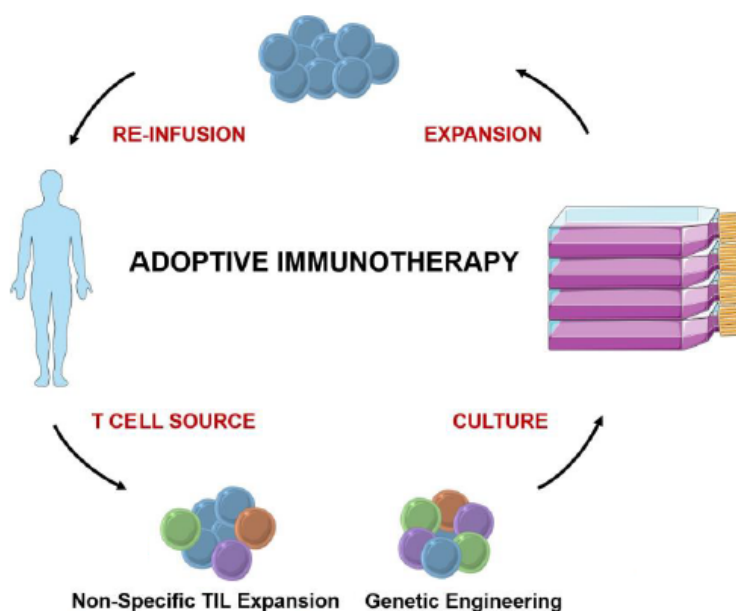


Figure 1. The process of adoptive T cell immunotherapy.

T cells are harvested either from tumor (TILs) or peripheral blood (peripheral blood lymphocytes, PBLs). TILs can be expanded non-specifically since they are preferentially tumor-specific prior to culture. In contrast, tumor specificity must be induced in PBLs, through genetic engineering. After several weeks of expansion in culture, tumor-specific T cells can be reinfused into the cancer patient; modified from (Perica *et al.*, 2015).

Consequently, cancer immunotherapy with tumor-reactive T cells is investigated as a novel treatment modality in patients with hematologic malignancies and solid tumors (Rosenberg *et al.*, 2008; Curran *et al.*, 2012; Restifo *et al.*, 2012; Maude *et al.*, 2014; Turtle *et al.*, 2016).

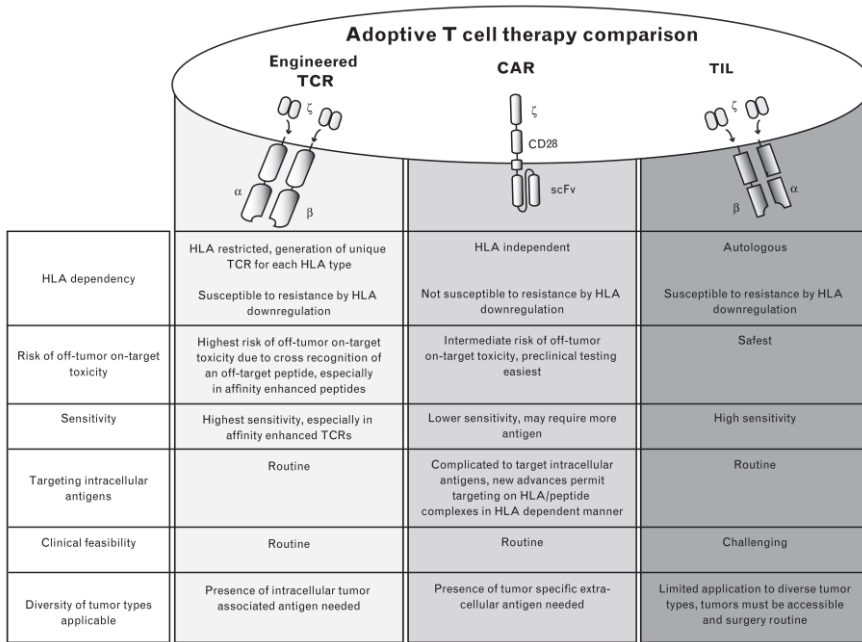


Figure 2. Adoptive T-cell therapies.

Strengths and limitations of ACT therapies. HLA, human leukocyte antigen (Smith *et al.*, 2014).

In this study, we aimed to develop two approaches for obtaining tumor-reactive T cells for clinical implementation in cancer immunotherapy of hematological malignancies.

2. Cytotoxic T Cells: Recognition of Tumor Antigens

The advance in the knowledge of immunology over the last 20 years has been a key issue to understand the molecular-level of the interplay between the T lymphocyte and the malignant cell that results in cytotoxic suppression of the malignancy.

The cytotoxic T lymphocytes (CTLs) are lymphocytes that kill target cells expressing target antigen in class I major histocompatibility complex (MHC-I) restricted manner. They are generally CD8+ T cells and play an effector role in the host response to virus-infected cells, organ transplants and tumor cells. Regarding tumor response, CTLs have the capacity to lysis tumor cells in an antigen-specific manner. Activation begins when receptors on the surface of T cells (TCR) recognize and bind to antigens or peptide fragments that are bound to MHC-I molecules, which are presented on the surface of specialized antigen presenting cells (APC) such as the dendritic cells (DC). The activation also requires the presence of co-stimulatory molecules. Once T cells are activated, there is recruitment of T helper cells that secrete cytokines such as interleukin-2 (IL-2) and granulocyte-macrophage colony-stimulating factor (GM-CSF), which further enhances T cell activation and proliferation (Figure 3) (Kumar, 2012). Tumor cell recognition occurs when an activated CTL ligates through TCR its antigen on

the tumor. If the avidity of the TCR to the antigen is sufficient, costimulatory molecules engage with ligands on the tumor cell and an immune synapse is formed between the T cell and its target, binding the two cells together and mediating the delivery of cytotoxic molecules into the tumor cell, leading to cell lysis by perforin and apoptosis by granzymes. Although CD4+ T cells are classically viewed as helper cells facilitating CD8+ T cell function, it is now clear that both cell subsets can exert cytotoxicity against tumor targets (Restifo *et al.*, 2012; Bollard and Barrett, 2014).

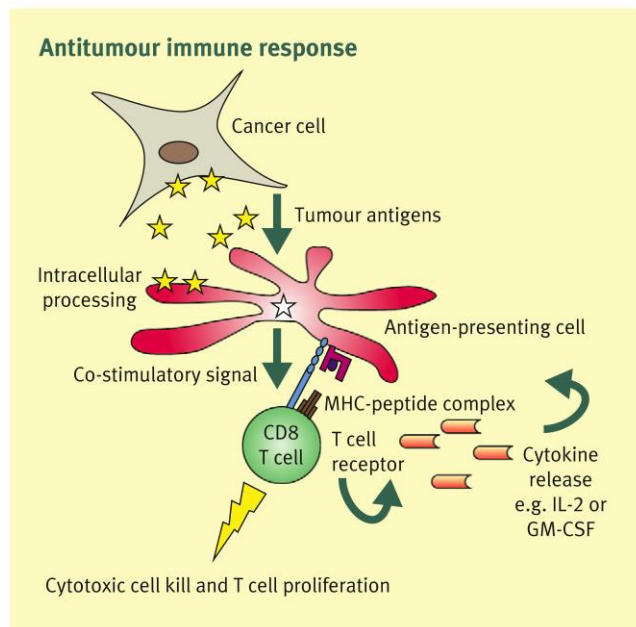


Figure 3. Antitumour immune response.

DCs capture antigens released by cancer cells. After intracellular processing, antigenic peptides are loaded onto MHC molecules on the surface of the DC. Specific T cells encounter these MHC-peptide complexes in conjunction with a co-stimulatory signal. The activated T cells proliferate and secrete cytokines (Kumar, 2012).

This idealized picture of T cell mediated toxicity is modified by factors involving the functionality of CTL, the tumor target, and the milieu in which the interaction occurs. These considerations are important in the successful generation and administration of functional tumor-specific T cells to the patient (Kershaw *et al.*, 2013; Perica *et al.*, 2015). Regarding functionality, CTL function is dependent on the maturational state of the effector cell. To expand into clones of effector cells, T cells must engage with their cognate antigen presented by an APC expressing the appropriate costimulatory molecules. DCs represent the most efficient type of APC for this purpose. Manufacturing of CTL in the laboratory include standard approaches based on the use of DCs generated from CD34 cells or CD14 monocytes. As T cells expand, they generally acquire CD45RO and lose CD45RA surface molecules. Other factors affecting CTLs include cell subpopulations that suppress T-cell proliferation and function, chiefly regulatory T cells (Tregs) and myeloid-derived suppressor cells (MDSCs) (Restifo *et al.*, 2012; Bollard and Barrett, 2014). Many tumors are immunogenic and provoke a host immune response, but this is normally not sufficient to overcome host tolerance or tumor microenvironment. For decades now, researchers have tried to develop new methods to enhance host immunological responses against tumor such as the infusion of tumor-specific T lymphocytes.

3. Conventional Methods for Obtaining Tumor-Specific Cytotoxic T Cells

Adoptive transfer of tumor-reactive cytotoxic T cells is a promising therapeutic approach for cancer treatment. To develop this strategy, it is necessary to isolate specific leukocyte subpopulations from peripheral blood or tumor tissue that will be reinfused into the patient after expansion *in vitro*.

Two approaches are widely applied for the detection and isolation of antigen-specific cytotoxic T lymphocytes:

The first is based on the assessment of specific T cells functions, such as cytokine (typically IFN- γ) production (Manz *et al.*, 1995; Becker *et al.*, 2001) or activation-induced phenotypical alterations, such as cell surface expression of CD107a (LAMP-1) and CD137 (4-1BB) (Rubio *et al.*, 2003). IFN- γ production is the most commonly used variable to detect T-cell reactivity against antigen-presenting targets. However, cytokine-producing CD8⁺ T cells are not exclusively cytotoxic (Panelli *et al.*, 2000; Snyder *et al.*, 2003), and consequently in the therapeutic context, it is important to distinguish T-cell reactivity from “functional cytotoxicity,” specifically the capacity of CTLs to destroy target cells. An alternative strategy uses soluble pMHC multimers to detect and separate antigen-specific T cells from the whole lymphocyte

population. pMHC multimers consist of multiple pMHC complexes that have been chemically linked together and conjugated to a detectable marker (Wooldridge *et al.*, 2009). Although, this technology has been successfully used (Cobbold *et al.*, 2005; Savage *et al.*, 2007), there are several obstacles that need to be solved. For example, the binding affinity threshold for pMHC class I (pMHC-I) tetramers is significantly higher than that required for T cell activation. As a result, pMHC-I tetramers can often fail to stain antigen specific T cells where the interaction between pMHC and TCR is weaker than $K_D = 80 \mu\text{M}$. Such pMHC-TCR affinities are not usually characteristic of CD8+ T cells specific for foreign, pathogen-derived antigens, and pMHC-I tetramers have excelled when used to characterize virus-specific cytotoxic T lymphocyte (CTL) populations. In contrast, the use of pMHC-I tetramers can be more problematic when the reagents are used to identify T cells specific for self-derived peptides (anti-tumor). Thus, at present, pMHC-I tetramers cannot be used to detect all antigen-specific CD8+ T cells (Wooldridge *et al.*, 2009; Dolton *et al.*, 2014). In addition, the use of MHC class II-based reagents to obtain antigen-specific CD4+ T cells is still challenging. The lower affinity of pMHC-II-TCR interactions combines with the fact that the CD4 co-receptor does not contribute to pMHC-II-TCR stabilization to ensure that the average CD4+ T cell is almost 50-fold more difficult to stain with

pMHC tetramers than the average CD8⁺ T cell (Hackett and Sharma, 2002; Wooldridge *et al.*, 2009). Thus, there is a currently a pressing need to extend pMHC multimer technology to a point where it can be used to stain all antigen-specific T cells in all biological systems.

In conclusion, both approaches have been used for obtaining tumor-specific CTLs, but there are still some limitations that need to be addressed. We present in this study two different approaches to obtain tumor-reactive T cells to treat hematologic malignancies: (1) a new method to select and isolate natural autologous tumor-specific T cells from patients based on cell sorting; and (2) a novel procedure to engineer T cells with tumor-specific chimeric antigen receptors (CAR).

4. The T Cell-Tumor Cell Interaction

The specificity of T cell activation clearly depends on the interaction of peptide-MHC (pMHC) complexes and TCR (van der Merwe, 2001). Other signals via coreceptors such as CD4 and CD8 or costimulatory interactions such as CD28 and CD80/CD86 appear to act as amplifiers that increase the magnitude and/or duration of the TCR signals, but do not act independently.

A kinetic model has been proposed that states that T cell signaling is highly dependent on the dissociation rate of pMHC from TCR. In this model, pMHC-TCR complexes with slow dissociation rates send positive signals to T cell, whereas fast off-rates result in negative signaling (McKeithan, 1995; Rabinowitz *et al.*, 1996). This model explains the experimentally observed relationship between T cell function and dissociation rate of ligand from receptor in some reports (Matsui *et al.*, 1994; Lyons *et al.*, 1996; Kersh *et al.*, 1998; Rosette *et al.*, 2001; Krogsaard *et al.*, 2003; Qi *et al.*, 2006).

Ding *et al.* were one of the first groups to show a correlation between the half-life of pMHC-TCR complexes and the type of functional signal generated by T cell. Thus, complexes pMHC-TCR with low dissociation constant (K_D) show specific lysis while complexes with high K_D do not present this ability suggesting that

long pMHC-TCR half-lives correlate tightly with agonist signals that induce T cell activation.(Ding *et al.*, 1999).

More recently, it has been reported that presentation of low-, medium- and high-potency pMHC complexes expressed by DCs *in vivo* leads to upregulation of T cell activation markers, but only high-potency pMHC complexes induce considerable T cell proliferation and production of IFN- γ (Skokos *et al.*, 2007).

To study the strength of the pMHC-TCR interaction, we performed molecular dynamics simulations. The model system chosen was the well-defined human A6 TCR which is specific to the TAX oligopeptide (LLFGYPVYV) of the human T cell lymphotropic virus HTLV-1 bound to the human class I MHC molecule HLA-A2 responsible to cause adult T-cell leukemia/lymphoma (Garboczi *et al.*, 1996). The TAX peptide is a strong agonist that induces T-cell activation at very low concentrations. Single mutations on TAX inhibit T-cell function instead of triggering it. The interactions of three peptide variants (P6A, V7R and Y8A) of TAX bound to HLA-A2 with the A6 T cell receptor have been extensively studied using T cell assays, kinetic and thermodynamic measurements, and X-ray diffraction (XRD). The V7R mutant weakly reacts and elicits the distinct cell responses at concentrations two orders of magnitude

higher than TAX. The P6A and V8A species can be considered unreactive, as they barely induce any response at concentrations several orders of magnitude higher than those at which the response to wild-type species saturates (Ding *et al.*, 1998; Ding *et al.*, 1999).

Altogether, these studies prompt us to hypothesize that tumor-reactive T cells may form strong interactions with tumor cells so that they could be identified and isolated by FACS-based cell sorting to pull out naturally occurring tumor-specific T cells in hematologic malignancies.

5. Tumor-Infiltrating Lymphocyte Therapy

It was convincingly shown that tumor-infiltrating lymphocytes (TILs) selected for reactivity towards autologous melanoma cells displayed high functional activity in metastatic melanoma patients. The earliest trials of ACT using TILs isolated from cancer samples were conducted at the surgical branch of the National Cancer Institute (NCI) in Bethesda, Maryland, USA in 1988 (Rosenberg *et al.*, 1988). Objective response rates (ORR) by Response Evaluation Criteria In Solid Tumors (RECIST) criteria were observed in 11 of 20 patients with metastatic melanoma, and in 34% of patients of a larger follow-up report in 1994 (Rosenberg *et al.*, 1994). Unfortunately, only 5 of the 29 responses were complete, and the median duration of response in these early studies was only 4 months.

A major breakthrough occurred with the addition of lymphodepletion prior to ACT (Figure 4). The benefits of total body irradiation and lymphodepleting chemo-therapy were first illustrated in mouse models of B16 melanoma (Gattinoni *et al.*, 2005). The addition of lymphodepletion increased response rates in stage IV melanoma patients to 49%, 52%, and 72% with three sequential protocols of increasing intensity total body irradiation (Rosenberg *et*

et al., 2011; Geukes Foppen *et al.*, 2015). Complete responses were achieved in 20 of 93 patients treated, and 19 of these 20 responses have persisted for at least 5 years. Comparable results have now been achieved outside of the NCI, as shown by a clinical trial that utilized a lymphodepleting chemotherapy regimen with no total body irradiation leading to a response rate of 48% (4 complete, 11 partial) (Besser *et al.*, 2010; Itzhaki *et al.*, 2011).

Several works have already shown new protocols to generate TILs. For example, in 2010 the first clinical trial, in which patients with metastatic melanoma were treated with TIL leaving out the selection step and also including a CD8 enrichment step, was reported (Dudley *et al.*, 2010). This was considered because of the risk of contamination with regulatory T lymphocytes (Tregs) which might in turn be infused as well, if bulk TIL were given. In this trial, 56 patients could be treated and the ORR for all treated patients was 54%.

TIL therapy is now explored in other cancers than melanoma, demonstrating that this approach is both feasible and efficacious. Prior work has shown that out of nine patients with metastatic cervical cancer treated with TIL therapy, three patients experienced an OR including two patients with complete tumor regression lasting over one year (Stevanovic *et al.*, 2015). Moreover, a recent

article characterized TILs obtained from head and neck cancer metastases. TILs were expanded with high efficiency (80% of patients, with massive expansion for up to 3500 folds), and recognition of tumor antigens could be demonstrated in 60% of patients (Junker *et al.*, 2011). More recently, the first report of successful treatment of a patient with epithelial cancer (cholangiocarcinoma) was reported. Whole-exome sequencing of the patient's tumor was used to identify a mutation in *erbb2* (HER2) that was recognized by a small subset of TIL. Subsequent expansion and reinfusion of mutant specific TIL resulted in dose-dependent durable clinical responses (Smith *et al.*, 2014; Tran *et al.*, 2014).

TIL therapy clearly demonstrates success in solid tumors; however, further work is needed to isolate tumor-reactive T cells in other cancers like hematologic malignancies. In fact, it has been recently reported that marrow-infiltrating lymphocytes (MILs) could be used to treat myeloma patients (Borrello and Noonan, 2016). In this sense, the first aim of this study was to develop a new procedure to identify and isolate anti-tumor T lymphocytes ("like TILs") from acute myeloid leukemia (AML) patients.

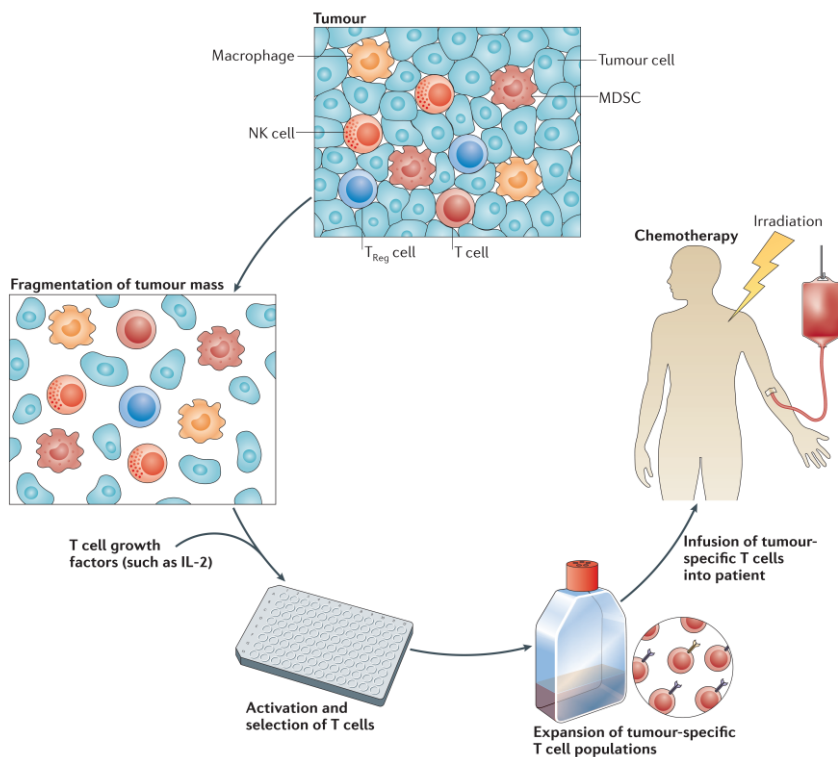


Figure 4. Isolation of TIL and expansion of tumor-specific T cells.

Tumors are often complex masses containing diverse cell types. These masses can be surgically resected and fragmented, and the cells can be placed in wells into which a T cell growth factor, such as interleukin-2 (IL-2), is added. T cell populations that have the desired T cell receptor (TCR) specificity can be selected and expanded, and then adoptively transferred into patients with cancer. Prior to this adoptive transfer, hosts can be immunodepleted by either chemotherapy alone or chemotherapy in combination with total-body irradiation. The combination of a lymphodepleting preparative regimen, adoptive cell transfer and a T cell growth factor can lead to prolonged tumor eradication in patients with metastatic melanoma. MDSC, myeloid-derived suppressor cell; NK, natural killer; TReg, regulatory T (Geukes Foppen *et al.*, 2015).

6. Gene-Modified T Cell Therapy

A significant advance in the field of ACT is the ability to confer to the T cells specificity for tumor antigens or tumor cell surface molecules by the introduction of genes that encode high affinity tumor-targeting T cell receptors (TCRs) or synthetic chimeric antigen receptors (CARs) respectively (Riddell *et al.*, 2014).

In the era of personalized medicine, T cells or defined T cell subsets with distinct functional attributes can be isolated from patient blood and genetically modified to express a transgene encoding a tumor targeting TCR or CAR. The genetically modified T cells are then expanded *in vitro* and if necessary, enriched before infusion into the patient. Conditioning chemoradiotherapy may be administered to the patient to induce lymphodepletion prior to T cell infusion in order to enhance the persistence of infused T cells. Figure 5 depicts an example of a general strategy for engineering autologous T cells for adoptive immunotherapy (Turtle *et al.*, 2012).

Genes encoding TCRs can be isolated from high avidity T cells that recognize cancer antigens and retroviral or lentiviral vectors can be used to redirect lymphocyte specificity to these cancer antigens (Rosenberg *et al.*, 2008). TCR gene transfer provides a mechanism to generate large numbers of autologous T cells directed against

epitopes from intracellular tumor-specific antigens presented on MHC. The best clinical example of TCR gene transfer therapy targeted the cancer/testis antigen NY-ESO-1 in patients with melanoma. Overall, nine out of 17 patients had objective clinical responses with two out of 11 melanoma patients achieving a complete remission lasting more than 1 year (Robbins *et al.*, 2011). Other targets have shown less efficacy, such as melanoma antigen recognized by T-cells 1 (MART1) (Morgan *et al.*, 2006). Several others have been highly toxic, such as carcinoembryonic antigen (Parkhurst *et al.*, 2011), and affinity enhanced MAGE-A3, which resulted in surprising off-target cytotoxicity (Linette *et al.*, 2013; Morgan *et al.*, 2013).

Additional studies are needed to address not only expected technical issues such as the necessity of unique TCRs for different human leukocyte antigen (HLA) types, or potential mispairing of TCR α/β chains, but also unfavorable efficacy:toxicity ratios seen in several early trials from molecular mimicry and 'off-target' cytotoxicity (Turtle *et al.*, 2012; Smith *et al.*, 2014). This has led to a current focus on the genetic modification of T cells with CARs.

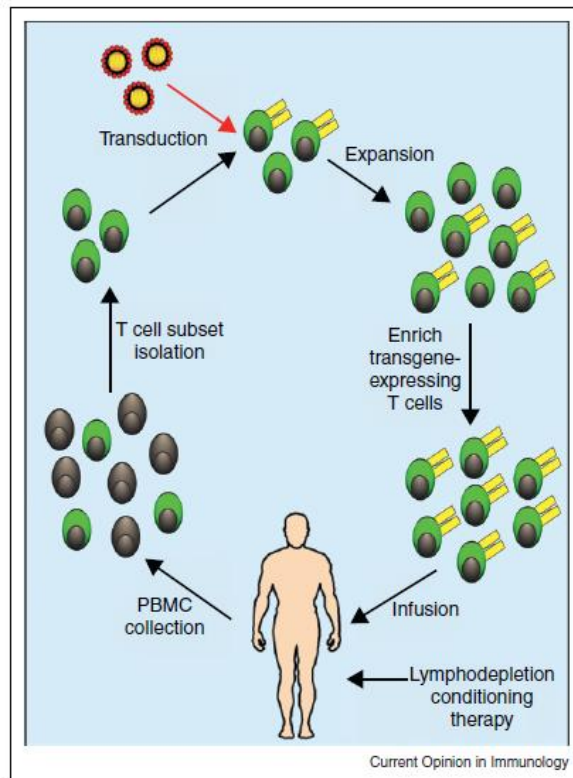


Figure 5. Schema for adoptive immunotherapy with genetically modified T cells.

T cells are isolated from peripheral blood mononuclear cells (PBMC) of patients and transduced with TCR or CAR transgenes. These cells are expanded *ex vivo* and then reinfused into the same patient. Lymphodepletion conditioning is needed before gene modified T cells infusion (Turtle *et al.*, 2012).

7. CAR Design and Mode of Action

Chimeric antigen receptors (CAR) are synthetic receptors that link the antigen specificity of a monoclonal antibody (mAb) to the killing and proliferation capabilities of T cells. CARs are comprised of an extracellular domain derived from single-chain variable fragment (scFv) of a mAb, which serves as the antigen binding moiety. The extracellular spacer domain provides flexibility and reach for antigen binding. A transmembrane (TM) domain links the extracellular domain to an intracellular signaling/activation module, most commonly composed of a T cell receptor (TCR)-derived CD3 ζ chain and one or more co-stimulatory domains such as CD28 or 4-1BB (Figure 6).

Compared with natural TCRs, CARs have several orders of magnitude higher affinities to target antigens that make them more potent in tumor eradication (Harris and Kranz, 2016). In addition, CARs recognize intact cell surface proteins in an MHC-independent manner. Therefore, most of the CAR-based approaches are insensitive to tumor escape mechanisms related to MHC loss variants (Zhou and Levitsky, 2012). Moreover, CAR therapy bypasses many other mechanisms through which cancer cells escape immunorecognition. These mechanisms include reduced expression of costimulatory molecules, induction of

suppressive cytokines and recruitment of regulatory T cells (Han *et al.*, 2013). In addition, they can be used in all individuals regardless of their human leukocyte antigen (HLA) type, which is a distinct advantage over TCRs. However, in contrast to natural TCRs, CARs only detect antigens that are expressed on the surface of tumor cells. Nonetheless, most tumor types can be targeted using CARs (Kershaw *et al.*, 2013).

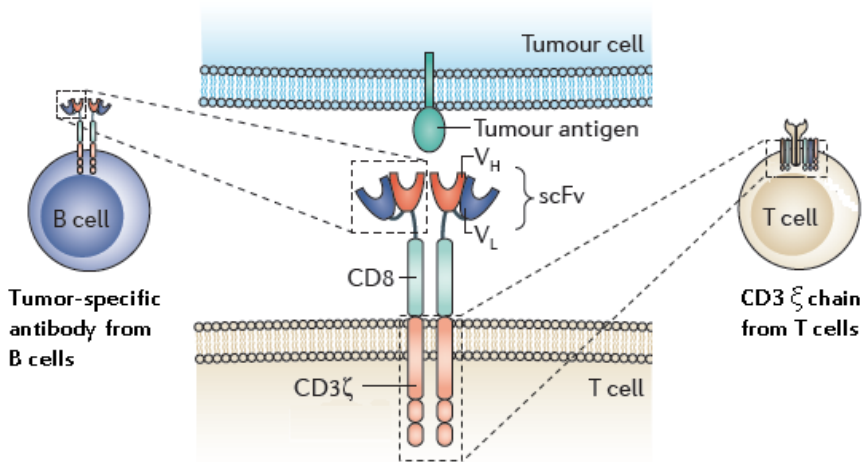


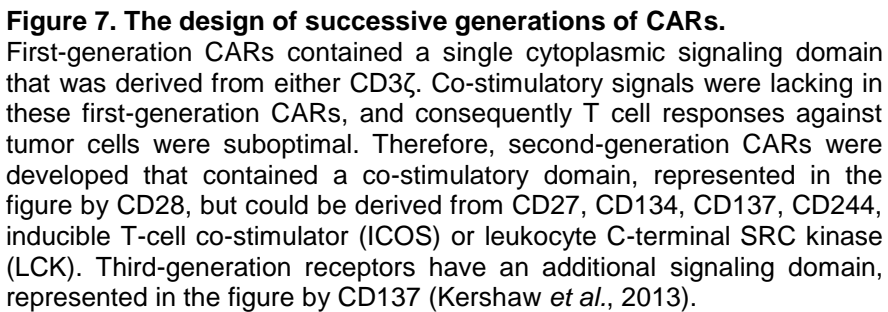
Figure 6: CAR design.

Chimeric antigen receptors (CARs) are composed of a single-chain antibody variable fragment (scFv) extracellular domain linked through hinge and transmembrane domains (represented in the figure by CD8) to a cytoplasmic signaling region that was derived from CD3ζ. Gene encoding the scFv is derived from a B cell that produces a tumor-specific antibody; modified from (Kershaw *et al.*, 2013).

Construction of a CAR relies on the identification of a suitable antibody which binds to a cell surface molecule of interest.

Because CAR recognition does not rely on peptide processing or presentation by MHC, the number of target epitopes is stoichiometrically equal to the number of target antigen molecules on the cell surface, and every surface expressed target molecule represents a potential CAR-triggering epitope, contributing to the potency of this approach. However, the identification of antigens uniquely expressed or overexpressed by tumor cells and to use those antigens as immunotargets to trigger antigen-specific T cell responses in patients is still a challenge (Gill and Kalos, 2013).

Intracellular signaling domain is of vital importance for CAR T cells to fulfill their antitumor function. The initial CAR of the first generation, which contained a single cytoplasmic signaling domain, provides a proof of concept of the targeting and activation of T cells. The CAR of the second and third generations have been developed by addition of dual or triple costimulatory signaling domains in order to increase their cytotoxicity, cytokines production and proliferation. The most important function of multiple signaling receptors is to enhance signaling strength and persistence, subsequently increasing their potency (Figure 7) (Han *et al.*, 2013).



Genetic modification of a T cell with a CAR successfully re-directs the T cell towards the desired target. Tumor cell recognition occurs when a CAR on a T cell ligates its antigen on the tumor cell. This

binding results in CAR clustering with the consequence that the immunoreceptor tyrosine-based activation motifs (ITAMs) of the signaling moiety become phosphorylated and initiate a downstream signaling cascade which finally induces T-cell activation. Activation can lead to direct cytotoxicity of tumor target by CAR T cell mediated release of granzyme and perforin. Tumor cell killing can also be mediated by activation of other components of the immune system through release of cytokines by CD4⁺ CAR T cells. Long-term eradication and prevention against tumor relapse may be provided by long-term memory CAR T cells that form after the initial activation (Figure 8) (Chmielewski *et al.*, 2013; Davila *et al.*, 2014).

The synthetic nature of CARs allows for the targeting of a variety of cancers by simply substituting various antigen-binding domains, encoded by scFv. The structural requirements for efficient targeting of tumor cells by CARs may differ according to the tumor antigen recognized and the tumor-antigen recognition domain itself (Baxevanis and Papamichail, 2004; Davila *et al.*, 2014).

Efforts to improve the functions of CARs have typically focused on the intracellular signaling domain. However, the affinity of the scFV selected for designing a CAR is an additional parameter that could affect T-cell recognition (Hudecek *et al.*, 2013).

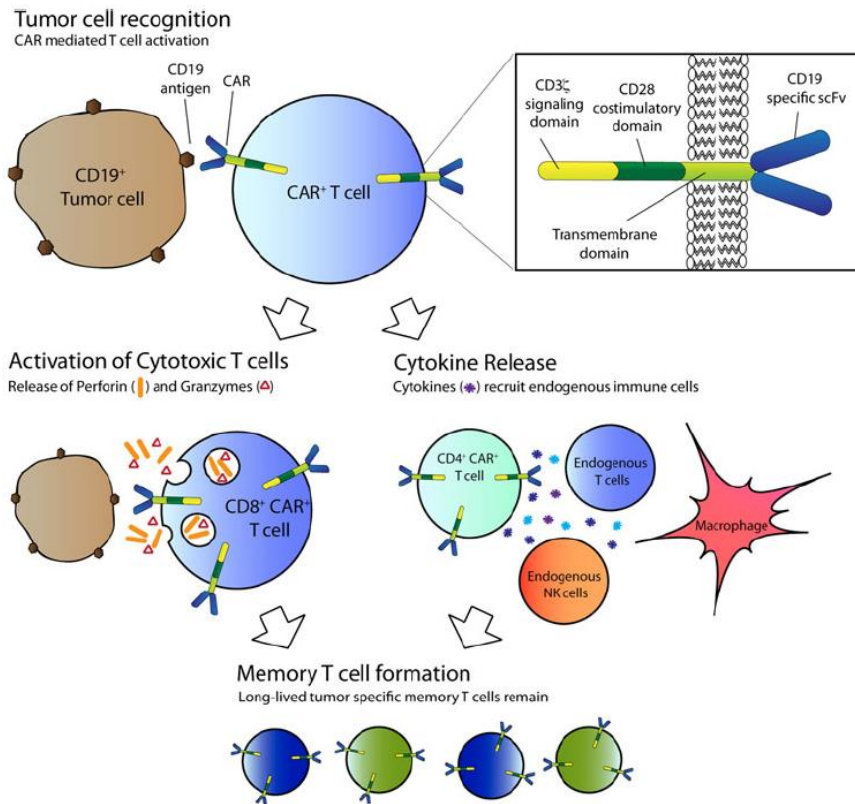


Figure 8: CAR T cell activation and killing of tumor cells.

The chimeric antigen receptor (CAR) is expressed on the surface of T cells. Ligation of the CAR to the target results in signal transduction through signaling moieties and leads to activation of the T cell and killing of the target directly or through engagement of other components of the immune system (Davila *et al.*, 2014).

8. CAR Clinical Trials

CAR therapy has already obtained successful results in the clinic. The most promising results have been achieved in hematologic malignancies. Several clinical trials have used CAR-transduced T cells targeting the CD19 antigen in patients with B cell malignancies (Brentjens *et al.*, 2011; Kalos *et al.*, 2011; Kochenderfer *et al.*, 2012). Some dramatic responses, together with a remarkable expansion of CAR T cells, as well as B cell aplasia, have been observed. CAR-modified T cells targeting another B cell antigen, CD20, have also shown promise for the treatment of lymphoid malignancy. The majority of patients who received anti-CD20 CAR T cells maintained stable disease, and two patients achieved partial responses (Till *et al.*, 2008). Several trials that targeted other tumor antigens like CD171 in neuroblastoma (Park *et al.*, 2007), carboxyl anhydrase IX (CAIX) in renal cell carcinoma (Lamers *et al.*, 2013) and prostate-specific membrane antigen (PMSA) for prostate cancer (Kloss *et al.*, 2013) have been reported. In this study, we also hypothesize that T cells can be targeted against the B-Cell Maturation Antigen (BCMA) by introducing a transgene that encoded a CAR. Therefore, the second aim of this study was to generate a second generation CAR against BCMA to treat multiple myeloma (MM) patients.

HYPOTHESIS

Adoptive transfer of tumor-reactive cytotoxic T cells is a promising therapeutic approach for the treatment of cancer. To develop this strategy, it is necessary to obtain tumor cytotoxic T lymphocytes (CTLs) that will be reinfused into the patient after expansion *in vitro*.

Several strategies have been used for obtaining tumor-specific CTLs, such as cytokine production assay or soluble pMHC multimers. However, there are some limitations that need to be addressed. **1)** Selection of CTL based on cytokine production assays does not necessarily represent functional cytotoxicity. **2)** In order to use this approaches the target antigen must be well known, which is not the case for most tumor cells. To address these issues, we hypothesized that:

- **Hypothesis 1:** *Tumor-reactive T cells may form strong interactions with tumor cells through TCR. This complex (T cell-tumor cell) may occur at sufficient frequency and shows enough functional avidity that could be isolated by FACS-based cell sorting to pull out naturally occurring tumor-reactive T cells.*

The isolation and use of naturally occurring tumor-reactive T cells have shown significant success in treating malignancies. However, there are some difficulties associated with the isolation process and feasibility. **1)** pMHC multimers can often fail to stain antigen specific T cells where the interaction between pMHC and TCR is weak. **2)** Reproducible results in the clinic with the use of these approaches are often hard to achieve based on the variability between patients. To address these issues we thought to generate tumor-specific T cells *ex vivo* by gene transfer in order to infuse them into the patient. Therefore, we also hypothesized that:

- **Hypothesis 2:** *Gene transfer could be exploited to redirect T cells against tumor specific antigens expressed on the surface of tumor cells by introducing transgenes that encoded chimeric antigen receptors (CAR).*

OBJECTIVES

With these hypotheses the aim of this research project is to develop novel strategies of cell therapy in patients with hematologic malignancies and more specifically:

- **Objective 1:** To analyze in silico the interaction between the TCR and the pMHC complex using Molecular Dynamics, to isolate natural autologous tumor-reactive T lymphocytes from acute myeloid leukemia (AML) patients using “Doublet Technology” and to confirm their anti-tumor reactivity against blast cells.
- **Objective 2:** To generate a second generation CAR against the B-Cell Maturation Antigen (BCMA) by genetic modification of T cells to treat multiple myeloma (MM) patients and to confirm the anti-tumor reactivity of BCMA CAR T cells against myeloma cells.

MATERIAL AND METHODS

1. Biological Material

1.1. Healthy Human Samples

Peripheral blood mononuclear cells (PBMC) from buffy coats of volunteer healthy donors were isolated by density gradient centrifugation using Ficoll–Paque solution (Amersham Biosciences, Uppsala, Sweden). Buffy coats were kindly donated by the Regional Centre for Blood Transfusions at Hospital Universitario Virgen del Rocío, Seville (Spain) and the Institutional Review Board of the University of Würzburg (Germany). The local ethics committee provided institutional review board approval for this study, and informed consent was obtained from all donors in accordance with the Declaration of Helsinki.

1.2. Tumor Human Samples

1.2.1. Acute myeloid leukemia (AML)

Blast cells were isolated from bone marrow of AML patients. The percentage of blast cells of the sample was higher than 90%. In addition, PBMC from AML patients were isolated once they achieved complete remission (CR). Informed consent was obtained from all patients in accordance with the Declaration of Helsinki.

1.2.2. Multiple myeloma (MM)

Myeloma plasma cells were isolated from bone marrow of MM patients using CD138 microbead selection (Miltenyi Biotec, Auburn, CA). Informed consent was obtained from all patients in accordance with the Declaration of Helsinki.

1.3. **Tumor Cell Lines**

1.3.1. Multiple myeloma cell lines

The MM.1S, OPM-2 and H929 human MM cell lines were purchased from DSMZ (Braunschweig, Germany). MM.1S/ffluc and OPM-2/ffluc cells were derived by lentiviral transduction with the GFP-firefly luciferase (ffluc)-genes. The MM cell line MM.1 was established from the peripheral blood cells of a patient with an IgA myeloma. The MM.1 cells are characteristic plasma cells. They are negative for CD19 and CD20 found on most normal and malignant B lymphocytes. They have low expression of CD10 (common lymphoblastic leukemia antigen), which is found on immature B cells, and have low expression of CD45. The MM.1 cells express the plasma cell surface marker CD38. The variant MM.1S is sensitive to dexamethasone (Greenstein *et al.*, 2003). OPM cell lines (OPM-1 and OPM-2) were established from the peripheral blood of a 56-year-old female myeloma patient at the stage of terminal leukemic evolution associated with loss of cytoplasmic

immunoglobulin heavy chain. The lines synthesized cytoplasmic λ -chain, but had no detectable surface immunoglobulins. The lines have very complex chromosomal abnormalities, but the patterns of chromosomes differed greatly between the two lines. OPM-2 is phenotypically negative for CD10, CD19 and CD20 although it express the plasma cell surface marker CD38 (Katagiri *et al.*, 1985). H929 is a highly differentiated human plasma cell line. This cell line was established from a malignant effusion in a 62-year-old female patient with myeloma. The cells have rearranged alpha and kappa genes and synthesize and secrete high amounts of IgAk. They are negative for CD10, CD19 and CD20 but possitive for CD38 (Gazdar *et al.*, 1986). All cell lines were cultured in tumor cell medium.

1.3.2. Other cell lines

The K562 and K562/BCMA were used as a negative and positive control cell lines. K562 was established from pleural effusion of 53-year-old female with chronic myelogenous leukemia (CML) in terminal blast crisis. Population highly undifferentiated and of the granulocytic series (Andersson *et al.*, 1979). K562/ffluc cells were derived by lentiviral transduction with the GFP-firefly luciferase (ffluc)-genes. Further, K562/BCMA ffluc cells were derived by

lentiviral transduction with GFP-firefly luciferase (ffluc) and BCMA genes. These cell lines were cultured in tumor cell medium. To produce the lentivirus, Lenti-X 293T cell line from Clontech was used (Cat.#632180). The 293T cell line is a highly transfectable derivative of human embryonic kidney 293 cells, and contains the SV40 T-antigen. To calculate the titration of the lentivirus production, Jurkat cell line Clone E6-1 was used (ATCC TIB-152). Jurkat is an acute T cell leukemia cell line originally derived from the peripheral blood of a 14-year-old boy. TM-LCL cell line from DSMZ (Braunschweig, Germany) was used for antigen dependent expansion of CAR T cells. TM-LCL is a lymphoblastoid cell line established from normal donor (donor initials: TM) in 1992.

2. Non-Biological Material

2.1. Equipment and Consumables

Equipment, consumables specification	Supplier
25, 75 cm ² surface area cell culture flasks	Corning, Kaiserslautern, Germany
96 well half-area plates, Corning® Costar®	Corning, Kaiserslautern, Germany
96 well plate ,white, flat bottom, Corning® Costar®	Corning, Kaiserslautern, Germany
96, 48, 12, 24 well plates, Corning® Costar® U bottom	Corning, Kaiserslautern, Germany
AutoMACS ProSeparator	Miltenyi, Bergisch Gladbach, Germany
Biological safety cabinets, Herasafe™ KS	Thermo Fisher, Waltham, MA, USA
Centrifuge tubes 15, 50 mL	Geriener, Frickenhausen, Germany
Centrifuge, Heraeus Megafuge 40R	Thermo Fisher, Darmstadt, Germany
CO ₂ Incubators, Heracell™ 150i and 240i	Thermo Fisher, Darmstadt, Germany
Electrophoresis power supply, Consort E802	Consort, Turnhout, Belgium
Facs Aria Fusion Cell Sorter	BD Biosciences, Heidelberg, Germany
Flow cytometer, BD FACSCanto™ II	BD Biosciences, Heidelberg, Germany
Flow cytometry tubes, Röhre 5 mL	Sarstedt, Nümbrecht, Germany
Gel electrophoresis system, Owl™ Minigel	Thermo Fisher, Darmstadt, Germany
Gel imaging system, ChemiDoc™ MP	Bio-Rad, Munich, Germany

Heat block, neoBlock1	neoLab, Heidelberg, Germany
Ice maker	Scotsman, Vernon Hills, IL, USA
Incubator	Memmert, Schwabach, Germany
Leucosep tubes	Gerier Bio-One, Frickenhausen, Germany
MACS separation columns, 25 LS	Miltenyi, Bergisch Gladbach, Germany
Microcentrifuge, Fresco 17	Thermo Fisher, Darmstadt, Germany
Microscope, Primo Vert	ZEISS; Jena, Germany
Mini-PROTEAN Tetra Cell	Bio-Rad, Munich, Germany
Multimode multiplate reader ,Infinite 200 PRO	TECAN- Männedorf, Switzerland
NanoDrop 2000	Thermo Fisher, Darmstadt, Germany
Refrigerator, -4 and -20 °C	Liebherr, Bulle, Switzerland
Shaker Incubator	INFORS HT, Basel, Switzerland
Trans-Blot Turbo Transfer Pack	Bio-Rad, Munich, Germany
Ultracentrifuge, Sorvall WX80	Thermo Fisher, Darmstadt, Germany
Ultra-low temperature freezer, -80 °C FORMA 900	Thermo Fisher, Darmstadt, Germany
UV transilluminator	neoLab, Heidelberg, Germany
Vivaspin 6 MWCO 50.000	GE Healthcare, Uppsala, Sweden
Water bath	Memmert, Schwabach, Germany

2.2. Software

Software	Application	Company
FlowJo X 10.0.7	FACS analysis	Tree Star Inc. Ashland, OR, USA
GraphPad Prism 6	statistical analysis	La Jolla, CA, USA
IBM SPSS	statistical analysis	New Orchard Road Armonk, NY
Image Lab™ Software	T7EI analysis	Bio-Rad, Munich, Germany
Infinicyt™	FACS analysis	Cytognos S.L., Salamanca, Spain
ModFit	Suppression analysis	Topsham ME, US

2.3. Chemicals and Reagents

2.3.1. Molecular biology

Name	Manufacturer
1 Kb DNA Ladder	NEB, Frankfurt am Main, Germany
100 bp DNA Ladder	NEB, Frankfurt am Main, Germany
Dual Xtra Standards	Bio-Rad, Munich, Germany
Ethanol absolute for molecular biology	AppliChem, Darmstadt, Germany
GelRed™ Nucleic Acid Gel Stain	Biotium, Fermont, CA, USA

Isopropyl alcohol	Sigma-Aldrich, Steinheim, Germany
LB Agar plates with 100 µg/mL Carbenicillin	TEKnova, Hollister, CA, USA
LB broth 1x	Thermo Fisher, Darmstadt, Germany
LDS Sample Buffer, Non-Reducing (4x)	Thermo Fisher, Darmstadt, Germany
Methanol	Sigma-Aldrich, Steinheim, Germany
NheI	NEB, Frankfurt am Main, Germany
NuPAGE® LDS Sample Buffer (4x)	Invitrogen, Karlsruhe, Germany
NuPAGE® Sample Reducing Agent (10x)	Invitrogen, Karlsruhe, Germany
Phosphatase Inhibitor Cocktail	Sigma-Aldrich, Steinheim, Germany
Precision Plus Protein™ Kaleidoscope	Bio-Rad, Munich, Germany
Protease Inhibitor Cocktail	Sigma-Aldrich, Steinheim, Germany
Tris-EDTA Buffer Solution (TE, pH 8.0)	Sigma-Aldrich, Steinheim, Germany
Water, molecular biology grade	AppliChem, Darmstadt, Germany
Western ECL substrate	Bio-Rad, Munich, Germany

2.3.2. Cell culture and immunology

Name	Manufacturer
2-Mercaptoethanol	Life Technologies, Darmstadt, Germany
Anti-biotin MicroBeads	Miltenyi, Bergisch Gladbach, Germany
Anti-PE MicroBeads	Miltenyi, Bergisch Gladbach, Germany

Cell trace CFSE	Life Technologies, Darmstadt, Germany
Dimethyl sulfoxide (DMSO)	Sigma-Aldrich, Steinheim, Germany
D-Luciferin firefly, Potassium Salt	Biosynth, Staad, Switzerland
Dulbecco's Phosphate-Buffered Saline (DPBS)	Life Technologies, Darmstadt, Germany
Dynabeads® Human T-Activator CD3/CD28	Life Technologies, Darmstadt, Germany
Ethylenediaminetetraacetic acid (EDTA) 0.5 M	Life Technologies, Darmstadt, Germany
Fetal calf serum (FCS)	Life Technologies, Darmstadt, Germany
GlutaMax-I 100X	Life Technologies, Darmstadt, Germany
HEPES 1M	Life Technologies, Darmstadt, Germany
Human Serum	Bayerisches Rotes Kreuz
Ionomycine	Sigma-Aldrich, Steinheim, Germany
PBS, pH 7.4, TWEEN® 20 (dry powder)	Sigma-Aldrich, Steinheim, Germany
PE Streptavidin 0.2 mg/mL	BioLegend, Fell, Germany
Penicillin/Streptomycin 10,000 U/mL	Life Technologies, Darmstadt, Germany
Phorbol 12-myristate 13-acetate (PMA)	Sigma-Aldrich, Steinheim, Germany
Polybrene (Millipore, 10 mg/mL)	Merck, Darmstadt, Germany
Human IL-2 (PROLEUKIN ® S)	Novartis, Basel, Switzerland
RPMI 1640 Medium, GlutaMAX™ Supplement	Life Technologies, Darmstadt, Germany
Trypan blue	Life Technologies, Darmstadt, Germany

2.4. Media and Buffers

T cell medium (TCM)

1640 RPMI, with 25 mM HEPES and Glutamax	500 mL
Human Serum (heat inactivated at 56 °C for 30 min)	10%
Penicillin/Streptomycin 10,000 U/mL	100 U/mL
GlutaMax-I 100X	1%
2-Mercaptoethanol 50 mM	0.1%

Tumor cells medium

1640 RPMI, with 25 mM HEPES and Glutamax	500 mL
FCS	10%
Penicillin/Streptomycin 10,000 U/mL	100 U/mL
GlutaMax-I 100X	1%

MACS buffer

DPBS	500 mL
EDTA 0.5 M	0.4%
FSC	0.5%

PBS/EDTA

DPBS	500 mL
EDTA 0.5 M	0.4%
FSC	0.5%

FACS buffer

DPBS	500 mL
EDTA 0.5 M	0.4%
FSC	0.5%
Sodium azide (NaN ₃)	0.1%

RIPA BUFFER

TRIS-HCL	50 mM
NaCl	150 mM
ddH ₂ O	75 mL

TBS 10x BUFFER

TRIS	24.2 g
NaCl	87.7 g
ddH ₂ O	700 mL

TBS-T 1x BUFFER

TBS 10x	50 mL
Tween 20	500 µL
ddH ₂ O	450 mL

2.5. Commercial Kits

Name	Manufacturer
CalPhos Mammalian Transfection Kit	Clontech, Taraka
CD3 MicroBeads, human	Miltenyi Biotec
CD4+ T Cell Isolation Kit, human	Miltenyi Biotec
CD8+ T Cell Isolation Kit, human	Miltenyi Biotec
DC Protein Assay Kit II	Bio-Rad
ELISA Max™ Set Deluxe (IL-2 and IFN γ kits)	BioLegend
Endofree Plasmid MAXI Kit	QIAGEN
Human BCMA/TNFRSF17 DuoSet ELISA	R&D Systems
MINI PROTEAN TGX™ Gels	Bio-Rad
PE Annexin V Apoptosis Detection Kit with 7-AAD	BD Biosciences
PKH67GL-1KT Kit	Sigma-Aldrich
Trans-Blot® Turbo™ RTA Mini LF PVDF Transfer Kit	Bio-Rad

2.6. Antibodies

2.6.1. Flow cytometry

Ligand	Clone	Conjugation	Isotype	Manufacturer
BCMA	19F2	APC	Mouse IgG2a, κ	Biolegend
CCR7	150503	PE	Mouse IgG2a	BD Biosciences
CD127	A019D5	PE	Mouse IgG1, κ	Biolegend

CD138	DL-101	PE	Mouse IgG1, κ	Biolegend
CD25	2A3	PE	Mouse IgG1, κ	BD Biosciences
CD25	BC96	PB	Mouse IgG1, κ	Biolegend
CD3	BW264/56	APC	Mouse IgG2a, κ	Miltenyi
CD3	SK7	PerCP	Mouse IgG1, κ	BD Biosciences
CD3	17A2	APC/Cy7	Mouse IgG1, κ	Biolegend
CD38	HIT2	BV421	Mouse IgG1, κ	Biolegend
CD4	SK3	PerCP	Mouse IgG1, κ	BD Biosciences
CD4	M-T466	VioBlue	Mouse IgG1, κ	Miltenyi
CD4	RPA-T4	APC/Cy7	Mouse IgG1, κ	BD Biosciences
CD45	HI30	PB	Mouse IgG1, κ	BD Biosciences
CD45	HI30	PE/Cy7	Mouse IgG1, κ	Biolegend
CD45	HI30	PO	Mouse IgG1, κ	BD Biosciences
CD69	FN50	FITC	Mouse IgG1, κ	Biolegend
CD8	BW135/80	VioBlue	Mouse IgG2a, κ	Miltenyi
CD8	SK1	APC	Mouse IgG1, κ	BD Biosciences
EGFR	C225	Biotin	Human IgG1, κ	ImClone LLC
EGFR	C225	AF 647	Human IgG1, κ	ImClone LLC
FoxP3	259D/C7	APC	Mouse IgG1, κ	BD Biosciences
TCR γ/δ	B1	PE/Cy7	Mouse IgG1, κ	Biolegend

2.6.2. Western blot

Name	Antibody	Dilution	Manufacturer
BCMA polyclonal goat	Primary	1:10000	R&D Systems
Goat-IgG HRP	Secondary	1:1000	R&D Systems

3. Molecular Dynamics

The published structures solved by XRD served as a starting point for this study. The HLA-A2/TAX/TCR-A6 system was chosen because it has been extensively studied experimentally, as the three peptide mutants (P6A, V7R, Y8A).

The initial coordinates of the complexes were downloaded from Protein Data Bank (Berman *et al.*, 2002) access codes: 1ao7 (TAX wild-type ternary complex), 1qse (V7R-TAX), 1qrn (P6A-TAX), 1qsf (Y8A-TAX). TAX (LLFGYPVYV) differs from the other peptides by single amino acid substitutions causing very different behaviors in T cells (Ding *et al.*, 1999).

MD trajectories were calculated with AMBER version 9. Standard protocols were used to carry out computational assays (Aroca *et al.*, 2011). Simulations were carried out under periodic boundary conditions in an orthorhombic cell solvated with TIP3P explicit water (Jorgensen *et al.*, 1983). A first energy minimization was performed on sidechains. Then, solvent was subjected to energy minimization followed by 300 ps NPT-MD computations. Temperature was regulated with Berendsen's algorithm (Berendsen *et al.*, 1984). Then, for each protein, the whole system was energy minimized and submitted to 1 ns NVT-MD at 298 K,

using 2.0 fs integration time steps for temperature equilibration. Production runs were computing under the microcanonical ensemble. The trajectories were analyzed with the PTRAJ module of the AMBER package, MatLab 7.11 (MathWorks) and Origin8.5 (OriginLab). Conformational entropies were estimated by using the standard approaches implemented in the PTRAJ module of AMBER. DelPhi v.5.1 was used to analyze protein electrostatics by solving the Poisson-Boltzmann equation by a finite difference method. Protein dielectric constant value was set to 4 and grid size to 0.5 Å.

4. Doublet Cell Culture and Functional Tests

4.1. PBMC Purification

Peripheral blood mononuclear cells (PBMC) were isolated from healthy donors peripheral blood (Donor) or AML patient peripheral blood in complete remission status (CR) by density centrifugation over Ficoll-Hypaque. Blood was mixed with room temperature DPBS at 8:1 ratio. Density centrifugation was performed for 30 min at 400xg with acceleration and deceleration settings of 9 and 2, respectively. The mononuclear cell layer, found between the Ficoll and the serum layer, was extracted and washed twice with TCM to eliminate traces of Ficoll. Finally, the PBMC were cultivated in a 48 well plate a final concentration of 1×10^6 cells/ml.

4.2. CD3 Depletion and Irradiation

PBMC or blast cells were isolated from healthy donors peripheral blood (target) or AML patient bone marrow, respectively. Samples were mixed with room temperature DPBS at 8:1 ratio. Density centrifugation was performed for 30 min at 400xg with acceleration and deceleration settings of 9 and 2, respectively. The mononuclear cell layer was extracted and washed twice with TCM. CD3+ cells (T cells) were depleted twice using CD3 MicroBeads,

human (Miltenyi Biotec) following the manufacturer's instructions. Then, the CD3 depleted-PBMC (CD3-PBMC) were irradiated at 25Gy. After irradiation, CD3-PBMC were stained with a nonspecific labeling PKH-67 which is FITC channel positive (CD3-PKH+PBMC).

PKH-67 Protocol
1-Determine number of cells
2- Add 500 μ l Diluent C per 5×10^6 cells (Solution 1)
3- Prepare 2 μ l PKH-67 per 500 μ l of Diluent C (Solution 2)
4- Mix Solution 1 and 2 in a ratio 1:1
5- Incubate on ice for 3 min and 45 sec in the dark and mixing
6- Add 2ml of human serum per ml of mixed solution to stop the staining
7- Incubate on ice for 1 min and wash twice with TCM

4.3. Primary Co-Culture

For setting up the technique, we co-cultured PBMC from donor 1 (donor) against irradiated CD3-PKH+PBMC from donor 2 (target) at 3:1 ratio in a 48 well plate with TCM (Figure 9A). Regarding clinical application, we co-cultured patient's blast cells against PBMC from the same patient in CR status (Figure 9B). The co-culture was incubated at 37°C without shaking. The cell cultures were analyzed

at different time points (2, 15, 24, 48 hours) by flow cytometry to study the percentage of doublet T cells (T cell bound to a tumor cell through TCR). The following panel was used: PKH-FITC/CD3-APC/CD45-PB.

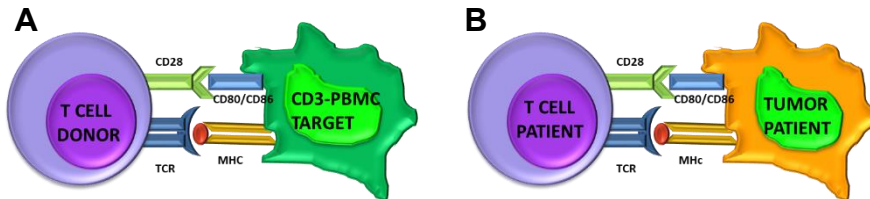


Figure 9. Co-culture in setting (A) and clinical (B) condition.

4.4. FACS-Based Cell Sorting

After 15 hours of co-culture, 2/3rds of the volume was removed from each well without touching the cells on the bottom of the well (the volume in the well was reduced e.g. 48-well from 1 mL to 333 μ L). The following antibodies were added directly to the well: CD25-PE/CD3-APC/CD45-PB. The antibodies were incubated at room temperature in dark for 30 min. Cells were harvested and washed with DPBS for 10 min at 220xg. After the second wash step, the supernatant was removed and the cells were resuspended in DPBS. FACS Aria Fusion Cell Sorter was used to sorter the different populations. The sorting strategy was: First, the viable region FSC/SSC and positive region for CD45 was selected. Then, double positive cells (CD3+PKH+) and non-doublet cells

(CD3+PKH-) were gated. Finally, within the non-doublet cells (CD3+PKH-), two different populations were sorted using the antibody CD25 (Figure 10). The nozzle size used to sort the doublet cells was 85 μ m. The sorted populations were analyzed in order to verify the purity of the sorting procedure.

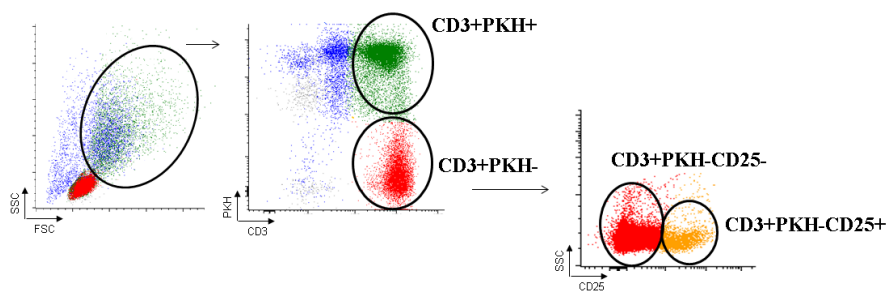


Figure 10. Sorting strategy

Once the cells were sorted, two washing steps were developed. The different populations were rested overnight (20 hours) in a 96 well plate with TCM. After the resting period, half medium change was performed.

4.5. Immunophenotype

Doublet/non-doublet T cells were analyzed by flow cytometry and groups were compared regarding CD4+/CD8+ proportions, naïve/effector/central memory/effector memory proportions and regulatory markers. Flow analyses were performed on a BD FACSCanto II and data analyzed using Infinicyt software (Cytognos).

4.6. Secondary Co-Cultures

4.6.1. Cytotoxicity assay

Secondary co-cultures were performed in a 96 well plate U-bottom at 37°C. Target CD3-PBMC (depleted of T cells) were thawed in TCM. After the second wash step, the supernatant was removed and the cells were stained with PKH-67 (CD3-PKH+PBMC). Co-cultures of sorted doublet/non-doublet T cells from donor with target CD3-PKH+PBMC (used in primary co-culture) were maintained for 7 hours. In the clinical application context, tumor cells from the same patient (used in primary co-culture) were stained with PKH-67 or a tumor marker. Co-cultures of patient's doublet /non-doublet T cells with autologous tumor cells were also maintained for 7 hours. The cytotoxic activity of doublet population vs non-doublet population was analyzed by flow cytometry using Annexin V / 7AAD staining. The viable cells were Annexin V negative and 7AAD negative.

4.6.2. Suppression assay

To test regulatory function, co-cultures of non-doublet T cells with activated conventional T cells were performed. PBMC from healthy donors were isolated by density gradient centrifugation.

Conventional T cells (CD3+ cells) were purified by positive isolation using Miltenyi MACS MicroBeads and magnetic cell separation protocol according to manufacturer's instruction. The conventional T cells were stained with PKH-67 and stimulated with plate bound anti-CD3 (10 µg/mL) and soluble anti-CD28 (1 µg/mL) mAbs. An increasing proportion of conventional T cells was used for studying the inhibition function of non-doublet T cells. After 4 days, cells were collected, stained with CD3-APC, 7AAD, CD25-PB and CD45-PO mAbs and analyzed by flow cytometry. ModFit software was used to calculate the percentage of resting and proliferating cells.

4.6.3. Activation assay

The sorted doublet/non-doublet T cells from donor were co-cultured with target CD3-PKH+PBMC. Moreover, the cells were activated with anti-CD3/CD28 beads in cell to bead ratio of 1:3 as a control and CD69 activation marker was studied by flow cytometry at 24 h after the secondary co-culture.

SUMMARY

Populations	Secondary Co-culture	Analyses
SETTING CD3+PKH+ <i>(doublet T cells)</i> CD3+ PKH- <i>(non-doublet T cells)</i>	Target CD3-PKH+PBMC Target CD3-PKH+PBMC	Immunophenotype Cytotoxicity Suppression Activation
CLINICAL APPLICATION pCD3+PKH+ <i>(patient doublet T cells)</i> pCD3+ PKH- <i>(patient non-doublet T cells)</i>	Tumor cell patient Tumor cell patient	Immunophenotype Cytotoxicity

5. CAR Manufacturing and Functional Tests

5.1. Preparation of BCMA CAR-Encoding Plasmids

DNA sequences encoding the BCMA CARs were designed. The sequence of each CAR followed this pattern from the 5' end to the 3' end: the GM-CSF signal sequence (22 amino acid; Uniprot Database: P15509), single chain variable fragments (scFv) of the anti-human BCMA 30 and 50 mAbs, IgG4 hinge (short: 12 amino acid; long: 229 amino acid; Uniprot Database: P01861) and transmembrane regions of the human CD28 molecule (27 amino acid; Uniprot Database: P10747), the cytoplasmic portion of the 4-1BB costimulatory molecule (42 amino acid; Uniprot Database: Q07011), and the cytoplasmic portion of the CD3 ζ molecule (112 amino acid, Uniprot Database: P20963). DNA encoding the CARs was codon optimized and synthesized by GeneArt AG with appropriate restriction sites. Products of GeneArt were transformed in competent cells of *Escherichia coli* strain Top10 (Invitrogen) and plated onto LB agar plates containing 100 μ g ampicillin/ml. Transformants were transferred to a mattress with LB Broth 1X medium containing 100 μ g ampicillin/ml and incubated overnight at 37°C with vigorous shaking (230 rpm). BCMA CAR-encoding plasmids DNA were extracted using EndoFree Plasmid Maxi Kit (QUIAGEN).

5.2. Preparation of Viral Vectors

Lentiviral vectors were produced in 293T-HEK cells (Lenti-X). To produce BCMA CARs lentiviral vectors, 15 µg of BCMA CAR-encoding plasmids and 10 µg, 1 µg and 2 µg of three helper plasmids, PCHGP-2, PCMV-Rev2 and PCMV-G, were used per 10 cm² petri dish, respectively. Lenti-X cells were cultured at 80% cell confluency in 10 cm² petri dishes, with three plates being used for one batch of lentivirus and incubated for six hours to allow the cells to settle. Transfection with the lentiviral and helper plasmids was performed using a calcium phosphate-based method (Clontech). The plasmids at the appropriate ratios and amounts were diluted in 2 M CaCl₂ solution and the final volume set to 500 µL per petri dish with dH₂O (1500 µL for 3 plates). The plasmid mixture was drop wise added to equal volume of 2x HEPES-buffered saline (HBS). The mixture (3 mL) was incubated for 20 min at room temperature, equal amount of DMEM/10%FCS were added to the mixture and 2 mL of the final DNA suspension was added to each plate in a slow drop-wise manner and the plates were gently twirled to distribute the DNA mixture evenly. Plates were incubated at 37 °C overnight. Viral supernatant from 3 plates were collected into one 50 mL centrifuge tube 72 hours after transfection, centrifuged at 2160 x g for 15 min at 8 °C to remove any cell debris, passed through a 0.45

µm vacuum filter unit and was added to one centrifuge tube. The tube was under laid with 4 mL of 20% sucrose. The sample was centrifuged at 138510 x g for 2 hours at 4 °C by an ultracentrifuge. The viral pellet was covered with 200 µL of DPBS and after at least 3 hours of incubation at 4 °C was resuspended and aliquoted in 20 µL fractions. Viral vectors were stored at -80 °C for future use.

5.3. Titration of Lentivirus

In order to determine the viral titration, Jurkat cells were plated in a 48-well plate at a cell density of 1×10^6 cells/mL in 250 µL of tumor cell lines culture medium with 5 µg/mL polybrene that facilitates viral entry into cells. Serial dilutions of lentivirus (0, 0.0626, 0.125, 0.25, 0.5, 1, 2.5 or 5 µL) were added to consecutive wells and incubated for 4 hours at 37 °C. Following incubation, the medium was topped up to 1 mL and the cells cultured for another 48 hours. CAR expression was analyzed by flow cytometry using the EGFRt transduction marker encoded within the lentiviral vector. The lentivirus titer in transforming units (TU)/mL was calculated using the following equation based on the percentage of EGFRt positive cells for CAR constructs:

$$\text{Virus titer } \left(\frac{\text{TU}}{\text{mL}} \right) = \frac{\text{Cell count at day of transduction} + \frac{\% \text{ EGFRt}^+ / \text{alive cells}}{100}}{\text{Volume of virus added (mL)}}$$

5.4. Isolation of Human T Cell Subsets

Peripheral blood mononuclear cells (PBMC) were isolated from healthy donor peripheral blood by density centrifugation over Ficoll-Hypaque. Blood was mixed with room temperature DPBS at maximum final volume of 35 mL and were carefully added to a 50 mL leucosep tube that was previously equilibrated with 15 mL of room temperature separation medium. Density centrifugation was performed for 15 min, at 350 x g, at 22 °C, with acceleration and deceleration settings of 9 and 2, respectively. The PBMC accumulate beneath the plasma and above of the leucospin tube filter. These cells were washed twice with cold (4 °C) PBS/EDTA buffer, and centrifuged at 4 °C at 220 x g for 15 min. These cells were then directly used for MACS separation. CD8 and CD4 bulk were purified by negative isolation using Miltenyi MACS MicroBeads and magnetic cell separation protocol according to manufacturer's instruction. For magnetic separation, LS columns were used for up to 150×10^6 cells. Isolated cells were activated by anti-CD3/CD28 Dynabeads in cell to bead ratio of 1:1 for further experimental procedures.

5.5. Lentiviral Transduction of T Cells

Prior to lentiviral transduction, T cells were cultured in a 48 well plate at a density of 0.5×10^6 T cells per well in TCM (T cell culture medium) with 50 U/mL rh IL-2 and were activated with anti-CD3/CD28 Dynabeads. The following day, 2/3 of medium was removed; CAR-encoding lentivirus at a multiplicity of infection (MOI) of 5, and polybrene at a final concentration of 5 μ g/mL were added to T cells, and inoculation performed by centrifugation at 800 x g for 45 min at 32 °C. Following centrifugation, the T cells were immediately transferred to 37 °C, rested for 4 hours, and then 1 mL of fresh, warm TCM and 50 U/mL rh IL-2 were added to each well. During subsequent days, a half-medium change with pre-warmed TCM was performed and rh IL-2 supplemented to a final concentration of 50 U/mL every second day. The anti-CD3/CD28 Dynabeads were removed using a hand-held magnet on day 6 post-stimulation and the T cells were transferred to larger plates or tissue culture flasks (12-well plate, then T25 flask) as appropriated to propagate.

5.6. Enrichment of CAR+ T Cells

Prior to functional testing, EGFRt-positive T cells transduced with BCMA CARs viral vectors were enriched using biotin-conjugated anti-EGFR mAb and anti-biotin MicroBeads and were expanded in

an antigen dependent manner with irradiated TM-LCL feeder cells for 7 days.

5.7. Antigen Dependent Expansion

Following enrichment, and before functional assays, EGFRt+ CD8+ and CD4+ T-cell subsets were expanded by irradiated TM-LCL (80 Gy) cells at a T cell: LCL ratio of 1:7. Next day, cultures were supplemented with 50 U/mL of rh IL-2 and cells were fed with fresh TCM and 50 U/mL rh IL-2 every second day. The phenotype of the expanded T cell lines was analyzed on day 7 of expansion.

5.8. Immunological and Functional Tests

5.8.1. Immunophenotype

T cells were washed by centrifugation at 200 x g for 4 min with FACS buffer and stained with the following conjugated mAbs: CD4, CD8, EGFRt in FACS buffer and incubated for 25 min at 4 °C, washed as above; cells were resuspended in FACS buffer before flow cytometry measurement. Viability staining solution 7-AAD was used for exclusion of dead cell. CAR+ (EGFRt+) T cells were detected by staining with biotin-conjugated anti-EGFR antibody (ImClone Systems Inc.) and streptavidin-PE or by staining with

anti-EGFR antibody conjugated to AlexaFluor 647. Flow analyses were performed on a BD FACSCanto II and data analyzed using FlowJo software (Treestar).

5.8.2. Cytotoxicity assay

Target cells expressing firefly luciferase were incubated in triplicate at 5×10^3 cells/well with effector T cells at various effector to target (E: T) ratios in 96-well white flat bottom plate in a final volume of 150 μ L. After 4-hour incubation, luciferin substrate was added to the final concentration of 0.3 mg/mL to the co-culture and the decrease in luminescence signal in wells that contained target cells and T cells was measured using a luminometer (Tecan) and compared to target cells alone. Specific lysis was calculated using the standard formula (Brown *et al.*, 2005) .

5.8.3. Cytokine secretion assay and ELISA

5×10^4 T cells were plated in triplicate wells with target cells at a ratio of 2:1 (MM1.S), or 4:1 (OPM-2, H929, K562/BCMA and K562), and IFN- γ and IL-2 production were measured in supernatant removed after a 24-hour incubation by ELISA kits (BioLegend) based on manufacturer's protocol.

5.8.4. CFSE proliferation assay

For analysis of proliferation, 5×10^4 T cells were labeled with 0.2 μ M carboxyfluorescein succinimidyl ester (CFSE, Thermo Fisher), washed and plated in triplicate wells with target cells at a ratio of 2:1 (MM1.S), or 4:1 (OPM-2, H929, K562/BCMA and K562) in medium without exogenous cytokines. After 72-hour incubation, cells were labeled with anti-CD8/CD4 mAbs and 7-AAD to exclude dead cells from analysis. Samples were analyzed by flow cytometry and division of living T cells was assessed by CFSE dilution. The proliferation index was calculated using FlowJo software.

5.9. Functional Tests in The Presence of Soluble BCMA

5.9.1. Cytotoxicity assay

MM1.S and K562/BCMA cells expressing firefly luciferase were incubated in triplicate at 5×10^3 cells/well with effector T cells at various effector to target (E: T) ratios in 96-well white flat bottom plate in the presence of 150 ng/ml of soluble BCMA protein. After 4-hour incubation, luciferin substrate was added to the final concentration of 0.3 mg/mL to the co-culture and the decrease in luminescence signal in wells that contained target cells and T cells was measured using a luminometer (Tecan) and compared to

target cells alone. Specific lysis was calculated using the standard formula (Brown *et al.*, 2005) .

5.9.2. Activation assay

1×10^5 T cells were plated in triplicate wells with soluble BCMA at different concentrations: 0, 37.5, 75 or 150 ng/ml and incubated for 24 hours. Activated T cells (CD25+CD69+ cells) were analyzed by flow cytometry using FlowJo software. Moreover, IFN- γ production was measured in supernatant removed after 24-hour incubation by ELISA kits (BioLegend) based on manufacturer's protocol.

6. Western Blotting

To analyze the soluble form of BCMA (sBCMA) Western Blot assay was developed. For that, 15-20 ml of supernatant of K562/BCMA and K562 cell lines was used. To concentrate the sBCMA, the supernatant was added into a Vivaspins 20 tube and centrifuged at 5000 x g for 120 min at 20 °C. Also, the membrane form of BCMA (mBCMA) was studied. For this purpose, K562/BCMA and K562 cells were harvested by centrifugation at 220 x g for 10 min at 20 °C. The cells were washed twice with cold DPBS and resuspended in 100 µl of RIPA buffer (supplemented with Protease Inhibitor Cocktail and Phosphatase Inhibitor Cocktail) and incubated on ice for 5 min. The samples were cracked in liquid nitrogen. After centrifugation at 8000 x g for 10 min at 4°C, the supernatant was transferred into a new tube. The protein concentration was determined using DC Kit (Bio-Rad). For non-reducing condition, LDS sample buffer Non-Reducing (4x) was used. For reducing condition, LDS sample buffer (4x) and Sample reducing agent (10x) were used. SDS-PAGE gels were prepared following standard protocols. The percentage of polyacrylamide was 4-20%. Electrophoresis was conducted at a constant voltage of 50 during the first 30 min and then increased to 100 V. Gels were transferred to PVDF membranes by semi-dry transfer. The

transfer was performed at constant amperage of 50 mA for 90 min. Membranes were blocked in TBS-T buffer + 5% BSA and incubated with primary antibody overnight on shaker at 4°C, followed by incubation with the appropriate horseradish peroxidase (HRP) conjugated secondary antibody for 1 h at room temperature. Finally, membranes were washed twice with TBS-T buffer and once with deionized water. Detection was performed with Western ECL substrate following the manufacturer's protocol. Bands were visualized by using ImageJ software.

7. Preclinical *in Vivo* Experiments

7.1. Multiple Myeloma Xenograft Model

The University of Würzburg Institutional Animal Care and Use Committee approved all mouse experiments. Six- to eight-week old female NSG mice were obtained from Charles River and inoculated by tail vein injection with 2×10^6 firefly luciferase expressing MM1.S tumor cells. On day 14, development of systemic myeloma was documented by bioluminescence imaging. Bioluminescence imaging was done on an IVIS Lumina (Perkin Elmer, Waltham, MA) following intraperitoneal injection of D-luciferin (0,3mg/g body weight), and data analyzed using Living Image Software.

7.2. Adoptive Transfer of T Cells and Analysis of Antitumor Efficacy

On day 14, groups of $n=4$ mice received intravenous injections of 5×10^6 BCMA CAR-modified or unmodified control (mock) T cells containing equal proportions of CD8+ and CD4+ T cells. Bioluminescence imaging was performed weekly to determine tumor burden and distribution in mice. Finally, survival of mice was analyzed by Kaplan-Meier analysis.

8. Statistical Analysis

All data are presented as mean \pm standard deviation/range of either absolute values or percentages. Statistical analyses were performed using IBM SPSS Statistics or GraphPad Prism softwares. Statistical significance was assessed by paired Student's t-test or Mann-Whitney test. In all the tests, p values were $p < 0.05$ (*), $p < 0.01$ (**) and $p < 0.001$ (***).

RESULTS

PART I

“DOUBLET TECHNOLOGY” TO OBTAIN TUMOR-REACTIVE T CELLS

The first objective of this study was to analyze the interaction between the TCR and the pMHC complex and to develop a new strategy for obtaining natural tumor-reactive T cells from the pool of patient's lymphocytes to treat hematologic malignancies. In particular, we developed the so called "Doublet Technology" to identify and isolate specific cytotoxic T lymphocytes (CTLs) in patients diagnosed with acute myeloid leukemia (AML) with the aim of tailoring therapy for each patient.

Therefore, we first performed molecular dynamics simulations to study the strength of the pMHC-TCR interaction using a range of peptides with different immune reactivity. To develop our "Doublet Technology" we used the cells of healthy donors due to the easy availability and feasibility. Once the co-culture conditions and sorting strategy were settled up, the "Doublet Technology" was confirmed with AML patient samples.

1. Reactivity of pMHC Complexes Correlates with The Strength of pMHC-TCR Interaction

1.1. Model system

The kinetic model states that T cell signaling is highly dependent on the dissociation rate of peptide-major histocompatibility (pMHC) from T cell receptor (TCR). Thus, pMHC-TCR complexes with slow dissociation rates send positive signals to T cell with the consequence that the T cell become activated (McKeithan, 1995; Rabinowitz *et al.*, 1996). Therefore, we performed molecular dynamics (MD) trajectories to study the interaction between pMHC and TCR at the molecular level.

The model system chosen was the well-defined human A6 TCR which is specific for an antigen of the human T cell lymphotropic virus HTLV-1, which is responsible to cause adult T-cell leukemia/lymphoma. The A6 TCR binds to the TAX oligopeptide (LLFGYPVYV) bound to the human class I MHC molecule HLA-A2 (Garboczi *et al.*, 1996). The TAX peptide is a strong agonist that induces T-cell activation at very low concentrations. Single mutations on TAX inhibit T-cell function instead of triggering it. The interactions of three peptide variants (P6A, V7R and Y8A) of TAX

bound to HLA-A2 with the A6 T cell receptor have been extensively studied using T cell assays, kinetic and thermodynamic measurements, and X-ray diffraction (XRD). The V7R mutant weakly reacts and elicits the distinct cell responses at concentrations two orders of magnitude higher than TAX. The P6A and Y8A species can be considered unreactive, as they barely induce any response even at concentrations which are several orders of magnitude higher than those at which the response to wild-type species saturates (Ding *et al.*, 1998; Ding *et al.*, 1999).

To summarize:

- TAX-HLA-TCR: wild-type reactive complex
- V7R-HLA-TCR: mutant weakly reactive complex
- P6A-HLA-TCR and Y8A-HLA-TCR: mutant non-reactive complexes

1.2. Stability of computational simulations

Ten MD trajectories were set up to simulate the behavior of isolated components of the different peptide-HLA-TCR complexes. We first demonstrated that all the complexes show a high structural similarity (Figure 11) but a different functional behavior (Ding *et al.*, 1999).

To evaluate the stability of the computational simulations (reliability of the simulations), the evolution of the structures along the trajectories was calculated (Figure 12). The evolution of the structures along the trajectories is displayed by the root mean-squared deviation (RMSD) values with respect to the initial structures.

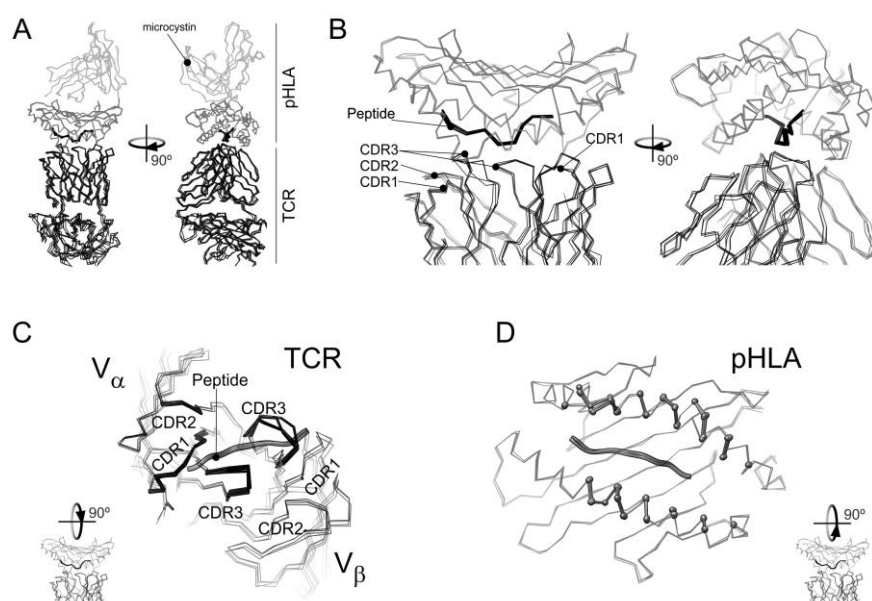


Figure 11. Overlay of the X-ray diffraction models for the WT and mutant TAX-HLA-TCR complexes. All the panels show an overlay of the C α atoms of the TAX-HLA-TCR complex (pdb: 1ao7) with those corresponding to V7R (pdb: 1qse) P6A (1qrn) and Y8A (pdb: 1qsf). A) Overlay of the full complex. TCR molecules are shown in black lines. Black ball-and-sticks represent the antigenic peptide. The HLA domain containing the peptide is depicted in dark grey lines while the remaining structure is shown in light grey. B) Detail of the ternary complex interface for the structure overlay in (A). C) Apical view of TCR and the antigenic peptide in the above overlay of the four structures. As in (A), TCR atoms are represented by lines, but those from residues closer than 6 Å from HLA are highlighted by stick representation. D) Apical view of HLA and the antigenic peptide for the four structures in the overlay. HLA residues closer than 6 Å from TCR are highlighted in a ball-and-stick representation.

In agreement with the statistical data in Table 1, the structure of the distinct pHLA binary complexes barely changes along simulations. Hence, comparing the average structures of HLA bound to reactive and non-reactive peptides reveals that they are highly similar. The RMSD values observed for the ternary complexes (pHLA-TCR) are marginally larger, but still not significant when considering that it is a complex involving 3 large polypeptides and the antigen oligopeptide.

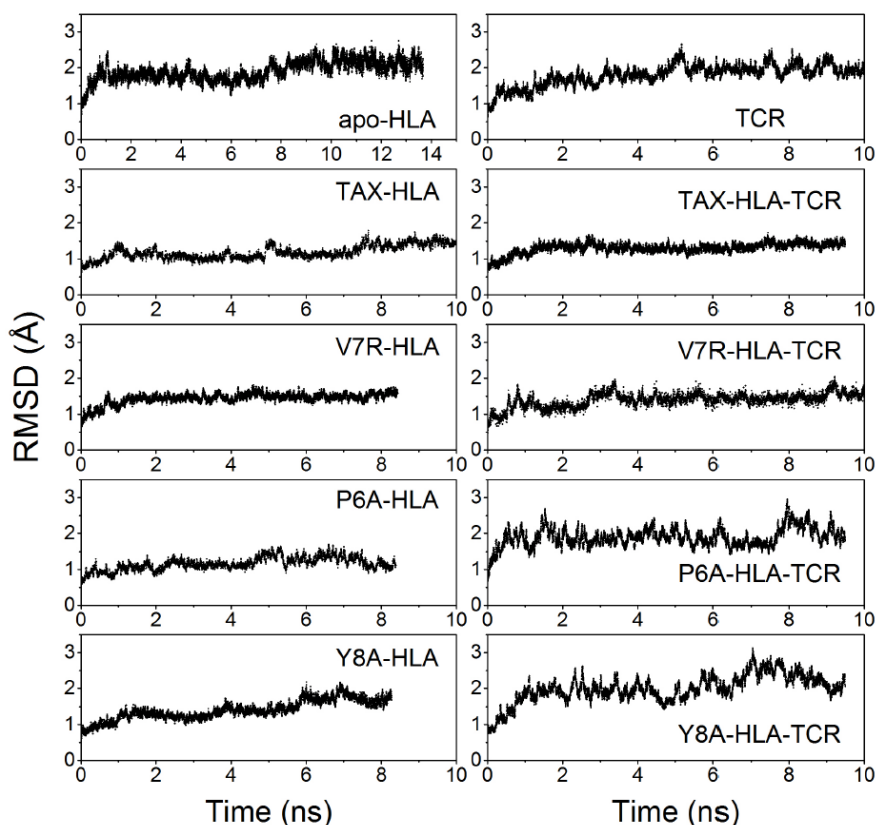


Figure 12. Time courses for the Root Mean Square Deviations along the simulations. RMSDs were calculated for the main-chain atoms, using the initial, energy minimized structure as reference.

Both, protein unfolding and complex dissociation are accompanied by an increase of the R_G values of the protein component of the simulated system. Hence, the radii of gyration (R_G) were also monitored along the computations. The initial R_G values for binary and ternary complexes were 17 Å and 30 Å, respectively. The absence of any increment or fluctuation in R_G values along the trajectories clearly indicates that the oligopeptides remain bound to the HLA domain in all the calculations. In other words, the trajectories were stable and reliable along the simulations.

Table 1. Summary of free HLA, free TCR and the various p-HLA and p-HLA-TCR complexes during MD trajectories.

Trajectory	Time of simulation (ns)	Average RMSD (Å)	Maximum RMSD (Å)	RMSD drift (pm ns ⁻¹)	$\langle R_G \rangle$ (Å)
Free HLA	13.67	1.83	2.65	4	15.22
TAX-HLA	10.00	1.36	1.89	5	17.10
V7R-HLA	8.29	1.19	1.68	6	17.20
P6A-HLA	8.43	1.45	1.81	2	17.17
Y8A-HLA	8.27	1.47	2.26	10	17.26
Free TCR	10.00	1.84	2.65	6	23.85
TAX-HLA-TCR	9.50	1.33	1.73	1	30.17
V7R-HLA-TCR	10.00	1.81	2.76	7	30.43
P6A-HLA-TCR	9.50	1.94	2.95	4	30.66
Y8A-HLA-TCR	10.00	1.61	2.60	6	30.37

HLA and TCR stand for the HLA-A2 and TCR-A6 species. RMSD means root mean square deviation with respect to the initial, energy-optimized structure. RMSD drift values were calculated from linear regressions. $\langle R_G \rangle$ is the average radii of gyration during the trajectory. R_G error was lower than 0.001 Å in all p-HLA trajectories.

1.3. Effect of the peptide in HLA structure

Next, we studied the effect of the presence of the peptide in HLA structure. The slightly larger RMSD values observed for the free HLA trajectory (2.65 Å on average) suggest that a small structural change takes place. In fact, the gyration radius of free HLA is smaller (15.22 Å) than those of the various pHLA complexes (ca. 17.2 Å). Indeed, the α -helical regions of free HLA relax and

approach each other due to the absence of the antigenic peptide in the cleft they define.

The differences between the pattern of atomic fluctuations within HLA in its free and binary (pHLA) forms are shown in Figure 13A. A positive value indicates a greater mobility of a residue in pHLA with respect to free HLA. As expected, the values were negative in the α -helix regions that define the groove of HLA housing the antigen. Thus, their mobility decreases when they clamp the antigenic peptide. In particular, the fluctuations of α helices 2 and 3 resulted to be more sensitive to the presence of the antigen than α helix 1. In fact, the hinge between these two elements is highly restrained by the oligopeptide.

When checking the root mean square fluctuations (RMSFs) of the binary pHLA complexes, t-student tests showed no difference between TAX-HLA and V7R-HLA complexes. However, P6A-HLA and Y8A-HLA showed a slight but significant increase of the average backbone fluctuations (Figure 13B), according to t-student tests at 5% confidence. In fact, although the pattern of fluctuations barely changed in the various pHLA complexes, there were differences in specific residues related to the reactivity of the peptide bound to HLA (Figure 13B,C). For instance, the region comprising the amino acid at positions 38–48 and 100–110 fluctuated more in the non-reactive than in the reactive complexes.

Notably, Trp107 shows the largest fluctuations in non-reactive P6A-HLA and Y8A-HLA complexes. Trp107 sidechain is in close contact with α helix 3, which is involved in TCR binding.

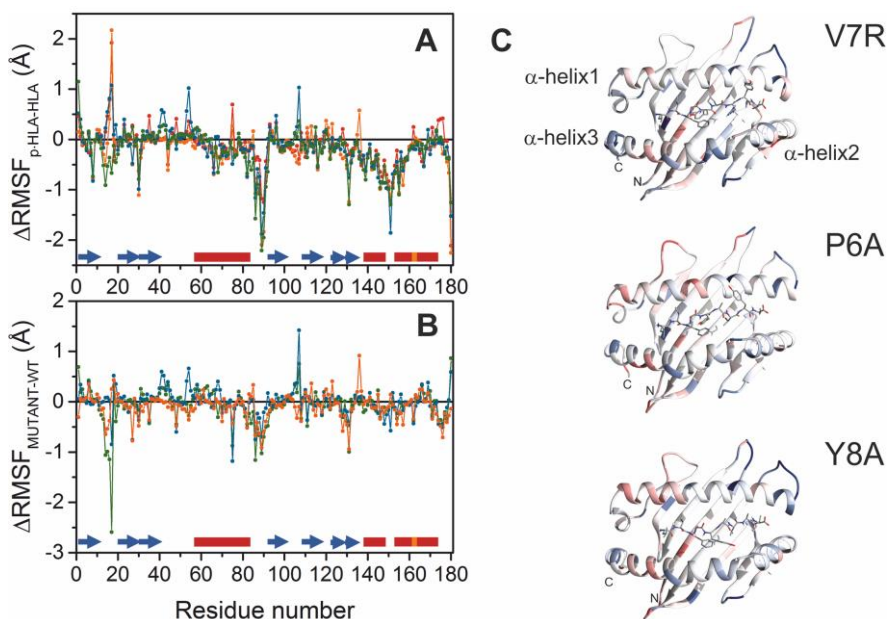


Figure 13. Root mean square fluctuations (RMSF) of HLA in the different complexes.

A) Differences between main-chain fluctuations of HLA in its free and binary forms, pHLA. Data corresponding to TAX-HLA, V7R-HLA, P6A-HLA and Y8A-HLA are in red, orange, blue and green, respectively. Secondary structure elements are shown on top of the abscissa axis. Blue arrows represent β -strands and helical regions (α in red, π in orange) are shown as boxes. B) Backbone fluctuations within V7R-HLA, P6A-HLA and Y8A-HLA complexes relative to the TAX-HLA complex. The N-terminus of the α -helix 1 and the central turns of the α -helix 3 present larger fluctuations (red) in the P6A-HLA and Y8A-HLA complexes than the reactive complex. C) Maps of the main-chain RMSD differences between the mutant binary complexes and TAX-HLA. Colors scales from -1.2 Å (blue) to 1.5 Å (red).

Nevertheless, the largest differences locate at loops out of the surface patch of pHLA that contacts TCR. Taking the wild-type TAX-HLA reactive complex as a reference, we examined the

fluctuations of the non-reactive P6A-HLA and Y8A-HLA complexes and the weakly reactive V7R-HLA (Fig 13B,C). However, data reveal a slight enhancement of fluctuations of the N-terminus region of α -helix 1, whereas the C-terminus of α -helices 2 and 3, the hinge region between these two elements and Gly162, which locates at the π -helix region in the middle of helix 3, decrease their mobility.

1.4. Effects of TCR binding on pHLA dynamics

We next sought to study the effect of TCR binding on pHLA dynamics. Interestingly, binding to the TCR hardly affects the structure of pHLA. In fact, the average RMSD of the binary reactive TAX-HLA complex is nearly identical (1.36 Å) to its average value computed in the ternary reactive TAX-HLA-TCR complex (1.33 Å). The average RMSD values of the non-reactive and weakly reactive complexes were also below 2 Å, though they were higher in the ternary complexes than in their respective binary forms (Table1).

To test the internal mobility within the various molecules, we analyzed the atomic fluctuations (RMSFs) of the main-chain atoms. The pattern of TCR fluctuations was very similar in the different complexes (data not shown). Notably, pHLA binding barely restrains the TCR motions besides those of the CDR3 loops responsible for the molecular recognition of the pHLA molecules,

and some flexible loops located at the constant α and β domains. Upon TCR binding, HLA displays an overall drop in its backbone fluctuations (data not shown), according to t-student tests at 1% significance—p values being lower than 10^{-8} . In addition, a specific loss of mobility was found for the unreactive pHLA complexes in the stretch comprising amino acids 85 to 92, which corresponds to the loop joining α -helix 1 to β -strand 4.

Hence, to investigate to which extent the differences in the atomic fluctuations may affect the binding equilibrium, we calculated the contribution of conformational (vibration) entropy (ΔS^{conf}) of free TCR, binary and ternary complexes and then of the association following the cycle $\Delta S^{\text{conf}} \text{ ternary} - \Delta S^{\text{conf}} \text{ freeTCR} - \Delta S^{\text{conf}} \text{ binary}$.

Data in Table 2, computed using all the protein atoms, indicate that vibrational entropy contribution is less favorable for the formation of ternary complexes involving non-reactive antigens, in agreement with the slightly higher fluctuations found in their binary complexes. In other words, these differences in conformational entropy are related to the higher pHLA entropy in the binary non-reactive pHLA complexes and the smaller entropies found in the non-reactive ternary ones.

Table 2. Vibrational entropy contributions ($-\Delta S^{\text{conf}}$) to binding-free energy.

	$-\Delta S^{\text{conf}}$ p-HLA	$-\Delta\Delta S^{\text{conf}}$ p-HLA-TAX-HLA	$-\Delta S^{\text{conf}}$ ternary	$-\Delta S^{\text{conf}}$ binding	$-\Delta\Delta S^{\text{conf}}$ binding
TAX	-9905.03	0.00	-30625.79	2828.31	0.00
V7R	-10314.69	-409.66	-30506.61	3357.16	528.84
P6A	-11396.40	-1491.37	-30763.30	4182.17	1353.86
Y8A	-11319.11	-1414.08	-30407.24	4460.94	1632.62

Units are kJ/mol. ΔS^{conf} stands for the vibrational entropy as computed by the PTRAJ module of AMBER. Ternary, p-HLA-TCR complexes. $-\Delta\Delta S^{\text{conf}}$ (kJ/mol) was calculated in each case with respect to TAX values. $-\Delta S^{\text{conf}}$ for free TCR was estimated to be -23549.07 kJ/mol.

To summarize, analysis at atomic level revealed that the binary non-reactive complexes (P6A-HLA and Y8A-HLA) show higher fluctuations than the reactive complex (TAX-HLA), therefore the formation of ternary complexes involving non-reactive antigens is less favorable.

1.5. Salt-bridge patterns and electrostatics

To evaluate the stability of the interaction pHLA and TCR, salt bridges and electrostatics were calculated. The salt bridges were studied in all the trajectories of the different binary and ternary complexes (Figure 14), considering ion-pairs with an oxygen-nitrogen distance lower than 3.2 Å in the peptide-HLA-TCR interface. Regarding the pHLA binary complexes, we observed ten salt bridges in TAX-HLA, six in V7R-HLA, eight in P6A-HLA and seven in Y8A-HLA (Figure 14A). These salt bridges are intramolecular interactions between charged groups of HLA. The electrostatic potential energy for a given pair of charges is inversely proportional to the distance between them, so we calculated the average of the inverse of the distances of every salt bridge during

the trajectory of the complexes. The resulting data were represented as a matrix for the four pHLA complexes.

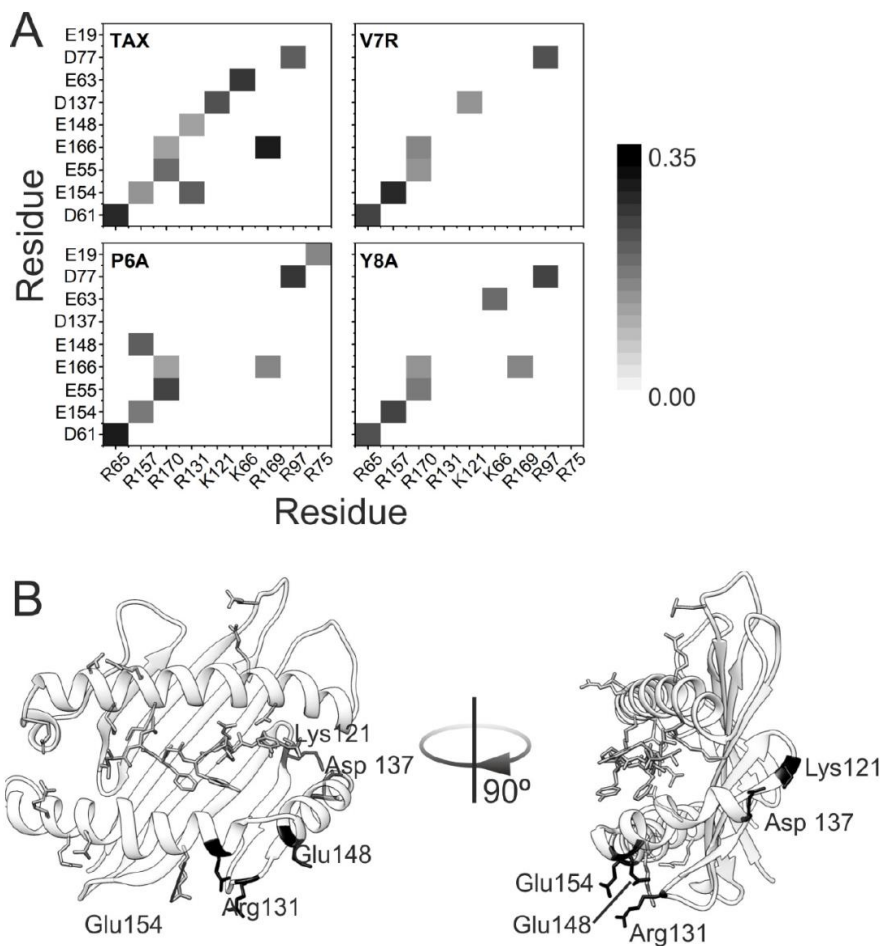


Figure 14. Salt bridges in binary complexes.

A) Patterns of salt bridges in the binary complexes, pHLA. The normalized weight (proportional to the inverse of the distance between the heavy atoms of the two charged groups) of each salt bridge is represented as a grey scale from 0 (white) to 0.35 (black). B) Representation of the TAX-HLA binary complex structure. Residues involved in salt bridges are represented in sticks. Labeled, black-colored residues are involved in salt bridges that are lost in non-reactive pHLA complexes.

The observed patterns in these matrices varied between them.

Notably, the weakly reactive and non-reactive complexes had

fewer salt bridges than the reactive one, agreeing with fluctuations results. The pattern of the weakly reactive complex (V7R-HLA) is intermediate between the patterns of the reactive (TAX-HLA) and non-reactive (P6A-HLA, Y8A-HLA) complexes. In fact, five salt bridges were common to all complexes (Asp61-Arg65, Glu154-Arg157, Glu55-Arg170, Glu166-Arg170 and Asp77-Arg97). In contrast, we noted the absence of three salt bridges from the non-reactive complexes (Glu148-Arg131, Glu154-Arg131 and Asp137-Lys121) that were present in the reactive complex (TAX-HLA). These salt bridges involve residues from α helices 2 and 3, and the rim of the β -sheet (Figure 14B). They may restrain the motion of these two helices in the reactive complexes, thereby favoring the interaction with TCR. In conclusion, we observed a signature salt bridge pattern in the peptide-HLA complexes that varied according to the reactivity of the complex. This pattern is consistent with the distinct backbone fluctuation profiles.

We next analyzed the salt bridges formed at the pHLA-TCR interface (Figure 15A). As observed within the binary pHLA complexes, we noted a significant loss of salt bridges in the non-reactive ternary complexes relative to the reactive complex. In particular, the reactive TAX-HLA-TCR complex had thirteen salt bridges; the intermediate V7R-HLA-TCR complex had ten, and the non-reactive P6A-HLA-TCR and Y8A-HLA-TCR complexes had

five and seven salt bridges, respectively. Accordingly, the number of intermolecular salt bridges between pHLA and TCR was also lower. The reactive complex had six intermolecular salt bridges whereas the intermediate complex had five and the non-reactive P6A-HLA-TCR and Y8A-HLA-TCR complexes had two and four intermolecular salt bridges, respectively. This may explain in part why the interaction between HLA and TCR is weaker in these complexes than in the reactive ones.

We noted an absence of seven salt bridges in the weakly reactive and non-reactive complexes. Three of these are intermolecular between HLA and TCR (Glu154 of HLA with Arg102 of the chain β of TCR, Glu154 of HLA with Lys55 of chain α of TCR, Glu55 of HLA with Arg27 of chain α of TCR). The two first are lost in the non-reactive complexes: those involving P6A and Y8A. Three salt bridges modulated the mobility of α helix 3 of HLA (Glu19-Arg75, Glu161-Arg157 and Glu166-Arg169). This may account also for the differences in vibrational entropies mentioned above. In addition, we found five salt bridges to be present in all complexes (Asp77 with Arg97 of HLA, Glu55 with Arg170 of HLA, Glu63 with Lys66 of HLA, Arg65 of HLA with Asp95 of the α -chain of TCR and Glu166 of HLA with Lys68 of the α -chain of TCR), thus suggesting them to be conserved and well-organized.

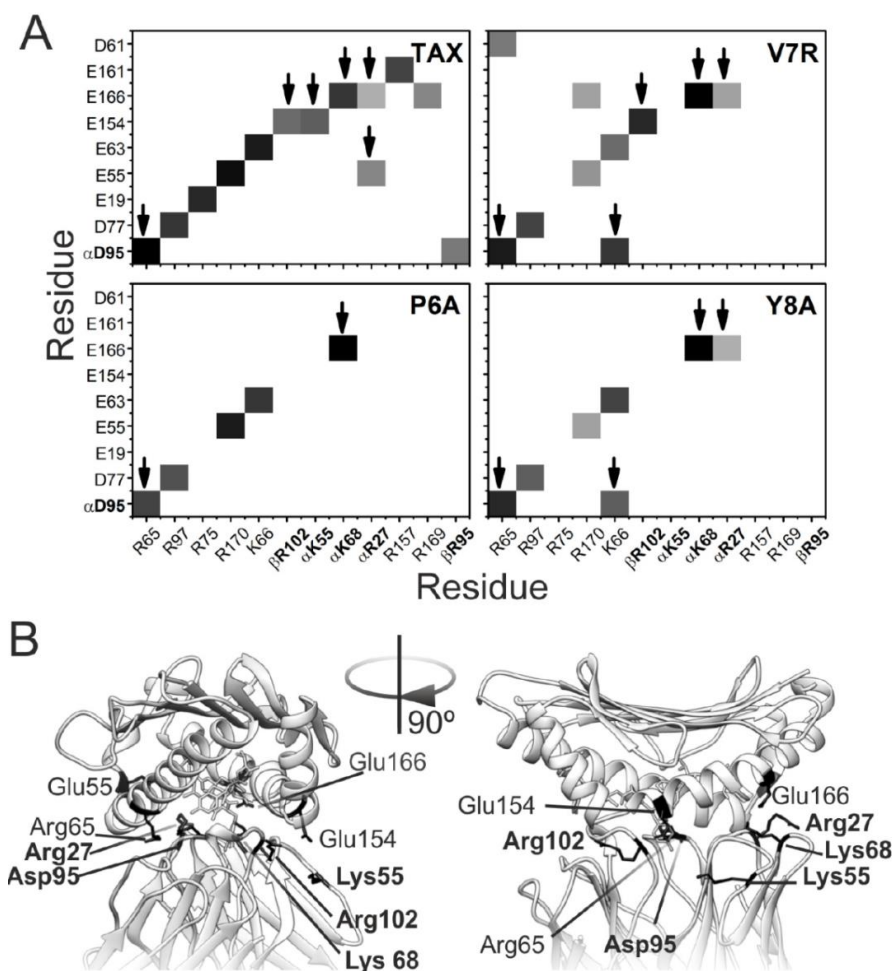


Figure 15. Salt bridges in ternary complexes.

A) Pattern of salt bridges in the ternary complex, pHLA-TCR. TCR residues are in bold font, and with a Greek letters indicating the chain to which the residue belongs. Arrows point to HLA-TCR intermolecular bridges. B) Detail of the structure of the TAX ternary complex (pdb code: 1ao7), displaying in sticks the antigen (in white) as well as the residues involved in intermolecular HLA-TCR salt bridges (in black). Bold font labels correspond to residues from TCR, plain font ones to HLA.

In the V7R-HLA-TCR complex, six salt bridges were lost, whereas three new ones were gained. One of them involves residues from both HLA (Lys66) and TCR (Asp95). In the Y8A-HLA-TCR

complex, only one new salt bridge was gained, and this was the same as that observed in the V7R-HLA-TCR complex (Lys66 of HLA with Asp95 of the α chain of TCR). In conclusion, we observed a signature salt bridge pattern in the ternary peptide-HLA-TCR complexes that differed in its reactive complex compared with weakly reactive and non-reactive ones.

To quantify these salt bridge signatures, we calculated the Frobenius' distances between the matrixes representing the distinct patterns (Table 3). This parameter measures how different two matrices of the same dimensions are. The larger the distance is, the more different are the two compared matrixes. Clearly, non-reactive ternary complexes are more similar to each other with respect their salt bridge pattern than they are to the reactive form. This trend is less pronounced in the binary complexes and more noticeable when only the intermolecular HLA-TCR salt bridges are considered.

Table 3. Normalized Frobenius' distances between salt bridge matrixes.

	TAX	V7R	P6A	Y8A	Y8A*
Y8A	0.34	0.25	0.31	0	0
P6A	0.46	0.34	0	0.29	0.11
V7R	0.44	0	0.46	0.34	0.31
TAX	0	0.59	0.51	0.57	0.32

Binary and ternary complexes are indicated by normal and bold type, respectively.

*Computed using intermolecular salt bridges matrixes.

Finally, we studied how the change in the salt bridges affects the electrostatics of the various binary complexes (Figure 16). A single

amino acid substitution in a peptide affects the electrostatic potential of the complex even if it does not modify the charge of the peptide, as is the case with the P6A-HLA and Y8A-HLA complexes. As the oligopeptide is held in a cleft, the mutations may affect pHLA solvation and the boundary between two phases with different dielectric constants: the protein and the solvent. In its turn, these changes may affect how the charged residues interact at the protein surface.

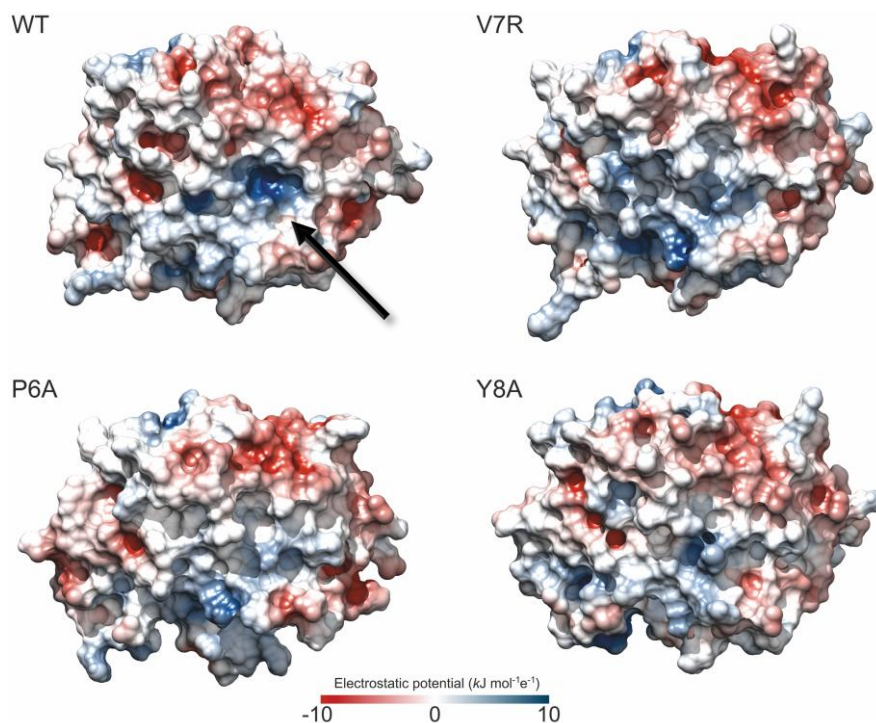


Figure 16. Electrostatics of the pHLA binary complexes.

Electrostatic potential maps at the surface of WT and mutant pHLA binary complexes. Color scales from dark blue (10 kJ mol⁻¹ e⁻¹) to dark red (-10 kJ mol⁻¹ e⁻¹). The electrostatic were calculated using DelPhi software. Arrow indicates the positive region of interest.

Nevertheless, in the V7R-HLA complex, the substitution modifies the charge, since a non-polar amino acid (valine) is replaced by a polar amino acid (arginine) at position seven. We observed that positive regions were strongly attenuated by this substitution. Surprisingly, this also occurred in the non-reactive complexes, even without a change of charge.

These studies have already been published (*García-Guerrero E et al.; PLoS One. 2016 Apr 28;11(4):e0154219.*)

In conclusion, the pHLA-TCR interactions that involve immune reactive peptides are more stable and strong than those which do not induce a triggering of the TCR activation. In our model, the stabilization of the reactive TAX-HLA-TCR complex was achieved due to less fluctuations and more salt bridges comparing with non-reactive peptides.

In aggregate, these results support our hypothesis that tumor-reactive T cells may form strong interactions with tumor cells. Consequently, our next point was to take advantage of the strength of these interactions to develop a new method to obtain CTLs from AML patients through FACS-based cell sorting.

2. The Basics of “Doublet Technology”: Co-Culture, Incubation Time and FACS-Based Cell Sorting

Therapies using tumor infiltrating lymphocytes (TILs) have made great progress in the treatment of solid tumors, especially melanoma (Rosenberg *et al.*, 1994; Dudley *et al.*, 2008). We aimed to transfer this therapeutic approach to the treatment of hematologic malignancy. Therefore, we strived to obtain tumor-reactive CTLs from AML patients to subsequently use them for autologous adoptive cell transfer therapy. To achieve this goal, we began by performing co-cultures of two different healthy donors to set up the best conditions to identify and select those T cells which recognize and bind the target cell (doublet T cells).

2.1. Co-culture conditions

We first checked the possibility to identify doublet T cells by flow cytometry indicating a T cell-target cell complex. To this end, co-cultures between donor 1 (Donor) and donor 2 (Target) were performed. T cell-depleted target PBMC were stained with PKH-67 (CD3-PKH+PBMC) to differentiate them from the donor's PBMC (Figure 17A). Furthermore, T-cell depletion in the target fraction allowed a better activation of donor's T cells (Figure 17B) (n=4,

p=0.005 for CD25; p=0.003 for CD69). Moreover, target CD3-PKH+PBMC were irradiated to avoid the immune response of these cells against donor's cells. Thereby, our cellular model allows us to study the response of donor's T cells against target cells.

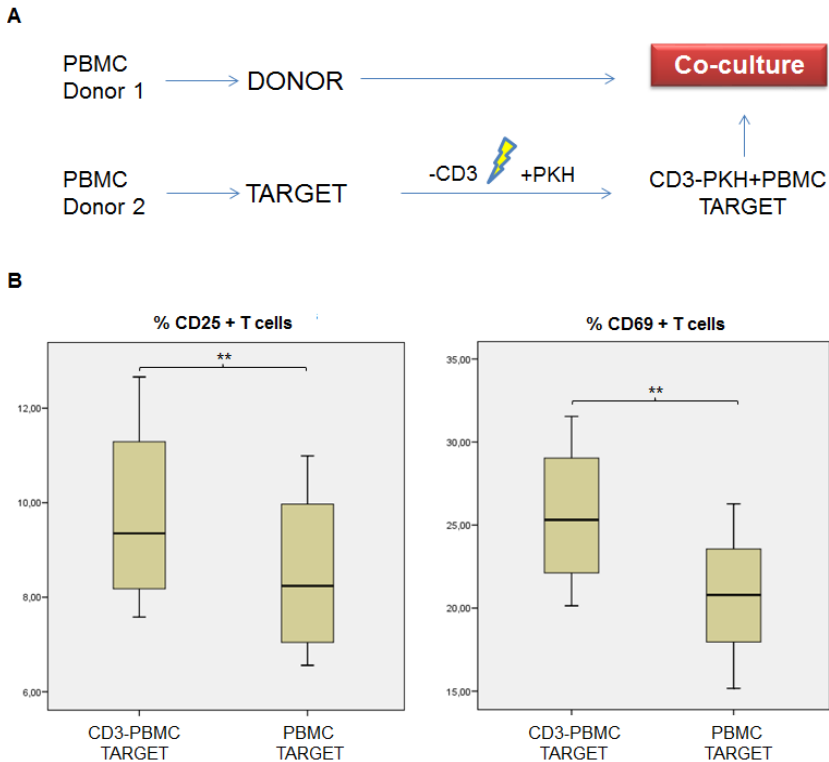


Figure 17. Schedule of the co-culture and T cell activation.

A) PBMC from two healthy donors were obtained by density gradient centrifugation. Target PBMC were depleted of CD3 cells, irradiated and stained with PKH-67 (CD3-PKH+PBMC). Co-cultures of donor's PBMC and target CD3-PKH+PBMC were performed. B) T cell activation markers (CD25 and CD69) were analyzed after 48h of co-culture. Shown are mean \pm SD of four independent experiments. P values between the indicated groups were calculated using paired Student t tests.

Then, we performed co-cultures at donor:target cell ratio of 3:1 and analyzed them by flow cytometry. Doublet-forming T cells were identified as a population that shows a higher FSC/SSC and expresses simultaneously CD3 and PKH. Thus, the doublet positive cells (CD3+PKH+) consist of CD3+ T cells from donor bound to PKH-stained target cells (Figure 18A). The doublet T cells were also identified under confocal microscope (Figure 18B).

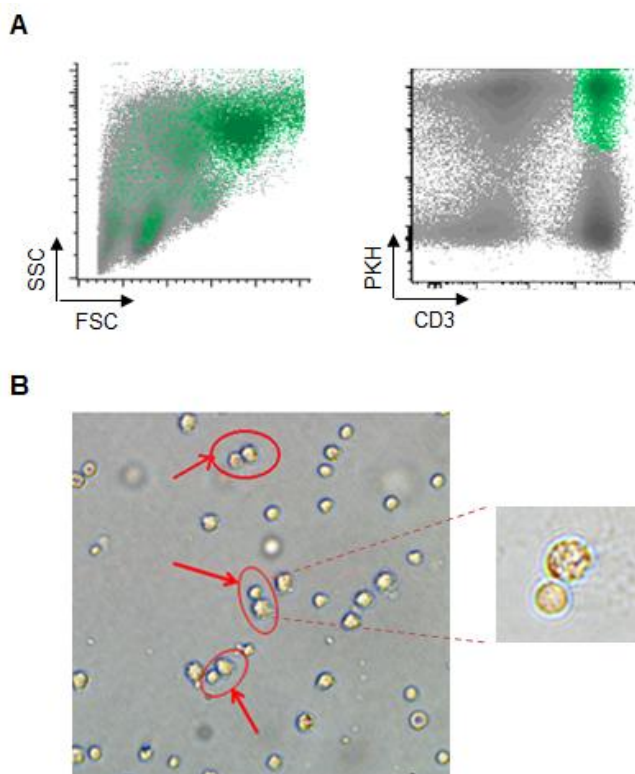


Figure 18. Identification by flow cytometry of the doublet cells.

A) Identification of doublet T cells. Co-cultures of donor's PBMC and target CD3-PKH+PBMC were performed. After 20h of co-culture, cells were directly stained and harvested for flow cytometry analyses. A population with higher FSC/SSC, CD3+ and PKH+ was gated. B) The co-cultures were also analyzed under confocal microscope at different time points (2, 6, 12, 24 h) and the doublet-forming T cells were observed.

The monitoring of co-cultures was performed within 15 hours using the incubator integrated with a confocal microscope and a camera. Hence, we could observe that CTLs bind target cells (green for the PKH emission) and form doublet cells (data not shown).

2.2. Incubation time

After identifying the doublet positive cells as a population which demonstrates higher FSC/SSC distribution and the expression of CD3 and PKH, we explored the optimal incubation time to obtain the highest proportion of doublet-forming T cells. Consequently, we performed co-cultures and analyzed the percentage of doublet population at different time points by flow cytometry. The time point of 15 hours resulted in the highest doublet percentage (Figure 19).

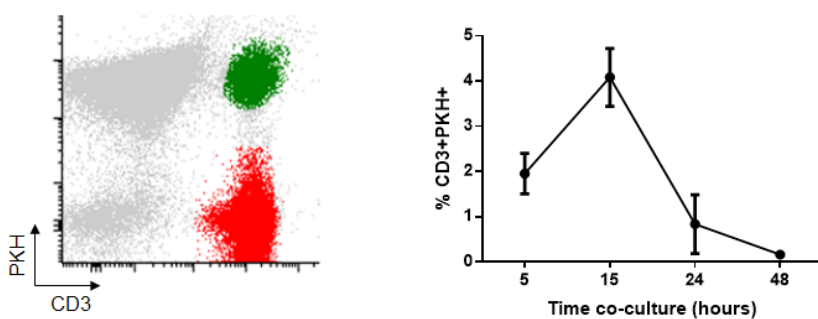


Figure 19. Time course of the co-culture.

Co-cultures of donor's PBMC and target CD3-PKH+PBMC were incubated in 48 well plates for 5, 15, 24 and 48 hours. After each time point, cells were directly stained and harvested for flow cytometry analyses. Representation of the percentage of doublet T cells vs co-culture time (hours) is shown. Depicted are the mean \pm SD of three independent experiments.

Once the doublet population was identified and the optimal time of co-culture was determined, we continued to select this population through cell sorting.

2.3. FACS-based cell sorting

Co-cultures of donor's PBMC and CD3-depleted, PKH-stained target PBMC (CD3-PKH+PBMC) were performed. After 15h of incubation, the cells were stained using the following panel: CD25-PE/CD3-APC/CD45-PB. Afterwards, the cells were washed and sorted based on their FSC/SSC as well as their positivity for both CD3 and PKH (doublet-forming T cells). The FACS Aria Fusion Cell Sorter was run with an 85 µm nozzle for sorting the doublet positive cells due to their large size and higher sensitivity (T cell bound to a target cell).

Doublet-forming T cells were identified in a range of 3% to 6% (n=10). The selected populations CD3+PKH+ (doublet T cells) and CD3+PKH- (non-doublet T cells) were further characterized. Within this last fraction, two populations were identified by the following phenotypes: CD3+PKH-CD25- and CD3+PKH-CD25+ (Figure 20).

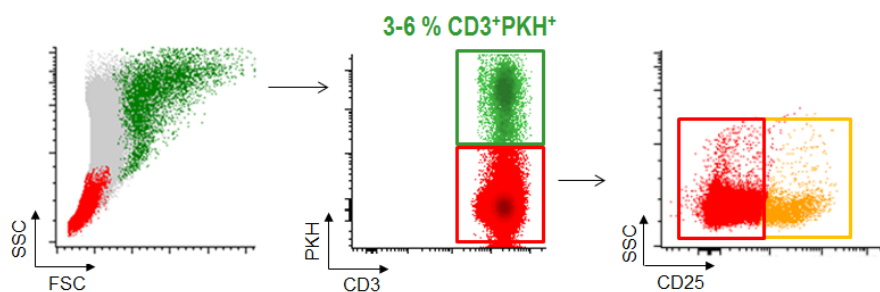


Figure 20. Sorting of doublet T cells and non-doublet T cells.

Co-cultures of donor's PBMC and target CD3-PKH+PBMC were performed at a ratio of 3:1 for 15h. After incubation, cells were stained, harvested and filtrated. Doublet population (high FSC/SSC, CD3+PKH+) and non-doublet cells (low FSC/SSC, CD3+PKH-) were identified and sorted.

After the sorting procedure, cells were analyzed by flow cytometry and observed under confocal microscope. The doublet T cells (CD3+PKH+) were still forming doublet positive population (>90%, n=3) and the non-doublet populations, both CD3+PKH-CD25+ and CD3+PKH-CD25-, were also highly purified (>95%, n=3).

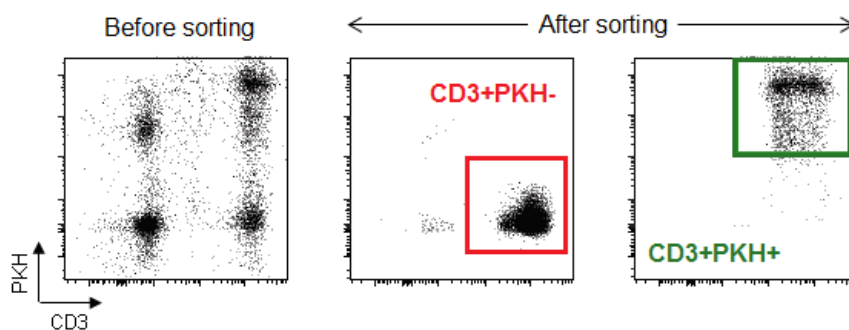


Figure 21. Purity of doublet T cells and non-doublet T cells.

Doublet positive population (CD3+PKH+) and non-doublet T cells (CD3+PKH-) were identified and sorted after 15h of the co-culture. The isolated cells were analyzed by flow cytometry after the sorting procedure.

3. Doublet T Cells Show Higher Percentage of Effector Cells and Specific Cytotoxic Activity as Compared to Non-Doublet T Cells

3.1. Immunophenotype

Immunophenotyping analysis demonstrated the difference between doublet-forming T cells (CD3+PKH+) and the T cells which did not form stable and strong interactions with target cells (CD3+PKH-CD25-). To compare the phenotype of both populations, we performed co-cultures for 15h. At this time point, cells were stained with the following panel: PKH-FITC/CCR7-PE/CD3-PerCP/CD45RA-PECy7/CD8-APC/CD4-APCCy7/CD45-PO.

Thereby, we studied not only the CD4+/CD8+ ratio, but also the percentage of T cell-subtypes (Figure 22). The T cell-subtypes were characterized by expression of CD45RA and CCR7 following the next criterion: Naïve (CD45RA+CCR7+), Effector (CD45RA+CCR7-), Central Memory (CD45RA-CCR7+) and Effector Memory (CD45RA-CCR7-).

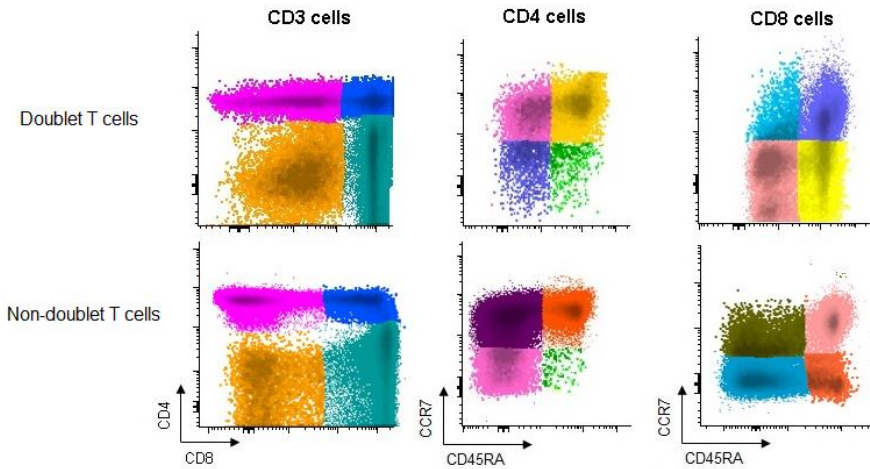


Figure 22: Immunophenotype of doublet and non-doublet T cells.

Co-cultures of donor's PBMC and target CD3-PKH+PBMC were performed. Cells were evaluated by flow cytometry (n=6). Dot plots show CD4, CD8, CD45RA and CCR7 expression on doublet T cells (upper panel) and non-doublet T cells (bottom panel). Within CD4+ and CD8+ cells, naïve (CD45RA+CCR7+), effector (CD45RA+CCR7-), central memory (CD45RA-CCR7+) and effector memory (CD45RA-CCR7-) T cells were analyzed. The Infinicyt software was used for data analysis.

Comparing doublet-forming T cells with non-doublet T cells, we could find differences regarding to the ratio CD4+/CD8+. As shown in figure 23A, doublet T cells showed a higher percentage of CD8+ T cells, while non-doublet T cells showed a higher percentage of CD4+ T cells. Within CD4+ T cells, similar percentage of naïve, central memory and effector memory between doublet cells and non-doublet cells was observed. The same result was noted in CD8+ T cells. However, different percentage of effector CD4+ and CD8+ T cells was observed when doublet T cells were compared with non-doublet T cells (Figure 23B, C).

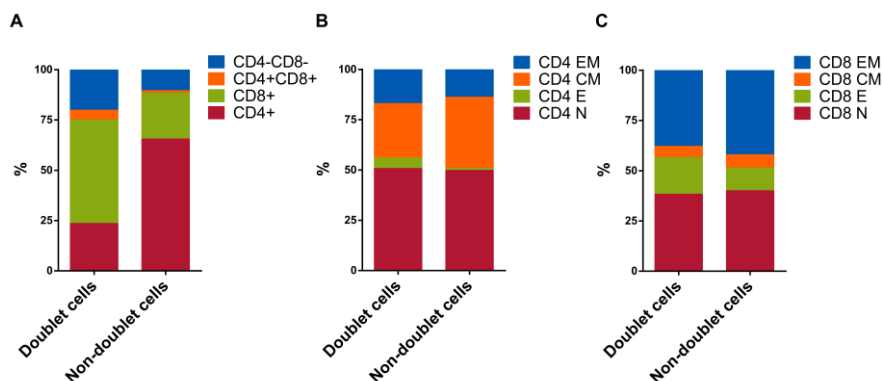


Figure 23: Percentage of T cell-subtypes in doublet and non-doublet populations.

A) Percentage of CD4+ (red), CD8+ (green), CD4+/CD8+ (orange) and CD4-/CD8- (blue) cells in doublet T cells compared to non-doublet T cells. B) Regarding CD4+ T cells, the percentage of naïve (red, CD45RA+CCR7+), effector (green, CD45RA+CCR7-), central memory (orange, CD45RA-CCR7+) and effector memory (blue, CD45RA-CCR7-) T cells is shown. The same analysis is shown in C) for CD8+ cells. Data show mean values of six independent experiments.

Accordingly, there was a significant difference in the percentage of CD4+ and CD8+ cells between doublet-forming T cells and non-doublet T cells (Figure 24A) ($n=6$, $p<0.001$). Furthermore, the percentage of effector CD4+ and CD8+ was significantly higher in doublet population (Figure 24B,C) ($n=6$, $p<0.001$ for effector CD4+; $p<0.05$ for effector CD8+). No significant differences were observed between the proportions of naïve, central memory or effector memory subtypes between both groups ($n=6$).

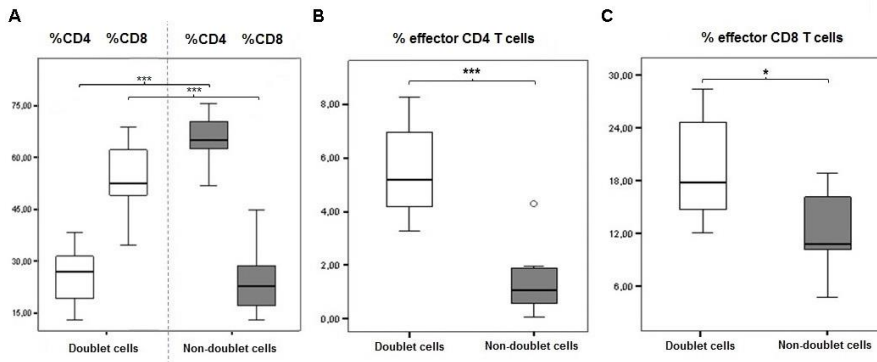


Figure 24: Statistic analyses of T cell-subtypes.

A) Percentage of CD4+ and CD8+ cells in doublet population vs non-doublet population. The mean percentage of CD4+ cells in doublet and non-doublet population was 25.73% vs 65.42%, respectively. The mean percentage of CD8+ cells in doublet and non-doublet population was 50.86% vs 23.42%, respectively. Percentage of effector CD4+ cells (B) and effector CD8+ cells (C) is shown. The mean percentage of effector CD4+ cells in doublet and non-doublet population was 5.57% vs 1.47%, respectively. Regarding effector CD8+ cells, the mean percentage comparing doublet and non-doublet population was 19.57% vs 12.43%, respectively. Depicted are the mean \pm SD of six independent experiments. P values between the indicated groups were calculated using paired Student t tests.

Finally, doublet T cells were negative for $\gamma\delta$ expression suggesting that they present the $\alpha\beta$ phenotype. A small proportion of $\gamma\delta$ T cells were identified in the population of non-doublet T cells (data not shown).

3.2. Cytotoxic activity

The cytotoxic effect of doublet-forming T cells (CD3+PKH+) was analyzed and compared to non-doublet T cells (CD3+PKH-CD25-) in secondary co-cultures (Figure 25). Thus, the sorted populations were again co-cultured with target cells. Therefore, doublet T cells (CD3+PKH+) as well as non-doublet T cells (CD3+PKH-CD25-) were washed and rested for at least 20h after sorting. During this time, doublet-forming T cells became single T cells due to the elimination of the target cells. CD3-depleted target PBMC were thawed and stained with PKH-67 (CD3-PKH+PBMC). Secondary co-cultures between doublet-forming T cells from donor and target CD3-PKH+PBMC were performed. Of note, target cells in secondary co-cultures were not irradiated in order to analyze the cytotoxic effect of donor's T cells.

Live target cells were determined by flow cytometry as a 7AAD and Annexin V negative population. The cytolytic activity was evaluated comparing the viability of target cells cultured alone or with doublet-forming T cells or non-doublet T cells.

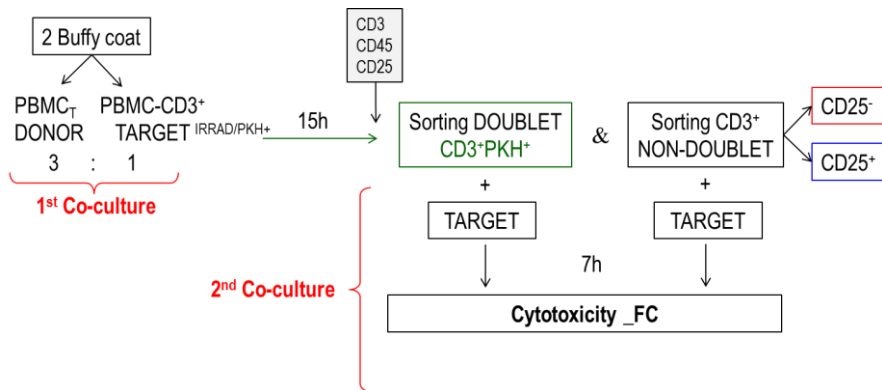


Figure 25: Schedule of the procedure with buffy coats.

PBMC from donor were co-cultured with target PBMC depleted of CD3 cells, irradiated and stained with PKH-67 (first co-culture). After 15h, cells were stained with CD3, CD45 and CD25 monoclonal antibodies for cell sorting. Doublet positive T cells (CD3+PKH+) and non-doublet T cells (CD3+PKH-) were sorted and rested for 20h. Target cells were thawed and stained with PKH-67 and secondary co-cultures between doublet-forming T cells or non-doublet T cells with target cells were performed (second co-culture). After 7 hours, cells were collected and stained with 7AAD and Annexin V.

As shown in figure 26A, significant increase of the specific lysis of target cells was obtained when doublet T cells were co-cultured compared to non-doublet T cells ($n=6$, $p=0,0029$). Further, we developed secondary co-cultures to analyze the CD69 activation marker after 24h of the co-culture (Figure 26B). A high percentage of CD69+ cells was observed in co-cultures with doublet-forming T cells against target cells compared to non-doublet T cells. When the activation was achieved using anti-CD3/anti-CD28 antibodies, the percentage of CD69+ cells was even higher indicating that the activation against target cells was specific.

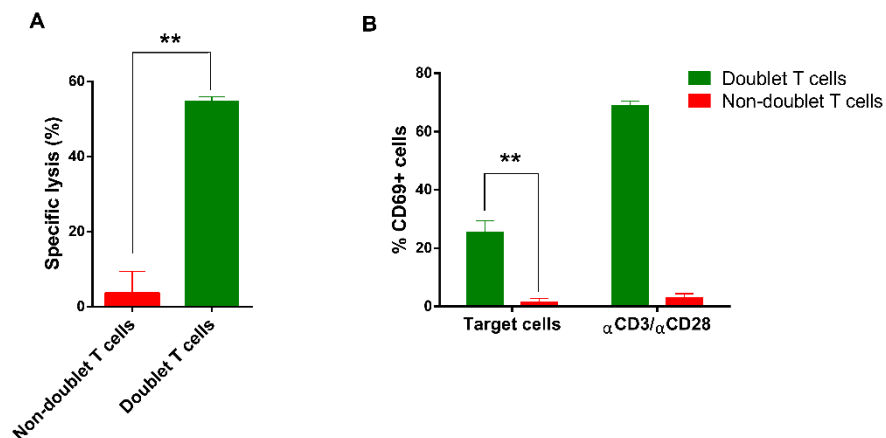


Figure 26: Functional assays of doublet-forming T cells vs non-doublet T cells.

A) Specific lysis of doublet-forming T cells. Secondary co-cultures between doublet-forming T cells or non-doublet T cells with target cells were performed. After 7 hours, cells were collected and stained with 7AAD and Annexin V. The specific lysis was calculated following the next formula: $[(\text{target viability alone} - \text{target viability with doublet or non-doublet T cells}) / \text{target viability alone}] \times 100$. Data show mean values \pm SD of six independent experiments. B) CD69 expression on secondary co-cultures. After 24 hours of co-culture, cells were analyzed by flow cytometry. Data show mean values \pm SD of three independent experiments. P values between the indicated groups were calculated using paired Student t tests.

4. A Subset of Non-Doublet T Cells Have Immuno-Suppressive Function

4.1. Immunophenotype

Non-doublet T cells (CD3+PKH-) were sorted based on their CD25 expression. Regarding the CD25+ T cells (CD3+PKH-CD25+), they showed regulatory phenotype expressing CD4, FoxP3 and CD25, but not CD127, thus suggesting that they are regulatory T cells (Figure 27) (>95%, n=6). The immunophenotype of non-doublet T cells that do not express CD25 (CD3+PKH-CD25-) was already shown in section 3.

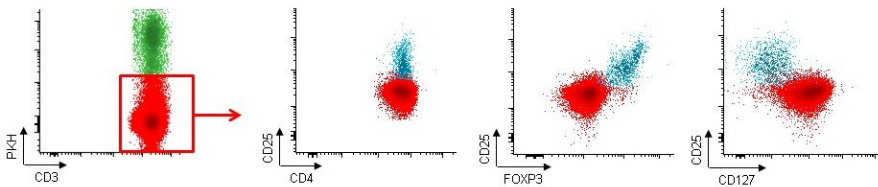


Figure 27: Immunophenotype of non-doublet cells CD3+PKH-CD25+. The regulatory phenotype was evaluated in non-doublet T cells that express CD25. Dot plots show the expression of CD4, CD25, FoxP3 and CD127 on non-doublet T cells CD25+ (CD3+PKH-CD25+). Data show one representative experiment of six independent experiments.

4.2. Immuno-suppressive function

Next, we investigated whether these non-doublet regulatory T cells showed suppressive capacity using functional assays. For this purpose, freshly isolated PKH-67 stained T cells (effector T cells)

were stimulated with anti-CD3 and anti-CD28 antibodies and co-cultured with non-doublet regulatory T cells. As controls, effector T cells were cultured alone, either unstimulated or stimulated with anti-CD3/anti-CD28. Moreover, freshly isolated CD4+CD25+ Treg cells and T cells depleted of Treg were used as controls. For that purpose, PBMC from a healthy donor were isolated. The CD4+CD25+ Treg cells were obtained by positive magnetic selection, and the negative fraction was used as T cells depleted of Treg. Furthermore, we were interested in studying the suppressive function of the population CD3+PKH-CD25-. Thus, escalating ratios of both non-doublet T cells and effector T cells were performed in order to evaluate the suppressive capacity of these cells. After four days of co-incubation, we analyzed the proliferation of effector T cells (Figure 28). The number of proliferating cells, as assessed by PKH fluorescence diminution, significantly decreased when co-incubated with non-doublet regulatory T cells (CD3+PKH-CD25+) (n=3, p=0.0369 for ratio 1:2; p=0.0150 for ratio 1:1). Surprisingly, non-doublet CD25- T cells (CD3+PKH-CD25-) also showed suppressive function (n=3, p=0.0058 for ratio 1:2; p=0.0151 for ratio 1:1). Accordingly, the CD25 activation marker expression was also significantly decreased when non-doublet regulatory T cells or non-doublet CD25- T cells were co-incubated with effector T cells (Figure 29).

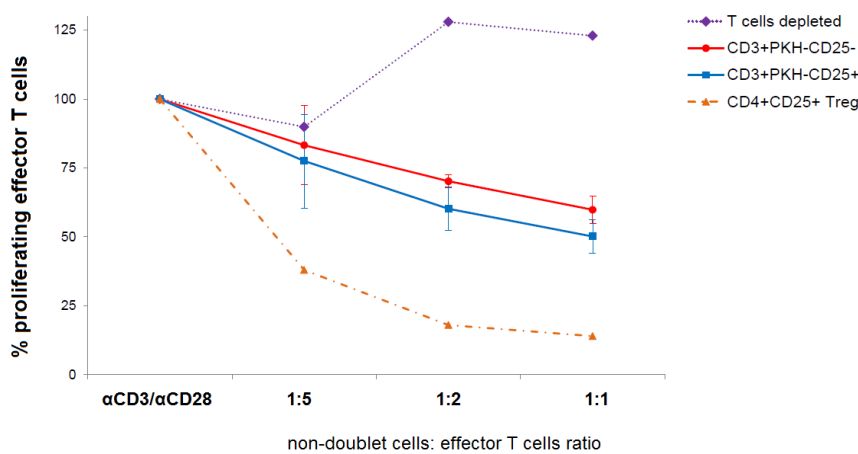


Figure 28: Titration of suppression capacity. The percentage of proliferating effector T cells monitored by PKH-67 dilution is shown. Titration assays showing the suppressive capacity of non-doublet T cells (CD3+PKH-CD25+ and CD3PKH-CD25-) at increasing ratios of non-doublet cells cultured versus effector T cells. Naturally occurring CD4+CD25+ Treg as well as T cells depleted of nTreg were used as controls. The proliferation of αCD3/αCD28 stimulated effector T cells was used as baseline.

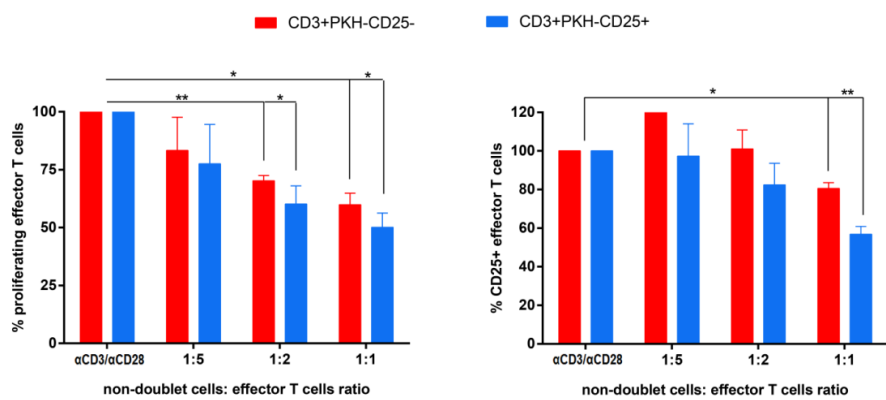


Figure 29: Suppression capacity assays. The percentage of proliferation (left bar diagram) and CD25 expression (right bar diagram) of effector T cells is shown. Proliferation was assessed by PKH fluorescence using ModFit software. PKH and CD25 expression were analyzed by flow cytometry. Depicted are the mean ± SD of three independent experiments. P values between the indicated groups were calculated using paired Student t tests.

5. Clinical Application: Doublet T Cells from AML Patients Have Specific Cytotoxic Activity against Primary Blast Cells

TIL from metastatic melanoma lesions comprise an enriched source of tumor-antigen reactive cells (Dudley *et al.*, 2008). Therefore, co-cultures of T cells from AML patients and autologous tumor cells were performed in order to obtain naturally occurring tumor-reactive T cells.

5.1. Patient samples

Bone marrow (BM) samples were obtained from patients with relapsed/refractory AML. The percentage of tumor cells in the BM samples was >90% in all cases (Figure 30A). After the treatment, patients with <5% blasts in the BM, recovery of neutrophils and platelets, and absence of extramedullary disease were considered in complete remission status (Figure 30B). Under this criterion, PBMC from AML patients in CR were obtained and co-cultured with PKH-67 stained and irradiated autologous tumor cells. After 15h of co-incubation, cells were stained and harvested for sorting. Doublet-forming T cells from AML patients were identified in a range of 2% to 6% (Figure 30C) (mean=3.83%, n=5).

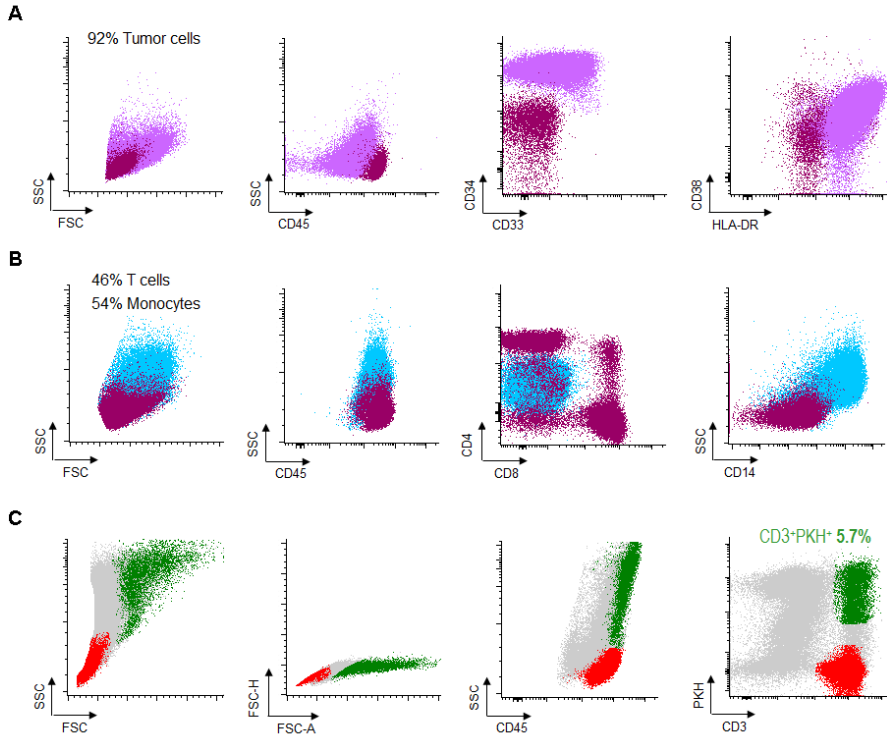


Figure 30: Doublet-forming T cells from an AML patient.

A) Blast cells from bone marrow of AML patient were obtained and frozen. The tumor sample contained 92% of blasts. The immunophenotype of blast cells were: $CD45^{low}$ $CD34^{++}$, $CD38^{+}$, $HLA-DR^{+}$. B) PBMC were obtained from peripheral blood when the patient was in CR and analyzed by flow cytometry. T cells represented the 46% of the total PMBC. C) T cells from the patient were co-incubated with blast cells for 15h. Then, cells were stained and sorted. Doublet-forming T cells were identified based on their FSC/SSC characteristics as well as their positivity for both PKH and CD3 (green). Non-doublet T cells were also isolated to use them as control (red). One representative case is shown.

5.2. Cytotoxic activity of doublet T cells against blast cells

Next, the sorted doublet-forming T cells and non-doublet T cells were rested overnight. Tumor cells from the same patient (autologous tumor cells) were thawed and stained with PKH-67 or

specific CD markers based on the immunophenotype at diagnosis. Secondary co-cultures of doublet-forming T cells and non-doublet T cells with autologous tumor cells were performed for 7 hours (Figure 31). Of note, tumor cells were not irradiated in order to analyze the cytotoxic effect of doublet-forming T cells from the patient. To determine the cytotoxic activity of doublet-forming T cells, the tumor viability was analyzed by flow cytometry using 7AAD and Annexin V staining.

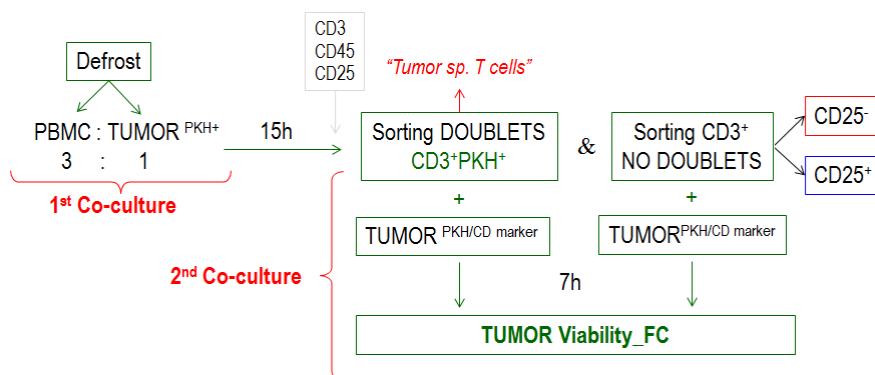


Figure 31: Schedule of the procedure performed with tumor samples. Tumor cells and PBMC from AML patients were obtained. Tumor cells were irradiated at 25Gy and stained with PKH-67. Co-culture of PBMC and tumor cells from the same patient was performed for 15 hours (first co-culture). Then, cells were stained and harvested for cell sorting. The sorted populations (CD3+PKH+ and CD3+PKH-) were rested overnight. Autologous tumor cells were thawed and stained with PKH-67 or specific CD markers. Secondary co-cultures between doublet-forming T cells or non-doublet T cells with autologous tumor cells were performed (second co-culture). After 7 hours, cells were collected and stained with 7AAD and Annexin V for cytometry analysis.

The cytolytic activity was evaluated comparing the viability of tumor cells cultured alone or with doublet-forming T cells or non-doublet cells from the same patient. As shown in figure 32A, significant increase of the specific lysis of tumor cells was obtained when doublet T cells were co-cultured compared to non-doublet T cells ($p=0,0424$; $n=3$). We also calculated the viability ratio and a significant difference between doublet-forming T cells and non-doublet T cells was observed (Figure 32B). Regarding the secondary co-cultures, tumor cells were also stained with tumor specific CD markers based on the immunophenotype of the AML at diagnosis instead of PKH-67 to analyze the tumor viability after co-cultures ($n=2$). The cytolytic activity of doublet-forming T cells against tumor cells in secondary co-cultures was observed in both conditions, PKH-67 or CD marker stained tumor cells (Figure 32C,D). Hence, we were able to obtain tumor-reactive T cells from AML patients by “Doublet Technology”.

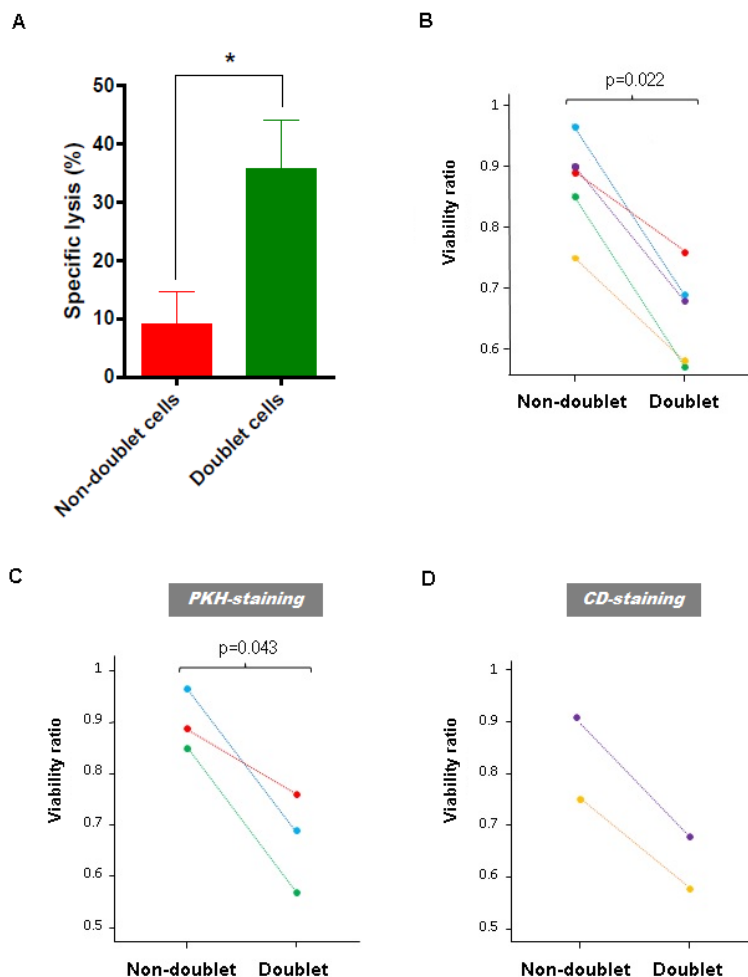


Figure 32: Specific lysis of doublet T cells against tumor cells.

Secondary co-cultures between doublet-forming T cells or non-doublet T cells with tumor cells from the same patient were performed. After 7 hours, cells were collected and stained with 7AAD and Annexin V. Viable cells were negative for both 7AAD and Annexin V. A) The specific lysis was calculated following the next formula: $[(\text{tumor viability alone} - \text{tumor viability with doublet or non-doublet cells}) / \text{tumor viability alone}] \times 100$. Data show mean values \pm SD of five independent experiments. B) The viability ratio was calculated as follows: $1 - [(\text{tumor viability alone} - \text{tumor viability with doublet or non-doublet cells}) / \text{tumor viability alone}]$. For secondary co-cultures, different staining of tumor cells was used. Tumor cells were stained with PKH-67 (n=3) or specific tumor CD marker (n=2). The viability ratio after co-cultures between doublet-forming T cells or non-doublet T cells with PKH-67 stained-tumor cells (C) or CD marker stained-tumor cells (D) are shown. P values between the indicated groups were calculated using paired Student t tests.

6. Interim Conclusion for “Doublet Technology”

In this study, our first objective was to analyze the interaction between the TCR and pMHC complex and to identify/isolate natural autologous tumor-reactive T lymphocytes from acute myeloid leukemia (AML) patients through FACS-based cell sorting.

We aimed to address several limitations related to the isolation of tumor-specific CTLs using conventional strategies, such as cytokine production assay or soluble pMHC multimers: **1)** Selection of CTL based on cytokine production assays does not exclusively represent functional cytotoxicity. **2)** In order to use this approaches the target antigen must be well known, which is not the case for most tumor cells.

We hypothesized that tumor-reactive T cells may form strong interactions with tumor cells through TCR so that they could be identified and isolated by our “Doublet Technology” to pull out naturally occurring tumor-specific CTLs in hematologic malignancies.

In summary, our data demonstrate that pHLA-TCR interactions that involve immune reactive peptides are more stable and strong than those which do not induce a robust triggering of the TCR. Moreover, we observed that when T cells from AML patients are

co-cultured with tumor cells, a doublet population appears. This population consists of T cells bound to tumor cells. We have shown that CTLs bound through TCR to tumor cells can be selected and isolated through FACS-based cell sorting. The CTLs from AML patients obtained with this technique have shown cytolytic activity against blast cells from AML patients suggesting the clinical use of these CTLs. Further, not only CD8+ tumor-reactive T cells are isolated with this approach, but also CD4+ effector T cells. Finally, the “Doublet Technology” represents a very useful advantage in cancer immunotherapy because it is not required a prior knowledge of the exact tumor antigen. Therefore, we are able to obtain tumor-specific T cells from each patient offering a personalized therapy.

PART II

CAR TECHNOLOGY TO GENERATE TUMOR-REACTIVE T CELLS

The second objective of this study was to genetically modify T lymphocytes with chimeric antigen receptors (CARs) to redirect autologous T cells against a specific tumor antigen expressed on the surface of tumor cells and to confirm their anti-tumor reactivity. In particular, we generated a second generation CAR against the B-Cell Maturation Antigen (BCMA) by genetic modification of T cells to target BCMA-expressing malignant plasma cells of multiple myeloma (MM) patients.

Therefore, we first designed two CAR constructs consist of two different recognition domains (BCMA 30 and BCMA 50) against the same epitope of BCMA. Furthermore, we designed each CAR construct in two different versions (short and long) to study the effect of the CAR design in the functionality. Moreover, we analyzed the serum from MM patients and determined whether the presence of soluble BCMA protein could abrogate the anti-myeloma function of BCMA CAR T cells.

1. Substantial Expression of BCMA on Myeloma Cells and Generation of BCMA CAR T Cells

1.1. BCMA expression on myeloma cells

We first evaluated B-cell maturation antigen (BCMA) as a target for immunotherapy. For this purpose, the BCMA expression level on malignant plasma cells from newly diagnosed and relapsed/refractory MM patients were evaluated by flow cytometry.

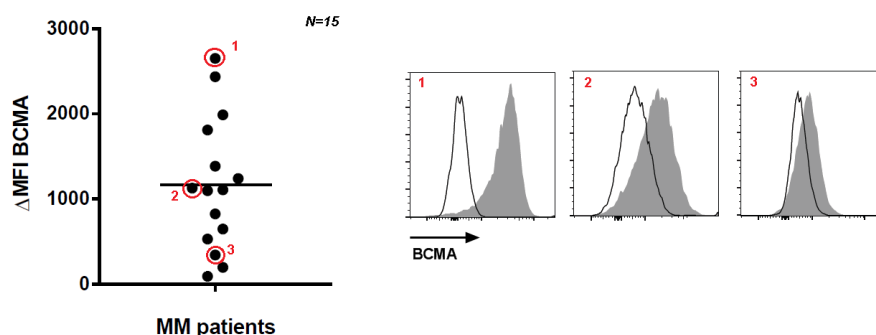


Figure 33: BCMA expression on plasma cells from MM patients.

Differential mean fluorescence intensity (MFI) of BCMA and isotype control staining is shown on CD38+ CD138+ myeloma cells from MM patients (n=15). Histograms display BCMA expression in representative cases showing high, intermediate and low expression. Shaded histograms show staining with anti-BCMA mAb, white histogram shows staining with isotype control antibody. 7AAD was used to exclude dead cells from analysis.

The 60% of the patients (9/15) showed a significant expression of BCMA on myeloma cells detected by flow cytometry. We next analyzed the BCMA expression on different tumor cell lines. For that, cell lines were stained with anti-BCMA mAb and analyzed by

flow cytometry (Figure 34). All three MM cell lines (MM1.S, OPM-2 and H929) show considerable expression of BCMA. In order to study the functional potency of BCMA CAR T cells, we additionally generated BCMA-expressing K562 cells by transducing them with BCMA-encoding plasmid.

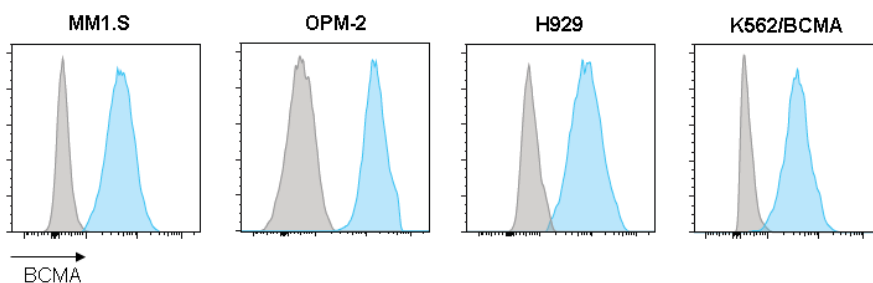


Figure 34: BCMA expression on cell lines.

Tumor cells were gated on GFP+CD138+ cells. Histograms display BCMA expression. Blue histograms show staining with anti-BCMA mAb, grey histogram shows staining with isotype control antibody. 7AAD was used to exclude dead cells from analysis.

1.2. BCMA expression on non-myeloma cells

Importantly, we analyzed the expression of BCMA on primary CD34+ hematopoietic stem cells (HSC) from healthy donors by flow cytometry. CD34+ HSC lacked cell-surface BCMA expression (Figure 35). We also evaluated *in silico* the antigen's expression pattern in normal tissues using The Human Protein Atlas (<http://www.proteinatlas.org>). The RNA expression of BCMA of the myeloma samples is dramatically higher than the expression of any other tissue (e.g. brain, endocrine tissues, muscle tissues, lung, liver, pancreas, skin, adipose and soft tissue).

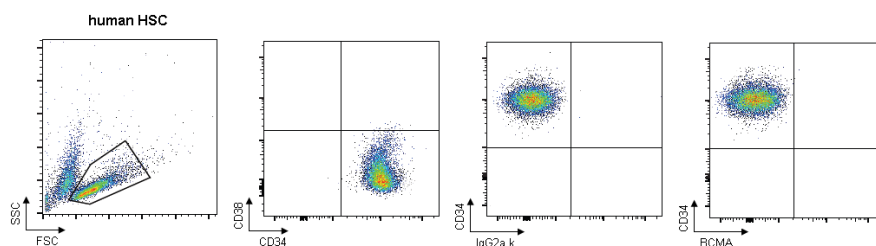


Figure 35: BCMA expression on human HSC.

Human HSC from healthy donors were stained with anti-CD38, anti-CD34 and anti-BCMA mAbs. An isotype control antibody IgG2a, κ was used. Cells were analyzed by flow cytometry.

Accordingly, BCMA has a restricted RNA expression pattern and is expressed on malignant plasma cells in MM patients. In conclusion, BCMA is an attractive target for immunotherapy due to its absent expression on essential normal tissues, except normal B-cells.

1.3. CAR design: 2^o generation CAR with 4-1BB domain

Due to the expression pattern of BCMA, we reasoned that BCMA would be an appropriate target for CAR T cells in MM. To further evaluate the suitability of BCMA as a therapeutic target for CAR T cells, we designed two CARs. Each CAR contained a single chain variable fragments (scFv) derived from one of two humanized anti-human-BCMA monoclonal antibodies (BCMA 30 and BCMA 50) in VL-VH configuration. Several studies have suggested the importance to tailor the extracellular spacer domain for different target molecules (Hudecek *et al.*, 2015). Thereby, we constructed

two versions of each BCMA CAR. The short version consisting of the IgG4 hinge domain (12 AA, short spacer) and the long version contains the IgG4 hinge-CH2-CH3 domain (229 AA, long spacer). Construction of the long 4/2 spacer CAR was accomplished by replacing the first six amino acids of the CH2 domain of IgG4 (APEFLG) with the corresponding five amino acids of IgG2 (APPVA) and an additional Asn297 to Gln mutation to abrogate the adverse consequences of FcγR binding *in vivo*. Each spacer was linked to a CD28 transmembrane domain and a signaling module composed of CD3ζ with a membrane-proximal 4-1BB costimulatory domain. All vectors encoded a truncated epidermal growth factor receptor (EGFRt) sequence downstream of the CAR linked by a T2A ribosomal skip element (Wang *et al.*, 2011). The EGFRt serves as a transduction marker and a tool for enrichment of CAR expressing T cells. Moreover, it can be used for depleting CAR T cells via EGFR binding antibodies (Figure 36).

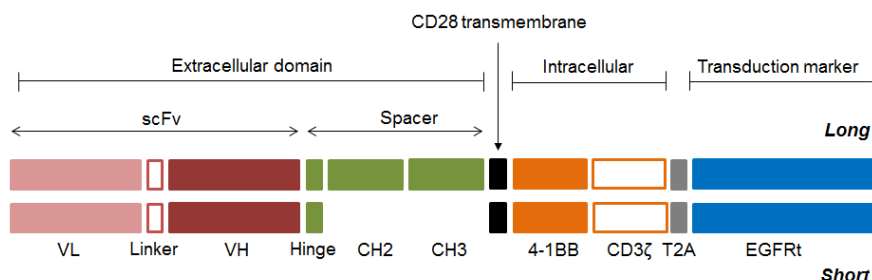


Figure 36: Lentiviral transgene inserts encoding BCMA CARs. Two BCMA CARs with different extracellular spacer lengths were designed. The scFv was derived from two anti-human BCMA mAbs.

After the amplification of BCMA CAR transgenes, the sequence of each plasmid was verified by sequencing and enzymes-restriction digestion to detect any non-desired mutation. The sequencing was performed by GATC Biotech AG. The digestion was performed using NheI and NotI enzymes. For that, 0.5µg of each plasmid was digested for 1h at 37°C. Then, digested-DNA was separated by gel electrophoresis.

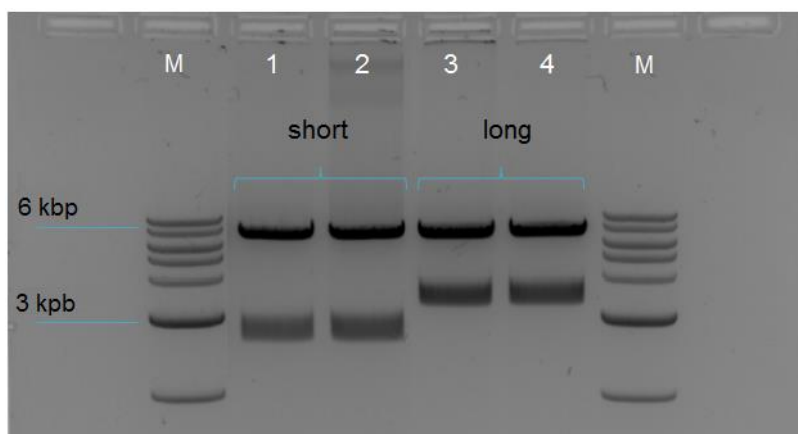


Figure 37: Validation of BCMA CAR short and long versions.

Restriction digestion analysis of BCMA CARs. Lane 1, BCMA 30 short digested with NheI and NotI; lane 2, BCMA 50 short digested with NheI and NotI; lane 3 BCMA 30 long digested with NheI and NotI; lane 4, BCMA 50 long digested with NheI and NotI. lane M, 1kb DNA ladder (NEB). The DNAs were analyzed on 1.2 % agarose gel.

The short versions of the two BCMA CARs (BCMA 30 short and BCMA 50 short) showed a band of 2,5 Kb corresponding with the CAR short transgene, whereas the long versions (BCMA 30 long and BCMA 50 long) showed a band of 3,2 Kb corresponding with the CAR long transgene.

1.4. Transduction of T cells by lentiviral gene transfer

Once the BCMA CAR plasmids were prepared, the lentiviral vectors were produced using 293-T cell line. The titration of BCMA CAR lentivirus was performed in Jurkat cells. An escalation dose of lentivirus vectors was used to transduce Jurkat cells. After 48 hours, the transduction efficiency was analyzed by flow cytometry (Figure 38). The lentivirus titer in transforming units (TU)/mL was calculated based on the expression of the EGFRt transduction marker. Replication-incompetent lentiviruses encoding the CARs were used to transduce human T cells. To generate BCMA CAR T cells, CD4⁺ and CD8⁺ T cells from PBMC of healthy donors were isolated by negative selection using magnetic beads (Figure 39).

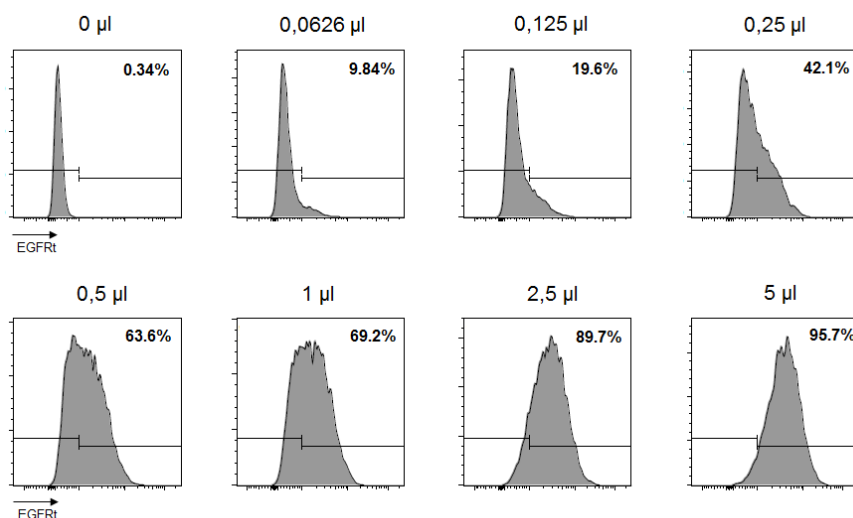


Figure 38: Titration of BCMA CAR lentiviral vector.

Jurkat cells were cultured at 250×10^3 cells/well in 48-well plates (Costar). BCMA lentiviral vector of each CAR was added to the cells. After 48 hours of incubation, cells were collected and stained with anti-EGFR mAb. The CAR expression was detected by flow cytometry.

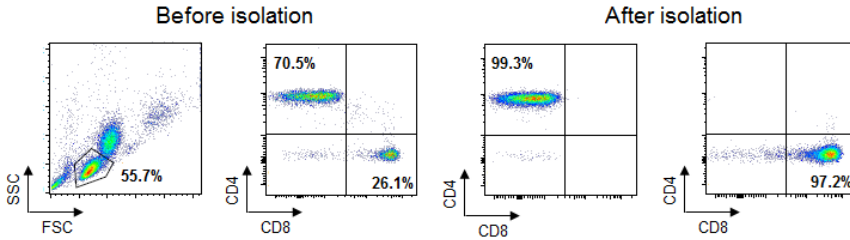


Figure 39: Purity of CD4+ and CD8+ cells after selection.

CD4+ and CD8+ T cells were isolated from PBMC of healthy donors. Cells were stained and analyzed by flow cytometry. 7AAD was used for discrimination of dead/alive cells. One representative case is shown.

The purity of CD4 and CD8 selections was >95% in all cases (n=3). Thereby, CD4+ and CD8+ T cells were transduced with BCMA CAR lentivirus vectors (BCMA 30 short/long; BCMA 50 short/long) after 24 hours of α CD3/ α CD28-bead stimulation. The transduction efficiency was analyzed at day 8 by flow cytometry (Figure 40, n=3). The percentage of CAR positive (EGFRt+) T cells was 15-30% for CD4+ subset and 7-15% for CD8+ subset. After enrichment using the EGFRt marker, the purity of CAR-expressing T cells was >90%. Then, T cells that were selected for EGFRt were expanded in an antigen-specific manner with BCMA+ feeder cells during 7 days. The expanded BCMA CAR T cells were analyzed at day 7 by flow cytometry (Figure 41, n=3). After antigen-dependent expansion, the percentage of CAR-expressing T cells was >90%. Importantly, BCMA CAR T cells showed stable transgene expression over multiple expansion cycles.

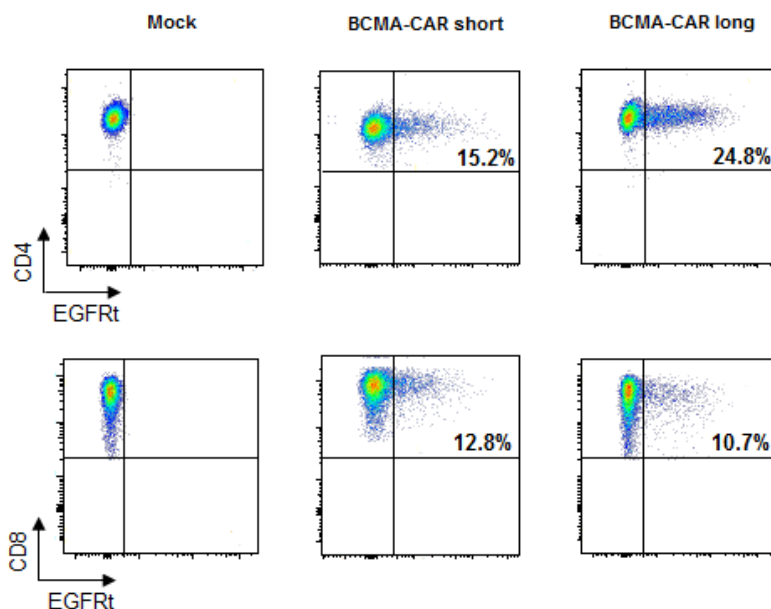


Figure 40: Transduction of CD4+ and CD8+ cells with BCMA CAR lentiviral vectors.

T cells were stimulated for 24 hours and cultured at 0.5×10^6 cells/well. BCMA lentiviral vector of each CAR was added to the cells at MOI of 5. At day 8 of transduction, cells were stained with anti-EGFR mAb and CAR expression was analyzed by flow cytometry. 7AAD was used for discrimination of dead/alive cells. One representative case is shown.

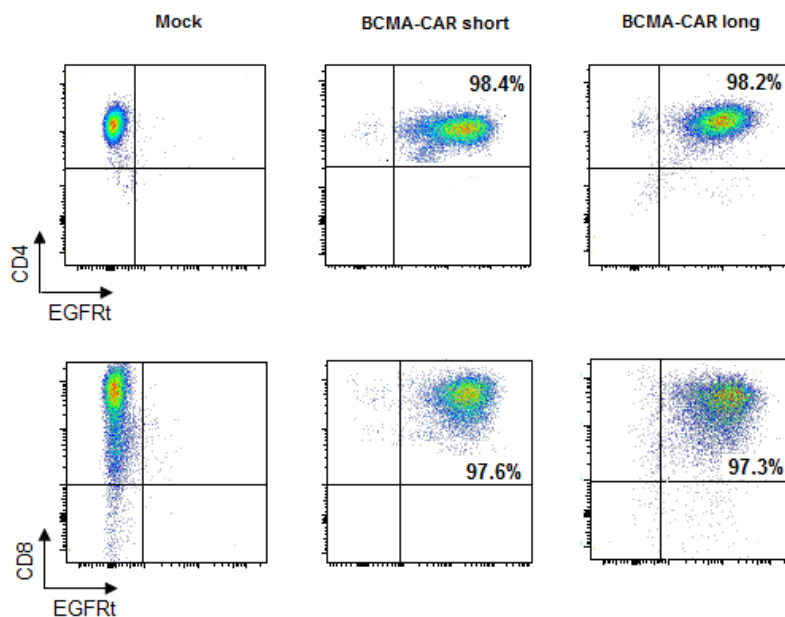


Figure 41: Enrichment and antigen-dependent expansion of CD4+ and CD8+ BCMA CAR T cells.

CD4+ and CD8+ BCMA CAR T cells were enriched using biotin-conjugated anti-EGFR mAb and anti-biotin MicroBeads (Miltenyi). Cells were cultured with irradiated TM-LCL feeder cells at ratio effector:target 1:7. At day 7 of the antigen-dependent expansion, cells were stained with anti-EGFR mAb and CAR expression was analyzed by flow cytometry. 7AAD was used for discrimination of dead/alive cells. One representative case is shown.

2. BCMA CAR Design Affects Anti-Myeloma Function

While the recognition domain is critical for CAR specificity, the connecting sequence between the recognition domain to the transmembrane domain, can also profoundly affect CAR T-cell function by producing differences in the length and flexibility of the resulting CAR (Dotti *et al.*, 2014). Therefore, we compare the functionality of two BCMA CAR versions, one with a short and one with a long spacer. For that, the cytolytic activity against myeloma cells was evaluated by bioluminescence. The long version showed higher anti-myeloma function in both BCMA CARs. Consequently, BCMA CAR 30 and 50 long were selected for further analyses.

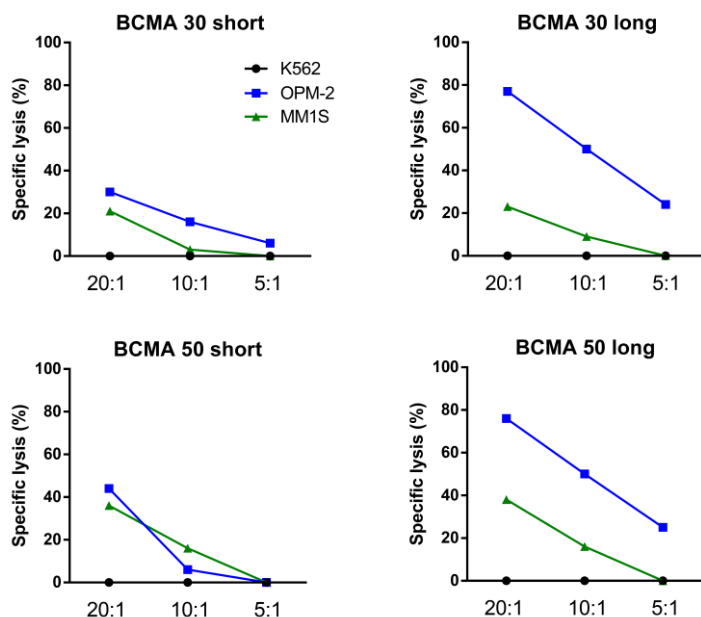


Figure 42: Comparison between short and long BCMA CAR T cells. CD8+ BCMA CAR T cells were co-cultured with target cells in 96-well plates at the indicated ratios. OPM-2 and MM.1S cell lines stably express firefly luciferase. After 4 hours, the cytotoxicity was evaluated with a bioluminescence-based assay.

3. BCMA CAR T Cells Eliminate Myeloma Cells *in Vitro*

3.1. Cytotoxic activity of BCMA CAR T cells

The next aim was to further analyze the functionality of BCMA CAR 30 and 50 long. We first evaluated the cytolytic activity of BCMA CAR modified and control untransduced T cells against BCMA+ tumor cells. For that, CD8+ T cells from three different healthy donors were genetically modified to express the BCMA CARs and their cytotoxic capability was analyzed against antigen-specific targets (Figure 43). Both BCMA CAR T cells showed specific killing of BCMA+ MM cell lines, without unspecific effect on the BCMA-control cell line (K562).

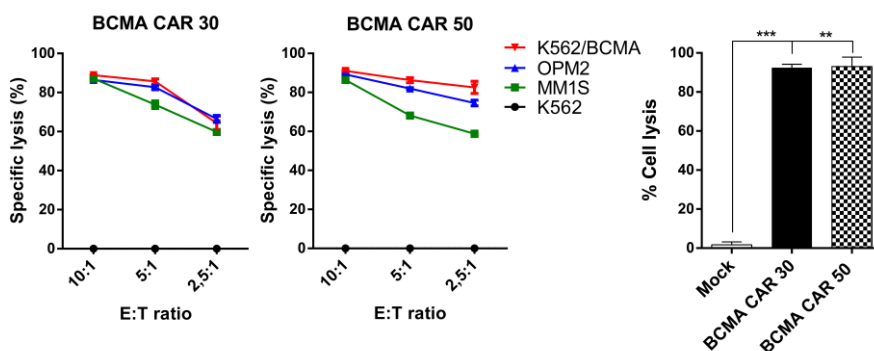


Figure 43: Specific cytolytic activity of CD8+ BCMA CAR T cells.

CD8+ BCMA CAR T cells were co-cultured with BCMA-expressing target cells, which stably express firefly luciferase. 4 hours later the cytotoxicity was evaluated with a bioluminescence-based assay. Right diagram shows specific lysis of K562/BCMA target cells (E:T=10:1) by BCMA CAR T cells prepared from n=3 different donors. P values between the indicated groups were calculated using paired Student t tests. Mock: no lentiviral vector.

3.2. Cytokine production of BCMA CAR T cells

Further, we analyzed the INF- γ and IL-2 release when CD4⁺ and CD8⁺ BCMA CARs were co-cultured with myeloma cells. After 20 hours, the supernatant was collected and the cytokines concentration was measured by ELISA.

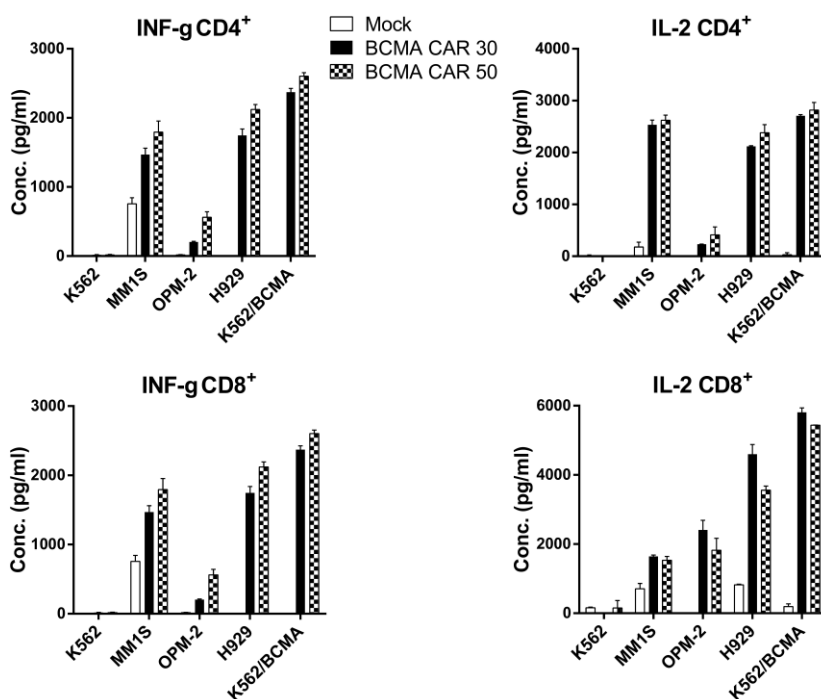


Figure 44: Cytokine production of BCMA CAR T cells.

BCMA CAR T cells were co-cultured with BCMA⁺ target cells for 24 hours. IFN- γ and IL-2 levels in supernatants were measured by ELISA (stimulation performed in triplicates). Data show mean values \pm SD of one representative experiment. Mock: no lentiviral vector.

Quantitative cytokine analysis showed that both BCMA CAR T cells produce INF- γ and IL-2 release when they were co-cultured with target-specific myeloma cells, while they did not produce cytokines release when they were co-cultured with the control K562 cell line.

3.3. Proliferation of BCMA CAR T cells

We next analyzed the proliferation capacity of BCMA CAR T cells. Therefore, co-cultures between CFSE-labeled BCMA CAR T cells with BCMA-expressing target cells were performed. After 72 hours, the BCMA CAR T cells proliferation was measured by flow cytometry (Figure 45).

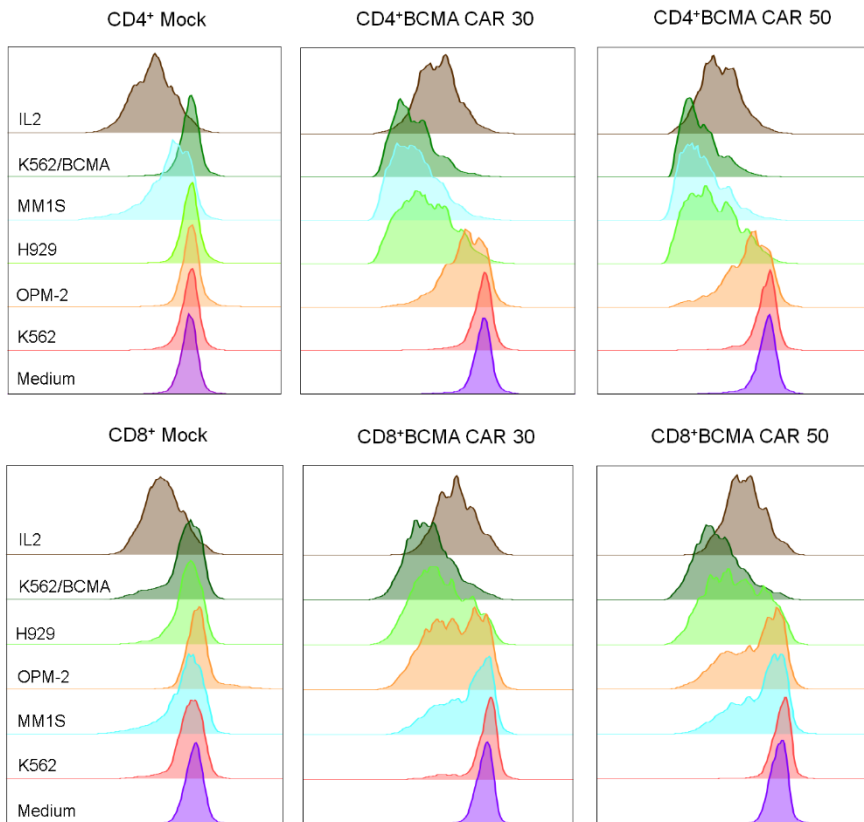


Figure 45: Proliferation of CD8+ and CD4+ BCMA CAR T cells.

CFSE labeled BCMA CAR T cells were co-cultured with BCMA+ target cells or the BCMA- K562 control cell line for 72 hours. Proliferation was assessed by CFSE dye dilution. No exogenous cytokines were added to the assay medium except in the control condition IL2 (positive proliferation control; IL2: 100 U/ml). One representative case is shown. Mock: no lentiviral vector.

The proliferation of CD4⁺ and CD8⁺ mock was only observed when cells were cultured in the presence of IL2, whereas BCMA CARs showed proliferative capacity when they were co-cultured with BCMA⁺ target cells. Accordantly, the increase of the percentage of proliferating cells against K562/BCMA target cells was statistically significant. For that, the proliferative capacity of BCMA CAR T cells from three different donors was compared to the proliferation rate of the mock (untransduced T cells).

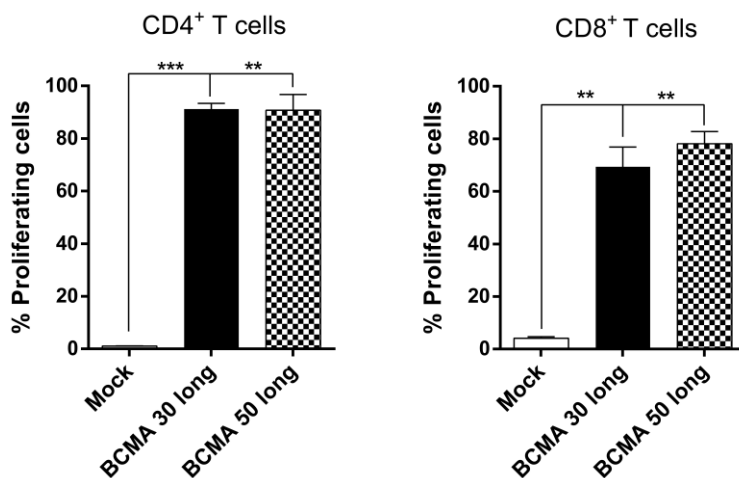


Figure 46: Percentage of proliferating cells of BCMA CAR T cells.

CFSE labeled BCMA CAR T cells were co-cultured with K562/BCMA cells during 72 hours. The percentage of proliferating cells (i.e. CFSE⁺ cells) was calculated from data obtained in n=3 independent experiments using FlowJo software. Data show mean values \pm SD. P values between the indicated groups were calculated using paired Student t tests.

Collectively, our data demonstrate that both BCMA CARs are specific and effective against myeloma cells. BCMA CAR 30 and 50 show cytolytic activity, INF- γ and IL-2 release and proliferative capacity against myeloma cells.

4. The Serum of Multiple Myeloma Patients Contains a Soluble Form of BCMA Which Is Correlated with Disease Status

The presence of soluble antigens would be a potential limitation for the clinical application of CARs. Thus, in addition to CAR affinity, the function can be also affected by soluble proteins (Cartellieri *et al.*, 2010). We next sought to determine whether the myeloma cell lines release soluble BCMA (sBCMA) protein. Therefore, several cell lines were cultured and supernatant was analyzed by ELISA.

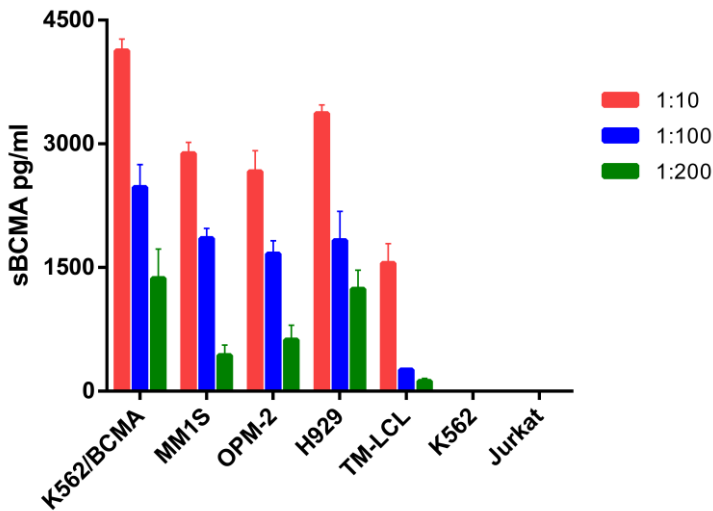


Figure 47: sBCMA concentration in the supernatant of cell lines.

Cell lines were cultured at 1×10^6 /well for 24 hours. After incubation, supernatant was collected and diluted at the indicated dilutions. sBCMA concentration was analyzed by ELISA (stimulation performed in triplicates). Data show mean values \pm SD.

Interestingly, BCMA+ cell lines showed sBCMA in the supernatant indicating that BCMA-expressing cell lines are able to release

sBCMA protein within 24 hours of culturing period. BCMA- cell lines like K562 and Jurkat did not show sBCMA released. The transduced cell line K562/BCMA showed the highest concentration of sBCMA. Moreover, we investigated whether the serum from MM patients contains soluble protein. For this purpose, peripheral blood from MM patients was centrifuged and the serum was collected and analyzed by ELISA for sBCMA concentration.

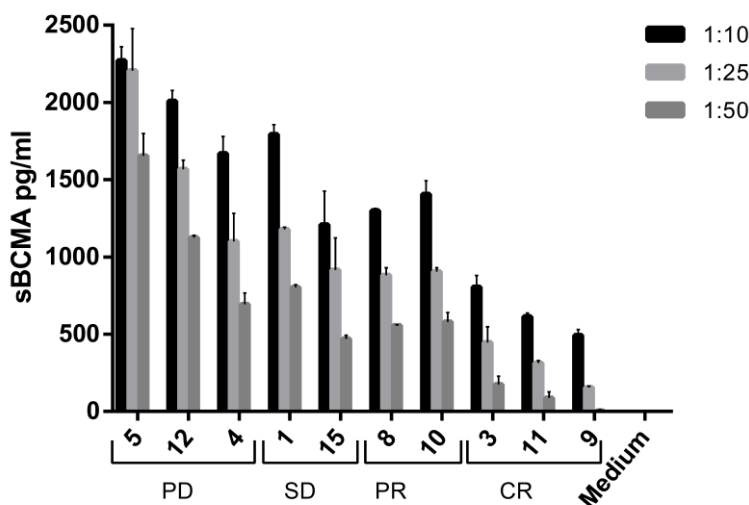


Figure 48: sBCMA concentration in the serum of MM patients.

Peripheral blood from MM patients was collected. Centrifugation at 3.000 rpm for 10 min was performed to obtain patient's serum. The serum was diluted at the indicated dilutions. sBCMA concentration was analyzed by ELISA (stimulation performed in triplicates). Data show mean values \pm SD. PD, progressive disease; SD, stable disease; PR, partial remission; CR, complete remission.

The concentration of sBCMA was higher in patients with progressive disease as compared to the sBCMA level on complete remission patients suggesting that soluble form of BCMA is correlated positively with disease burden.

5. Soluble BCMA Does Not Abrogate the Efficacy of BCMA CAR T Cells

5.1. Cytotoxic activity in the presence of sBCMA

We next sought to determine whether the presence of sBCMA could affect the functionality of BCMA CAR T cells. In order to evaluate the influence of soluble protein on cytolytic activity, CD8+ BCMA CAR T cells were co-cultured with target cells in different effector:target ratio in the presence or absence of sBCMA protein. The specific lysis was measured at 4 hours.

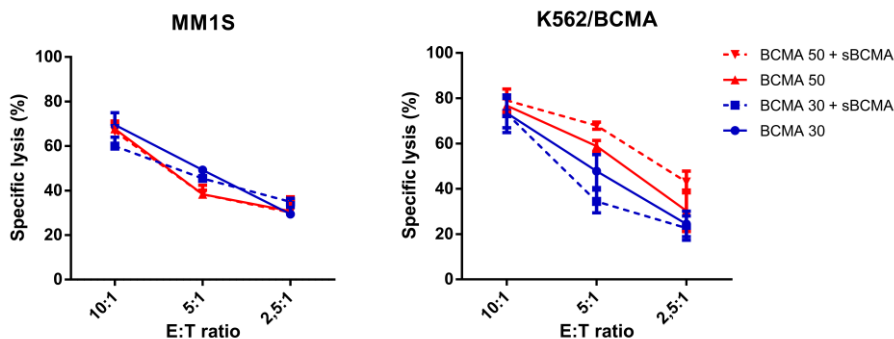


Figure 49: Specific cytolytic activity of CD8+BCMA CAR T cells in the presence of sBCMA.

CD8+ BCMA CAR T cells were co-cultured with MM1.S and K562/BCMA target cells in absence (continuous line) or presence (discontinuous line) of 150 ng/ml of soluble BCMA. After 4 hours, luciferin was added to the culture and the cytotoxicity was evaluated with a bioluminescence-based assay. Data show mean values \pm SD.

The cytolytic activity of both BCMA CARs against tumor cell lines in the presence of sBCMA vs. fresh medium was similar suggesting

that sBCMA protein is not interfering with the cytotoxic function of BCMA CAR T cells.

5.2. Activation in the presence of sBCMA

Further, we were interested to analyze the percentage of activated BCMA CAR T cells in the presence of sBCMA to determine whether the soluble form of the protein could load the aggregation of BCMA CARs. Thus, cultures of CD4⁺ and CD8⁺ BCMA CAR T cells were performed using an increasing dose of sBCMA and the percentage of CD69⁺/CD25⁺ T cells was analyzed by flow cytometry (Figure 50)

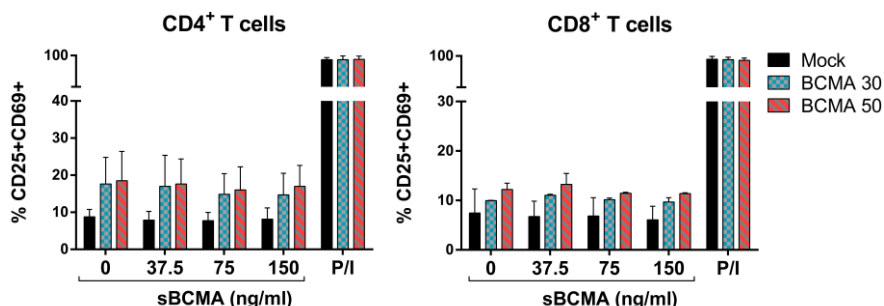


Figure 50: Percentage of activated T cells in the presence of sBCMA. BCMA CAR T cells were incubated with soluble BCMA protein at the indicated concentrations for 24 hours. No target cells were added to the assay. P/I condition: PMA (25 ng/ml) and Ionomycin (1 µg/ml) were added to the culture. The percentage of activated T cells (CD25⁺CD69⁺) was calculated from data obtained in n=2 independent experiments using FlowJo software. Data show mean values ± SD. Mock: no lentiviral vector.

No differences in the percentage of activated CD69⁺/CD25⁺ T cells were observed when BCMA CAR T cells were cultured with or without sBCMA protein. Moreover, as indication of cell activation,

we investigated the INF- γ release when BCMA CAR T cells were cultured with an increasing dose of sBCMA. The supernatant was collected after 24 hours and analyzed by ELISA (Figure 51). Concordantly, the INF γ secretion was similar when BCMA CAR T cells were cultured with or without sBCMA. In aggregate, these results suggest that sBCMA protein does not interfere with BCMA CAR 30 and 50 neither abrogating the cytotoxicity activity nor inadvertent T-cell activation with cytokine release due to aggregation of several BCMA CARs.

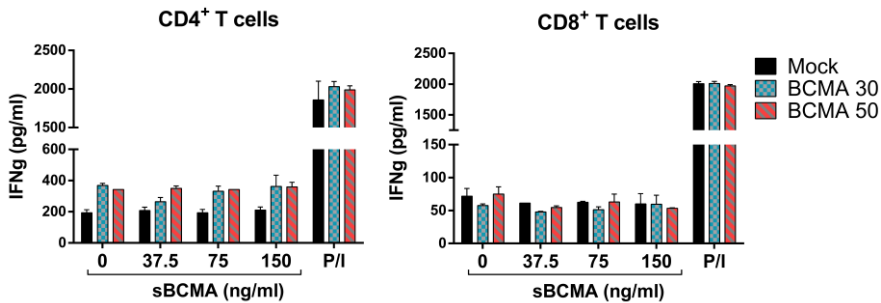


Figure 51: INF gamma secretion in the presence of sBCMA.

BCMA CAR T cells were incubated with soluble BCMA protein at the indicated concentrations for 24 hours. No target cells were added to the assay. P/I condition: PMA (25 ng/ml) and Ionomycin (1 μ g/ml) were added to the culture. INF- γ level in supernatants was measured by ELISA (stimulation performed in triplicates). Diagrams show the concentration of INF- γ calculated from data obtained in n=2 independent experiments. Data show mean values \pm SD. Mock: no lentiviral vector.

5.3. sBCMA protein detection

Finally, we performed western blot analyses of K562 and K562/BCMA cells and their supernatant to determine whether the

target epitope of sBCMA protein is hidden so that BCMA CARs are not affected.

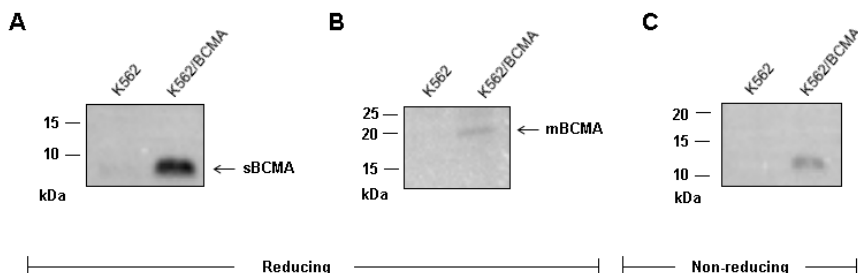


Figure 52: Western blot analysis of soluble and membrane BCMA. K562 and K562/BCMA cell lines were cultured at 1×10^6 / ml for 24 hours. A) and C) The supernatant was concentrated in soluble BCMA using Vivaspin tubes (Sartorius). B) Cells were harvested and treated with RIPA buffer. A 4-20% polyacrylamide gel was used.

A band of 6 kDa was observed when supernatant of K562/BCMA was analyzed in reducing condition. This band corresponds in size to the soluble BCMA protein. However, a 20 kDa band was visualized when K562/BCMA cells were analyzed corresponding with the membrane BCMA. Interestingly, when the supernatant of K562/BCMA was analyzed in non-reducing condition (the secondary structure is maintained), a ≈ 12 kDa band was observed suggesting that sBCMA could form homodimers. Altogether, these results indicate that the efficacy of BCMA CAR T cells is not affected by the presence of soluble BCMA protein probably due to the non-accessibility of the BCMA CAR to the target epitope of the soluble protein.

6. BCMA CAR T Cells Eradicate Tumor *in Vivo*

Finally, we analyzed anti-tumor efficacy of generated BCMA CAR T cells in a systemic BCMA+ multiple myeloma xenograft model (NSG/MM1.S-ffLuc) (Figure 53).

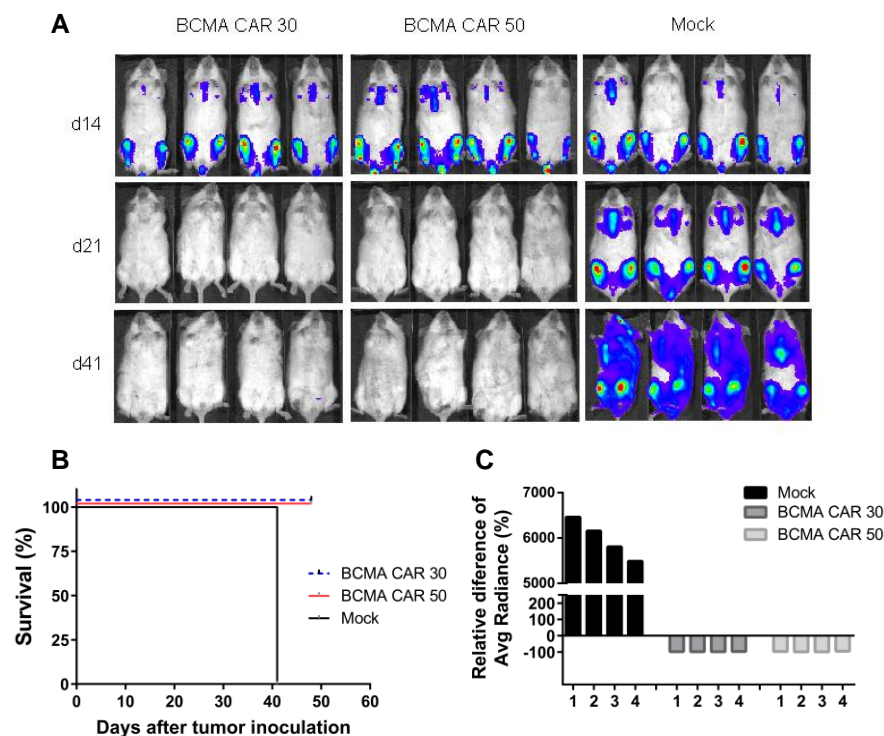


Figure 53. *In vivo* antitumor reactivity of BCMA CAR T cells.

A) NSG mice were inoculated with MM1.S-ffluc/eGFP cells and 14 days later treated with 5×10^6 BCMA CAR T cells (1:1 ratio of CD8+ and CD4+ T cells, 2.5×10^6 each) or unmodified control T cells (mock). BCMA CAR T cells were generated by lentivirus transduction. Bioluminescence images were obtained on day 14 (before T-cell infusion, upper row), on day 21 (7 days after T-cell infusion, middle row) and on day 41 (27 days after T-cell infusion, lower row). B) Kaplan-Meier analysis of survival in groups of mice treated with BCMA CAR 30 T cells (n=4), BCMA CAR 50 T cells (n=4) and mock T cells (n=4). C) Waterfall plot shows the relative difference in average radiance of each experimental animal between day 14 and day 21 in percent.

A potent anti-tumor effect was mediated by a single dose of CD8+ and CD4+ BCMA CAR T cells. These cells rapidly eradicated myeloma cells in all treated mice (n=4), whereas the mice receiving control T cells showed progressive, deleterious myeloma (Figure 53A). Relative difference in average radiance was calculated between day 21 (7 days after T cells infusion) and day 14 (before T cells infusion, already established tumor). As shown in Figure 53C, infusion of BCMA CAR 30 and 50 T cells dramatically reduce the tumor burden compared to control T cells (>6000 units of difference).

Collectively, our data demonstrate that BCMA CAR engineered-T cells are highly potent *in vitro* and *in vivo*. Hence, we were able to redirect T cells against the tumor-specific antigen BCMA by CAR Technology and successfully trigger multiple myeloma disease.

7. Interim Conclusion for CAR Technology

As the second objective of this study we aimed to create a second generation CAR against the B-Cell Maturation Antigen (BCMA) by genetic modification of T cells and to confirm their anti-tumor reactivity against myeloma cells to treat multiple myeloma (MM) patients.

Generating tumor-specific CTLs *ex vivo* may address some difficulties associated with the isolation and use of conventional strategies to obtain them, such as cytokine production assay or soluble pMHC multimers: **1)** pMHC multimers can often fail to stain antigen specific T cells where the interaction between pMHC and TCR is weak. **2)** Reproducible results in the clinic with the use of these approaches are often hard to achieve based on the variability between patients. We hypothesized that gene transfer could be exploited to redirect T cells against tumor specific antigens expressed on the surface of tumor cells by introducing transgenes that encoded chimeric antigen receptors (CAR). Hence, the generation of CAR T cells may solve these problems due to the possibility to use different antibodies affinities and to select desired subsets of T cells from the patients.

Collectively, we have designed and developed several BCMA CARs to trigger myeloma cells. Further, we have observed that the

long spacer confers higher anti-myeloma function than the short one. BCMA CAR T cells showed specific cytolytic activity, production of cytokines including IFN- γ and IL-2, as well as productive proliferation against BCMA-expressing target cells. Moreover, we have confirmed the presence of soluble BCMA in the serum of MM patients. We also demonstrated that the presence of soluble BCMA does not abrogate the efficacy of BCMA CAR T cells suggesting that BCMA CARs can be used in the clinical setting to trigger multiple myeloma disease. Furthermore, different subsets of T cells like CD4 and CD8 can be successfully engineered against BCMA by gene transfer and those subsets show an appropriate and significant efficacy. Hence, our data indicate the great advantage of CAR Technology to trigger tumor-specific antigens in order to efficiently eradicate the tumor.

DISCUSSION

1. “Doublet Technology” to Obtain Tumor-reactive T Cells from Acute Myeloid Leukemia Patients

Harnessing the immune system to recognize and destroy tumor cells has been the central goal of anti-cancer immunotherapy. Currently, there is an increasing interest to optimize anti-tumor technologies in order to develop clinically feasible therapeutic approaches. One of the main treatment modalities in cancer immunotherapy is based on adoptive transfer of T cells (ACT). Using this approach, tumor-specific cytotoxic T cells (CTLs) are infused into cancer patients with the goal of recognizing, targeting, and destroying tumor cells (Perica *et al.*, 2015). T lymphocytes are multifunctional effector cells with exquisite antigen specificity and with a clear biologic role in the defense of the organism. The importance of T cells in the control of malignancy is inferred from studies showing increased susceptibility to neoplasia in immunodeficient patients or experimental animal models, and from decades of experience with allogeneic bone marrow transplantation that have established the central role of T cells in the “graft-versus-tumor” response (Gill and Kalos, 2013). The conventional methods to obtain tumor-specific CTLs are cytokine production assays and soluble pMHC multimers (Becker *et al.*, 2001; Savage *et al.*, 2007). The first one is based on selecting those CTLs that highly release

INF- γ . However, cytokine-producing T cells are not necessarily cytotoxic, so that they would not present the capacity to destroy target cells. Furthermore, we should take in consideration the “bystander effect” which is antigen non-specific stimulation due to some T cells could release INF- γ not because they are tumor-reactive cells, but because they are stimulated through cytokines released from bystander lymphocytes (Panelli *et al.*, 2000; Snyder *et al.*, 2003; Boyman, 2010). Prior work showed that IFN- γ secretion and cytotoxic ability are regulated independently. Thus, the secretion of IFN- γ without killing by some CD8⁺ T cells was confirmed by combining the Lysispot with an IFN γ Elispot in a two-color assay (Snyder *et al.*, 2003). On the other hand, the use of soluble pMHC multimers consist of multiple pMHC complexes that have been chemically linked together and conjugated to a detectable marker (Wooldridge *et al.*, 2009). Although, this technology has been successfully used (Cobbold *et al.*, 2005; Savage *et al.*, 2007), there are several obstacles that need to be solved. For example, the binding affinity threshold for pMHC class I (pMHC-I) tetramers is significantly higher than that required for T cell activation. As a result, pMHC-I tetramers cannot be used to detect all antigen-specific CD8⁺ T cells (Wooldridge *et al.*, 2009; Dolton *et al.*, 2014). Moreover, pMHC multimers can fail for isolation of antigen-specific CD4⁺ T cells due to the lower affinity of

pMHC-II tetramers (Hackett and Sharma, 2002; Wooldridge *et al.*, 2009). In this study, we show for the first time the feasibility to isolate of tumor-specific CTLs from acute myeloid leukemia (AML) patients. First, we have analyzed the dynamics of various binary complexes (pHLA), and their corresponding ternary ones (pHLA-TCR), with a different degree of immune reactivity in order to clarify the interaction of pHLA and TCR at the molecular level. The TAX/HLA-A0201/TCR-A6 was chosen as a model system because it has been extensively studied experimentally. Ding *et al.* were one of the first groups to study these peptides in the context of different T cell signals. They calculated the binding thermodynamics of three structures of HLA-A2/TCR-A6 complexes containing singly substituted variants of the reactive TAX peptide of the human T cell lymphotropic virus HTLV-1, which is known to cause adult T-cell leukemia/lymphoma. Their work provided direct evidence that the capacity of variant TAX peptides (V7R, P6A and Y8A) to produce different biological effects upon interaction with the TCR-A6 is correlated with the strength of the interaction pMHC-TCR (Ding *et al.*, 1998; Ding *et al.*, 1999). T cell assays demonstrated that TAX peptide induces specific lysis, secretion of INF- γ and macrophage inflammatory protein 1 β (MIP-1 β), while P6A and Y8A peptides do not. The complex between TAX-HLA and TCR shows a low

dissociation constant and V7R-TAX shows a ten-fold decrease in the affinity and, finally, P6A and Y8A complexes are too weak to be analyzed by biophysical methods suggesting that long pMHC-TCR half-lives correlate tightly with agonist signals that induces T cell activation. Our data demonstrate that pHLA-TCR interactions that involve reactive peptides are more stable and strong compared to non-reactive interactions. As shown in section 1 (Part I) molecular dynamics enable us to discern patterns of salt bridges, in pHLA and pHLA-TCR complexes that differ according to the reactivity of the complex. Thus, we note a significant loss of salt bridges in the non-reactive ternary complexes relative to the reactive complex: reactive complex TAX-HLA-TCR (13 salt bridges) > intermediate complex V7R-HLA-TCR (10 salt bridges) > non-reactive complexes P6A-HLA-TCR and Y8A-HLA-TCR (5 and 7 salt bridges, respectively). This may explain why the interaction between HLA and TCR is weaker in non-reactive complexes than in the reactive ones. Taking this data into consideration, we sought to take advantage of this stable and strong interaction and isolate tumor-specific CTLs through FACS-based cell sorting. In fact, we observe that when T cells from AML patients are co-cultured with tumor cells, doublet population appears. This population consists of T cells bound with strong interactions to tumor cells. Following the sorting strategy explained in material and methods (section 4.4),

we were able to isolate tumor-specific CTLs from AML patients. These AML-specific CTLs have shown cytolytic activity against primary blast cells suggesting the potential use of these CTLs in the clinical setting. Further, not only CD8+ tumor-reactive T cells are isolated with this approach, but also CD4+ effector T cells. Although CD4+ T cells are classically viewed as helper cells facilitating CD8+ T cell function, it is now clear that both cell subsets can exert cytotoxicity against tumor targets (Restifo *et al.*, 2012; Bollard and Barrett, 2014). Moreover, we have demonstrated that selecting doublet-forming T cells, we are depleting regulatory T cells with immune suppressive function from the pool of patient's T cells. Altogether, "Doublet Technology" allows us to identify and isolate tumor-specific T cells from patients diagnosed with hematologic malignancies and warrant further studies to investigate the safety and efficacy of this new strategy to treat hematologic malignancies.

2. CAR Technology to Generate Tumor-reactive T cells from Multiple Myeloma Patients

The abilities of T cells to coordinate immunity and to deliver lethal hits against diseased cells can be directed towards tumors by genetically modifying T cells. Genes encoding tumor specific antigens can be inserted into T cells to enable them to recognize and respond to cancer cells. CAR technology may solve the problems that conventional approaches for obtaining tumor-specific T cells present. In this study, we create a second generation CAR against the tumor B-Cell Maturation Antigen (BCMA) by genetic modification of T cells to treat multiple myeloma (MM) patients. A critical factor for any antigen being considered as a target for immunotherapies is the expression pattern of the antigen in normal tissues. Therefore, we first confirmed the expression of BCMA on malignant cells of myeloma patients and on myeloma cell lines and verified the absence of BCMA expression on hematopoietic stem cells (HSC), in agreement with other works (Laabi *et al.*, 1992; Novak *et al.*, 2004). We designed CARs with different recognition domains targeting the same BCMA epitope. Each of these CAR constructs was tested as two different versions (short and long) to study the effect of the CAR design in the functionality. Several studies have already suggested the importance to tailor the

extracellular spacer domain of every CAR individually for different target molecules and epitopes (Hudecek *et al.*, 2015). While the recognition domain is critical for CAR specificity, the connecting sequence between the recognition domain and the transmembrane domain (the hinge region), can also profoundly affect CAR T-cell function by producing differences in the length and flexibility of the resulting CAR (Dotti *et al.*, 2014). A study of CD22-specific CARs suggested that the distance of the target epitope from the cell membrane plays an important role in CAR design (Haso *et al.*, 2013). This theory is supported by the observation that tumor recognition by 5T4- and NCAM-specific CARs that recognize membrane-proximal epitopes was improved with a long spacer (Guest *et al.*, 2005). Therefore, we tested two different versions of the hinge region, one short version consisting of the IgG4 hinge domain (12 AA, short spacer) and one long version containing the IgG4 hinge-CH2-CH3 domain (229 AA, long spacer). We could find that our BCMA-specific CARs showed more potent and efficient killing of myeloma cells when they were designed with the long spacer. This result matches with the fact that BCMA-CARs recognize a membrane-proximal epitope (24 - 41 AA) of the extracellular domain of BCMA. In addition, the extracellular domain of BCMA is very short (54 AA) compared to others proteins (CD19:

272 AA; CD20: 668 AA) so that the long spacer of BCMA CAR offers better flexibility to access the target. One further important point in the design of a CAR is the costimulatory domain. Although both CD28 and 41BB costimulatory domains augment cytokine secretion compared to first-generation CARs, several studies have already shown that the incorporation of 4-1BB signaling domain in second-generation CARs prevent anergy and promote T cell proliferation and memory, with the anticipation of a greater effect on T cell maintenance than on functional activation compared to CD28 (Kalos *et al.*, 2011; van der Stegen *et al.*, 2015; Kawalekar *et al.*, 2016). Hence, we incorporated the 4-1BB costimulatory domain into BCMA CARs. The functional tests show that T cells expressing BCMA CARs 30 and 50 designed with a long spacer have potent antitumor effect against myeloma cell lines, show antigen-specific INF- γ and IL-2 release as well as proliferative capacity. Our BCMA CARs were compared to a recently published BCMA CAR (Ali *et al.*, 2016) and they present similar cytolytic activity, cytokine production and proliferation *in vitro* (data not shown). The presence of soluble target protein in the serum of MM patients promotes controversial issues due to the possibility to abrogate the functionality of CARs. Therefore, we analyzed the serum of MM patients to study the presence of soluble BCMA (sBCMA) protein. Soluble BCMA was detected and, in fact, it did correlate with

disease status. Thus, serum BCMA levels are higher among patients with progressive disease as compared to those with responsive disease confirming a positive correlation between sBCMA concentration and disease burden. This conclusion is in agreement with the previous report by Sanchez *et al.* (Sanchez *et al.*, 2012). In addition to CAR affinity, function can be also affected by soluble antigen proteins (Cartellieri *et al.*, 2010). Hence, we determined whether the sBCMA could abrogate the anti-myeloma function of BCMA CAR T cells using a synthetic sBCMA protein and/or supernatant containing released sBCMA. Cytotoxic activity in the presence of high concentration of sBCMA (150 ng/ml, which is 10x more than the concentration observed in patients with progressive disease) shows that soluble protein does not abrogate the cytolytic function of BCMA CARs. We also consider the hypothesis that sBCMA could aggregate BCMA CAR T cells triggering unspecific CAR activation. Thus, CD69+CD25+ T cells and INF- γ release were analyzed in the presence of increasing amount of sBCMA and without antigen-specific target cells. No activation of BCMA CAR T cells or INF- γ release were detected even at the highest amount of sBCMA (150 ng/ml) suggesting that sBCMA does not interfere with BCMA CAR T cells *in vitro*. One possible explanation for these results is that sBCMA is part of

homodimeric or heterodimeric complexes so that the target epitope of the soluble protein is not accessible. sBCMA has a molecular weight (MW) of ≈ 6 kDa demonstrated by western blot analysis. This is consistent with the previous report by Laurent *et al.* (Laurent *et al.*, 2015). Non-reducing western blot analyses also revealed ≈ 12 kDa band suggesting that sBCMA can form homodimeric complexes. In this regard, it has been already reported that sBCMA can form large complexes with APRIL (a proliferation-inducing ligand, (Hymowitz *et al.*, 2005) and BAFF (B-cell activating factor, (Liu *et al.*, 2003) supporting the idea that the target epitope of sBCMA could be hidden so that the functionality of BCMA CARs is not affected. This fact is also seen in other CARs. *In vitro* studies have shown that anti-carcinoembryonic antigen (anti-CEA) CARs are not inhibited by soluble CEA, even at high concentrations (Hombach *et al.*, 1999; Gilham *et al.*, 2002). Finally, we developed a systemic BCMA+ myeloma xenograft model (NSG/MM1.S-ffluc) to study the BCMA CARs function *in vivo*. A potent antitumor effect was mediated by a single dose of BCMA CAR T cells. Collectively, we are able to generate BCMA CARs that eradicate myeloma cells *in vitro* and *in vivo* and warrant clinical trials to investigate the safety and efficacy of this approach to treat MM patients.

3. Clinical Translation

Adoptive transfer of tumor-reactive cytotoxic T cells is a promising therapeutic approach for cancer treatment. To develop this strategy, it is necessary to obtain tumor cytotoxic T lymphocytes (CTLs) that will be reinfused into the patient after expansion *in vitro*. Here, we present two strategies to obtain tumor-specific T cells.

“Doublet Technology” is a personalized therapy. With this technique, we can obtain tumor-specific T cells from hematologic patients, being the equivalent of TIL in solid tumor. The protocol starts obtaining tumor cells from patients either at diagnosed or after relapse and freezing down. After chemotherapy regimens and when the patient achieves the complete remission status, peripheral blood is extracted. Once the co-culture between PBMC and tumor cells is performed, tumor-specific T cells can be sorted in 15 hours. Those T cells have the advantage that they are already cytotoxic tumor-specific T cells so that they can be directly and rapidly expanded with IL2 or soluble anti-CD3/anti-CD28 without a selection step like measure of INF- γ , which is usually needed in TIL therapy (Restifo *et al.*, 2012). Therefore, “Doublet Technology” is a fast, cost-effective approach to obtain tumor-reactive T cells. The principal advantage of this strategy is that

there is no need for a priori knowledge of exact tumor antigen, emphasizing the broadly applicability of this technology. Moreover, we isolate not only CD8+ tumor-reactive T cells, but also CD4+ tumor-reactive T cells, which are also important in tumor eradication (Restifo *et al.*, 2012; Bollard and Barrett, 2014). One disadvantage is the variability between patients, but this is an assumed factor in cell therapies. Recently, the existence of marrow-infiltrating lymphocytes (MIL) and their use in MM patients has been reported, supporting our approach for tumor-specific T cell sorting. In fact, “Doublet Technology” presents the advantage to obtain tumor-specific CTLs from peripheral blood, without bone marrow aspiration surgery which might also be a potential source of CTL using our technology. Several works have reported that the bone marrow is a reservoir for regulatory T cells (Tregs) (Zou *et al.*, 2004). Taking this result in consideration and combine with the fact that we are able to deplete Tregs from the pool of tumor-specific T cells, “Doublet technology” is presented as a safe strategy.

CAR T-cell Therapy is a transformative novel way for treating advanced malignancies. In fact, CAR Therapy has been reached successful results in hematologic malignancies. The clinical protocol is the standard in gene-modified therapies (Turtle *et al.*, 2012). The principal advantage of this strategy is the specificity.

Compared with natural TCRs, CARs have several orders of magnitude higher affinities to target antigens that make them more potent in tumor eradication (Harris and Kranz, 2016). In addition, CARs recognize intact cell surface proteins in an MHC-independent manner, so that they are insensitive to tumor escape mechanisms related to MHC loss variants. Compared to “Doublet Technology”, CAR Therapy presents higher reproducibility; however, it is necessary to know the tumor antigen a priori. Moreover, with this strategy we are able to select the specific subset of T cells which would be engineered and infused into the patient. In this study, we used CARs targeting the BCMA antigen. BCMA is expressed on malignant plasma cells in MM and is an attractive target for immunotherapy due to its absent expression on normal tissues, except normal B-cells. Thus, low on-target off-tumor toxicity should be expected. Finally, therapeutically relevant CAR T-cell numbers could be obtained for the clinical setting with our CAR-based approach.

In conclusion, our developed strategies pave the way for broader and advanced clinical application of T-cell therapies for the treatment of hematologic malignancies.

4. Final remarks and Further Work

“Doublet technology” is a new procedure to obtain tumor-specific T cells for clinical implementation in cancer immunotherapy. There is no need for a priori knowledge of exact tumor antigen, emphasizing the broadly applicability of this technology. However, the identification of new tumor antigens is needed for the development of therapeutic strategies against cancer. Thus, we could sequence and clone the region CDR3 of the tumor-reactive CTLs isolated and, through a mathematical model, to identify the antigens or groups of antigens against which the cytotoxic antitumor response is generated. Moreover, TCR sequence of these natural tumor-reactive CTLs can be used to redirect lymphocyte specificity to cancer antigens by genetic engineering.

CAR T cell therapy is a highly innovative and very potent new modality for treating advanced malignancies. However, it has been documented that targeting a single antigen on tumor cells with CAR T cells may lead to the selection and outgrowth of tumor cells that have learnt to lose that antigen (antigen-loss as escape mechanism). To reduce the risk of antigen loss, we could explore the concomitant targeting of two tumor-specific antigens and investigate whether simultaneous targeting of these two antigens is advantageous compared to targeting each antigen alone.

CONCLUSIONS

“Doublet Technology”

1. pHLA-TCR interactions that involve immune reactive complexes are more stable and strong as compared to those which do not induce immune activation.
2. The complex T cell-tumor cell occurs at sufficient frequency and shows enough functional avidity that can be isolated by FACS-based cell sorting.
3. Tumor-reactive T cells from AML patients can be identified and isolated based on their capability to form stable and strong interactions through TCR with tumor cells.
4. The CTLs from AML patients obtained with “Doublet Technology” show cytolytic activity against blast cells.
5. Using this approach, there is no need to know a priori the exact tumor antigen; therefore, we might be able to obtain tumor-specific T cells from each patient offering a personalized therapy.

CAR Technology

1. BCMA is highly expressed on myeloma cells and T cells can be genetically modified with BCMA-specific CARs.
2. A long spacer domain confers higher anti-myeloma function to BCMA CARs.
3. BCMA CAR T cells show antigen-specific cytolytic activity, production of cytokines, as well as productive proliferation against myeloma cells.
4. Serum from MM patients contains soluble BCMA protein which is correlated positively with disease status.
5. Soluble BCMA does not abrogate the efficacy of BCMA CAR T cells indicating the potential use of these T cells in the clinical setting.

REFERENCES

- Ali, S. A., V. Shi, I. Maric, M. Wang, D. F. Stroncek, J. J. Rose, J. N. Brudno, M. Stetler-Stevenson, S. A. Feldman, B. G. Hansen, V. S. Fellowes, F. T. Hakim, R. E. Gress and J. N. Kochenderfer (2016). "T cells expressing an anti-B-cell maturation antigen chimeric antigen receptor cause remissions of multiple myeloma." Blood 128(13): 1688-1700.
- Andersson, L. C., K. Nilsson and C. G. Gahmberg (1979). "K562--a human erythroleukemic cell line." Int J Cancer 23(2): 143-147.
- Aroca, A., A. Diaz-Quintana and I. Diaz-Moreno (2011). "A structural insight into the C-terminal RNA recognition motifs of T-cell intracellular antigen-1 protein." Febs Letters 585(19): 2958-2964.
- Baxevanis, C. N. and M. Papamichail (2004). "Targeting of tumor cells by lymphocytes engineered to express chimeric receptor genes." Cancer Immunol Immunother 53(10): 893-903.
- Becker, C., H. Pohla, B. Frankenberger, T. Schuler, M. Assenmacher, D. J. Schendel and T. Blankenstein (2001). "Adoptive tumor therapy with T lymphocytes enriched through an IFN-gamma capture assay." Nat Med 7(10): 1159-1162.
- Berendsen, H. J. C., J. P. M. Postma, W. F. Vangunsteren, A. Dinola and J. R. Haak (1984). "Molecular-Dynamics with Coupling to an External Bath." Journal of Chemical Physics 81(8): 3684-3690.
- Berman, H. M., T. Battistuz, T. N. Bhat, W. F. Bluhm, P. E. Bourne, K. Burkhardt, L. Iype, S. Jain, P. Fagan, J. Marvin, D. Padilla, V. Ravichandran, B. Schneider, N. Thanki, H. Weissig, J. D. Westbrook and C. Zardecki (2002). "The Protein Data Bank." Acta Crystallographica Section D-Biological Crystallography 58: 899-907.
- Besser, M. J., R. Shapira-Frommer, A. J. Treves, D. Zippel, O. Itzhaki, L. Hershkovitz, D. Levy, A. Kubi, E. Hovav, N. Chermoshniuk, B. Shalmon, I. Hardan, R. Catane, G. Markel, S. Apter, A. Ben-Nun, I. Kuchuk, A. Shimoni, A. Nagler and J. Schachter (2010). "Clinical responses in a phase II study using adoptive transfer of short-term cultured tumor infiltration lymphocytes in metastatic melanoma patients." Clin Cancer Res 16(9): 2646-2655.
- Bollard, C. M. and A. J. Barrett (2014). "Cytotoxic T lymphocytes for leukemia and lymphoma." Hematology Am Soc Hematol Educ Program 2014(1): 565-569.

- Borrello, I. and K. A. Noonan (2016). "Marrow-Infiltrating Lymphocytes - Role in Biology and Cancer Therapy." Front Immunol 7.
- Boyman, O. (2010). "Bystander activation of CD4(+) T cells." Eur J Immunol 40(4): 936-939.
- Brentjens, R. J., I. Riviere, J. H. Park, M. L. Davila, X. Y. Wang, J. Stefanski, C. Taylor, R. Yeh, S. Bartido, O. Borquez-Ojeda, M. Olszewska, Y. Bernal, H. Pegram, M. Przybylowski, D. Hollyman, Y. Usachenko, D. Pirraglia, J. Hosey, E. Santos, E. Halton, P. Maslak, D. Scheinberg, J. Jurcic, M. Heaney, G. Heller, M. Frattini and M. Sadelain (2011). "Safety and persistence of adoptively transferred autologous CD19-targeted T cells in patients with relapsed or chemotherapy refractory B-cell leukemias." Blood 118(18): 4817-4828.
- Brown, C. E., C. L. Wright, A. Naranjo, R. P. Vishwanath, W. C. Chang, S. Olivares, J. R. Wagner, L. Bruins, A. Raubitschek, L. J. Cooper and M. C. Jensen (2005). "Biophotonic cytotoxicity assay for high-throughput screening of cytolytic killing." J Immunol Methods 297(1-2): 39-52.
- Cartellieri, M., M. Bachmann, A. Feldmann, C. Bippes, S. Stamova, R. Wehner, A. Temme and M. Schmitz (2010). "Chimeric antigen receptor-engineered T cells for immunotherapy of cancer." J Biomed Biotechnol 2010: 956304.
- Chmielewski, M., A. A. Hombach and H. Abken (2013). "Antigen-Specific T-Cell Activation Independently of the MHC: Chimeric Antigen Receptor-Redirected T Cells." Front Immunol 4: 371.
- Cobbold, M., N. Khan, B. Pourgheysari, S. Tauro, D. McDonald, H. Osman, M. Assenmacher, L. Billingham, C. Steward, C. Crawley, E. Olavarria, J. Goldman, R. Chakraverty, P. Mahendra, C. Craddock and P. A. Moss (2005). "Adoptive transfer of cytomegalovirus-specific CTL to stem cell transplant patients after selection by HLA-peptide tetramers." J Exp Med 202(3): 379-386.
- Curran, K. J., H. J. Pegram and R. J. Brentjens (2012). "Chimeric antigen receptors for T cell immunotherapy: current understanding and future directions." J Gene Med 14(6): 405-415.
- Davila, M. L., D. C. Bouhassira, J. H. Park, K. J. Curran, E. L. Smith, H. J. Pegram and R. Brentjens (2014). "Chimeric antigen receptors for the adoptive T cell therapy of hematologic malignancies." Int J Hematol 99(4): 361-371.
- Ding, Y. H., B. M. Baker, D. N. Garboczi, W. E. Biddison and D. C. Wiley (1999). "Four A6-TCR/peptide/HLA-A2 structures that

- generate very different T cell signals are nearly identical." Immunity 11(1): 45-56.
- Ding, Y. H., K. J. Smith, D. N. Garboczi, U. Utz, W. E. Biddison and D. C. Wiley (1998). "Two human T cell receptors bind in a similar diagonal mode to the HLA-A2/Tax peptide complex using different TCR amino acids." Immunity 8(4): 403-411.
- Dolton, G., A. Lissina, A. Skowera, K. Ladell, K. Tungatt, E. Jones, D. Kronenberg-Versteeg, H. Akpovwa, J. M. Pentier, C. J. Holland, A. J. Godkin, D. K. Cole, M. A. Neller, J. J. Miles, D. A. Price, M. Peakman and A. K. Sewell (2014). "Comparison of peptide-major histocompatibility complex tetramers and dextramers for the identification of antigen-specific T cells." Clin Exp Immunol 177(1): 47-63.
- Dotti, G., S. Gottschalk, B. Savoldo and M. K. Brenner (2014). "Design and development of therapies using chimeric antigen receptor-expressing T cells." Immunol Rev 257(1): 107-126.
- Dudley, M. E., C. A. Gross, M. M. Langhan, M. R. Garcia, R. M. Sherry, J. C. Yang, G. Q. Phan, U. S. Kammula, M. S. Hughes, D. E. Citrin, N. P. Restifo, J. R. Wunderlich, P. A. Prieto, J. J. Hong, R. C. Langan, D. A. Zlott, K. E. Morton, D. E. White, C. M. Laurencot and S. A. Rosenberg (2010). "CD8+ enriched "young" tumor infiltrating lymphocytes can mediate regression of metastatic melanoma." Clin Cancer Res 16(24): 6122-6131.
- Dudley, M. E., J. C. Yang, R. Sherry, M. S. Hughes, R. Royal, U. Kammula, P. F. Robbins, J. Huang, D. E. Citrin, S. F. Leitman, J. Wunderlich, N. P. Restifo, A. Thomasian, S. G. Downey, F. O. Smith, J. Klapper, K. Morton, C. Laurencot, D. E. White and S. A. Rosenberg (2008). "Adoptive cell therapy for patients with metastatic melanoma: evaluation of intensive myeloablative chemoradiation preparative regimens." J Clin Oncol 26(32): 5233-5239.
- Fabre, J. W. (2001). "The allogeneic response and tumor immunity." Nat Med 7(6): 649-652.
- Garboczi, D. N., P. Ghosh, U. Utz, Q. R. Fan, W. E. Biddison and D. C. Wiley (1996). "Structure of the complex between human T-cell receptor, viral peptide and HLA-A2." Nature 384(6605): 134-141.
- Gattinoni, L., S. E. Finkelstein, C. A. Klebanoff, P. A. Antony, D. C. Palmer, P. J. Spiess, L. N. Hwang, Z. Yu, C. Wrzesinski, D. M. Heimann, C. D. Surh, S. A. Rosenberg and N. P. Restifo (2005). "Removal of homeostatic cytokine sinks by lymphodepletion enhances the efficacy of adoptively

- transferred tumor-specific CD8+ T cells." J Exp Med 202(7): 907-912.
- Gazdar, A. F., H. K. Oie, I. R. Kirsch and G. F. Hollis (1986). "Establishment and characterization of a human plasma cell myeloma culture having a rearranged cellular myc proto-oncogene." Blood 67(6): 1542-1549.
- Geukes Foppen, M. H., M. Donia, I. M. Svane and J. B. Haanen (2015). "Tumor-infiltrating lymphocytes for the treatment of metastatic cancer." Mol Oncol 9(10): 1918-1935.
- Gilham, D. E., A. O'Neil, C. Hughes, R. D. Guest, N. Kirillova, M. Lehan and R. E. Hawkins (2002). "Primary polyclonal human T lymphocytes targeted to carcino-embryonic antigens and neural cell adhesion molecule tumor antigens by CD3 zeta-based chimeric immune receptors." Journal of Immunotherapy 25(2): 139-151.
- Gill, S. and M. Kalos (2013). "T cell-based gene therapy of cancer." Transl Res 161(4): 365-379.
- Greenstein, S., N. L. Krett, Y. Kurosawa, C. Ma, D. Chauhan, T. Hideshima, K. C. Anderson and S. T. Rosen (2003). "Characterization of the MM.1 human multiple myeloma (MM) cell lines: a model system to elucidate the characteristics, behavior, and signaling of steroid-sensitive and -resistant MM cells." Exp Hematol 31(4): 271-282.
- Guest, R. D., R. E. Hawkins, N. Kirillova, E. J. Cheadle, J. Arnold, A. O'Neill, J. Irlam, K. A. Chester, J. T. Kemshead, D. M. Shaw, M. J. Embleton, P. L. Stern and D. E. Gilham (2005). "The role of extracellular spacer regions in the optimal design of chimeric immune receptors - Evaluation of four different scFvs and antigens." Journal of Immunotherapy 28(3): 203-211.
- Hackett, C. J. and O. K. Sharma (2002). "Frontiers in peptide-MHC class II multimer technology." Nat Immunol 3(10): 887-889.
- Han, E. Q., X. L. Li, C. R. Wang, T. F. Li and S. Y. Han (2013). "Chimeric antigen receptor-engineered T cells for cancer immunotherapy: progress and challenges." J Hematol Oncol 6: 47.
- Harris, D. T. and D. M. Kranz (2016). "Adoptive T Cell Therapies: A Comparison of T Cell Receptors and Chimeric Antigen Receptors." Trends Pharmacol Sci 37(3): 220-230.
- Haso, W., D. W. Lee, N. N. Shah, M. Stetler-Stevenson, C. M. Yuan, I. H. Pastan, D. S. Dimitrov, R. A. Morgan, D. J. Fitzgerald, D. M. Barrett, A. S. Wayne, C. L. Mackall and R. J. Orentas (2013). "Anti-CD22-chimeric antigen receptors targeting B-cell precursor acute lymphoblastic leukemia." Blood 121(7): 1165-1174.

- Hombach, A., D. Koch, R. Sircar, C. Heuser, V. Diehl, W. Kruis, C. Pohl and H. Abken (1999). "A chimeric receptor that selectively targets membrane-bound carcinoembryonic antigen (mCEA) in the presence of soluble CEA." Gene Ther 6(2): 300-304.
- Hudecek, M., M. T. Lupo-Stanghellini, P. L. Kosasih, D. Sommermeyer, M. C. Jensen, C. Rader and S. R. Riddell (2013). "Receptor affinity and extracellular domain modifications affect tumor recognition by ROR1-specific chimeric antigen receptor T cells." Clin Cancer Res 19(12): 3153-3164.
- Hudecek, M., D. Sommermeyer, P. L. Kosasih, A. Silva-Benedict, L. Liu, C. Rader, M. C. Jensen and S. R. Riddell (2015). "The nonsignaling extracellular spacer domain of chimeric antigen receptors is decisive for in vivo antitumor activity." Cancer Immunol Res 3(2): 125-135.
- Hymowitz, S. G., D. R. Patel, H. J. A. Wallweber, S. Runyon, M. H. Yan, J. P. Yin, S. K. Shriver, N. C. Gordon, B. L. Pan, N. J. Skelton, R. F. Kelley and M. A. Starovasnik (2005). "Structures of APRIL-receptor complexes - Like BCMA, TACI employs only a single cysteine-rich domain for high affinity ligand binding." Journal of Biological Chemistry 280(8): 7218-7227.
- Itzhaki, O., E. Hovav, Y. Ziporen, D. Levy, A. Kubi, D. Zikich, L. Hershkovitz, A. J. Treves, B. Shalmon, D. Zippel, G. Markel, R. Shapira-Frommer, J. Schachter and M. J. Besser (2011). "Establishment and large-scale expansion of minimally cultured "young" tumor infiltrating lymphocytes for adoptive transfer therapy." J Immunother 34(2): 212-220.
- Jorgensen, W. L., J. Chandrasekhar, J. D. Madura, R. W. Impey and M. L. Klein (1983). "Comparison of Simple Potential Functions for Simulating Liquid Water." Journal of Chemical Physics 79(2): 926-935.
- Junker, N., M. H. Andersen, L. Wenandy, S. L. Dombernowsky, K. Kiss, C. H. Sorensen, M. H. Therkildsen, C. Von Buchwald, E. Andersen, P. T. Straten and I. M. Svane (2011). "Bimodal ex vivo expansion of T cells from patients with head and neck squamous cell carcinoma: a prerequisite for adoptive cell transfer." Cytotherapy 13(7): 822-834.
- Kalos, M., B. L. Levine, D. L. Porter, S. Katz, S. A. Grupp, A. Bagg and C. H. June (2011). "T Cells with Chimeric Antigen Receptors Have Potent Antitumor Effects and Can Establish Memory in Patients with Advanced Leukemia." Sci Transl Med 3(95).

- Katagiri, S., T. Yonezawa, J. Kuyama, Y. Kanayama, K. Nishida, T. Abe, T. Tamaki, M. Ohnishi and S. Tarui (1985). "Two distinct human myeloma cell lines originating from one patient with myeloma." Int J Cancer 36(2): 241-246.
- Kawalekar, O. U., R. S. O'Connor, J. A. Fraietta, L. Guo, S. E. McGettigan, A. D. Posey, P. R. Patel, S. Guedan, J. Scholler, B. Keith, N. Snyder, I. Blair, M. C. Milone and C. H. June (2016). "Distinct Signaling of Coreceptors Regulates Specific Metabolism Pathways and Impacts Memory Development in CAR T Cells." Immunity 44(2): 380-390.
- Kersh, G. J., E. N. Kersh, D. H. Fremont and P. M. Allen (1998). "High- and low-potency ligands with similar affinities for the TCR: the importance of kinetics in TCR signaling." Immunity 9(6): 817-826.
- Kershaw, M. H., J. A. Westwood and P. K. Darcy (2013). "Gene-engineered T cells for cancer therapy." Nat Rev Cancer 13(8): 525-541.
- Kloss, C. C., M. Condomines, M. Cartellieri, M. Bachmann and M. Sadelain (2013). "Combinatorial antigen recognition with balanced signaling promotes selective tumor eradication by engineered T cells." Nat Biotechnol 31(1): 71-+.
- Kochenderfer, J. N., M. E. Dudley, S. A. Feldman, W. H. Wilson, D. E. Spaner, I. Maric, M. Stetler-Stevenson, G. Q. Phan, M. S. Hughes, R. M. Sherry, J. C. Yang, U. S. Kammula, L. Devillier, R. Carpenter, D. A. N. Nathan, R. A. Morgan, C. Laurencot and S. A. Rosenberg (2012). "B-cell depletion and remissions of malignancy along with cytokine-associated toxicity in a clinical trial of anti-CD19 chimeric-antigen-receptor-transduced T cells." Blood 119(12): 2709-2720.
- Kolb, H. J. (2008). "Graft-versus-leukemia effects of transplantation and donor lymphocytes." Blood 112(12): 4371-4383.
- Kolb, H. J., A. Schattenberg, J. M. Goldman, B. Hertenstein, N. Jacobsen, W. Arcese, P. Ljungman, A. Ferrant, L. Verdonck, D. Niederwieser, F. van Rhee, J. Mittermueller, T. de Witte, E. Holler and H. Ansari (1995). "Graft-versus-leukemia effect of donor lymphocyte transfusions in marrow grafted patients." Blood 86(5): 2041-2050.
- Krogsgaard, M., N. Prado, E. J. Adams, X. L. He, D. C. Chow, D. B. Wilson, K. C. Garcia and M. M. Davis (2003). "Evidence that structural rearrangements and/or flexibility during TCR binding can contribute to T cell activation." Mol Cell 12(6): 1367-1378.

- Kumar, S. G. (2012). "Principles of cancer treatment by immunotherapy." Surgery 30(4): 198–202.
- Laabi, Y., M. P. Gras, F. Carbonnel, J. C. Brouet, R. Berger, C. J. Larsen and A. Tsapis (1992). "A New Gene, Bcm, on Chromosome-16 Is Fused to the Interleukin-2 Gene by a T(4-16)(Q26-P13) Translocation in a Malignant T-Cell Lymphoma." Embo Journal 11(11): 3897-3904.
- Lamers, C. H. J., S. Sleijfer, S. van Steenbergen, P. van Elzakker, B. van Krimpen, C. Groot, A. Vulto, M. den Bakker, E. Oosterwijk, R. Debets and J. W. Gratama (2013). "Treatment of Metastatic Renal Cell Carcinoma With CAIX CAR-engineered T cells: Clinical Evaluation and Management of On-target Toxicity." Molecular Therapy 21(4): 904-912.
- Laurent, S. A., F. S. Hoffmann, P. H. Kuhn, Q. Y. Cheng, Y. Y. Chu, M. Schmidt-Supprian, S. M. Hauck, E. Schuh, M. Krumbholz, H. Rubsamen, J. Wanjgren, M. Khademi, T. Olsson, T. Alexander, F. Hiepe, H. W. Pfister, F. Weber, D. Jenne, H. Wekerle, R. Hohlfeld, S. F. Lichtenthaler and E. Meinel (2015). "gamma-secretase directly sheds the survival receptor BCMA from plasma cells." Nat Commun 6.
- Linette, G. P., E. A. Stadtmauer, M. V. Maus, A. P. Rapoport, B. L. Levine, L. Emery, L. Litzky, A. Bagg, B. M. Carreno, P. J. Cimino, G. K. Binder-Scholl, D. P. Smethurst, A. B. Gerry, N. J. Pumphrey, A. D. Bennett, J. E. Brewer, J. Dukes, J. Harper, H. K. Tayton-Martin, B. K. Jakobsen, N. J. Hassan, M. Kalos and C. H. June (2013). "Cardiovascular toxicity and titin cross-reactivity of affinity-enhanced T cells in myeloma and melanoma." Blood 122(6): 863-871.
- Liu, Y. F., X. Hong, J. Kappler, L. Jiang, R. G. Zhang, L. G. Xu, C. H. Pan, W. E. Martin, R. C. Murphy, H. B. Shu, S. D. Dai and G. Y. Zhang (2003). "Ligand-receptor binding revealed by the TNF family member TALL-1." Nature 423(6935): 49-56.
- Lyons, D. S., S. A. Lieberman, J. Hampl, J. J. Boniface, Y. Chien, L. J. Berg and M. M. Davis (1996). "A TCR binds to antagonist ligands with lower affinities and faster dissociation rates than to agonists." Immunity 5(1): 53-61.
- Manz, R., M. Assenmacher, E. Pfluger, S. Miltenyi and A. Radbruch (1995). "Analysis and sorting of live cells according to secreted molecules, relocated to a cell-surface affinity matrix." Proc Natl Acad Sci U S A 92(6): 1921-1925.
- Matsui, K., J. J. Boniface, P. Steffner, P. A. Reay and M. M. Davis (1994). "Kinetics of T-cell receptor binding to peptide/I-Ek

- complexes: correlation of the dissociation rate with T-cell responsiveness." Proc Natl Acad Sci U S A 91(26): 12862-12866.
- Maude, S. L., N. Frey, P. A. Shaw, R. Aplenc, D. M. Barrett, N. J. Bunin, A. Chew, V. E. Gonzalez, Z. Zheng, S. F. Lacey, Y. D. Mahnke, J. J. Melenhorst, S. R. Rheingold, A. Shen, D. T. Teachey, B. L. Levine, C. H. June, D. L. Porter and S. A. Grupp (2014). "Chimeric antigen receptor T cells for sustained remissions in leukemia." N Engl J Med 371(16): 1507-1517.
- McGuire, S. (2016). "World Cancer Report 2014. Geneva, Switzerland: World Health Organization, International Agency for Research on Cancer, WHO Press, 2015." Adv Nutr 7(2): 418-419.
- McKeithan, T. W. (1995). "Kinetic proofreading in T-cell receptor signal transduction." Proc Natl Acad Sci U S A 92(11): 5042-5046.
- Morgan, R. A., N. Chinnasamy, D. Abate-Daga, A. Gros, P. F. Robbins, Z. Zheng, M. E. Dudley, S. A. Feldman, J. C. Yang, R. M. Sherry, G. Q. Phan, M. S. Hughes, U. S. Kammula, A. D. Miller, C. J. Hessman, A. A. Stewart, N. P. Restifo, M. M. Quezado, M. Alimchandani, A. Z. Rosenberg, A. Nath, T. Wang, B. Bielekova, S. C. Wuest, N. Akula, F. J. McMahon, S. Wilde, B. Mosetter, D. J. Schendel, C. M. Laurencot and S. A. Rosenberg (2013). "Cancer regression and neurological toxicity following anti-MAGE-A3 TCR gene therapy." J Immunother 36(2): 133-151.
- Morgan, R. A., M. E. Dudley, J. R. Wunderlich, M. S. Hughes, J. C. Yang, R. M. Sherry, R. E. Royal, S. L. Topalian, U. S. Kammula, N. P. Restifo, Z. Zheng, A. Nahvi, C. R. de Vries, L. J. Rogers-Freezer, S. A. Mavroukakis and S. A. Rosenberg (2006). "Cancer regression in patients after transfer of genetically engineered lymphocytes." Science 314(5796): 126-129.
- Novak, A. J., J. R. Darce, B. K. Arendt, B. Harder, K. Henderson, W. Kindsvogel, J. A. Gross, P. R. Greipp and D. F. Jelinek (2004). "Expression of BCMA, TACI, and BAFF-R in multiple myeloma: a mechanism for growth and survival." Blood 103(2): 689-694.
- Panelli, M. C., A. Riker, U. Kammula, E. Wang, K. H. Lee, S. A. Rosenberg and F. M. Marincola (2000). "Expansion of tumor-T cell pairs from fine needle aspirates of melanoma metastases." Journal of Immunology 164(1): 495-504.

- Papaioannou, N. E., O. V. Beniata, P. Vitsos, O. Tsitsilonis and P. Samara (2016). "Harnessing the immune system to improve cancer therapy." Ann Transl Med 4(14): 261.
- Park, J. R., D. L. DiGiusto, M. Slovak, C. Wright, A. Naranjo, J. Wagner, H. B. Meechoovet, C. Bautista, W. C. Chang, J. R. Ostberg and M. C. Jensens (2007). "Adoptive transfer of chimeric antigen receptor re-directed cytolytic T lymphocyte clones in patients with neuroblastoma." Molecular Therapy 15(4): 825-833.
- Parkhurst, M. R., J. C. Yang, R. C. Langan, M. E. Dudley, D. N. Nathan, S. A. Feldman, J. L. Davis, R. A. Morgan, M. J. Merino, R. M. Sherry, M. S. Hughes, U. S. Kammula, G. Q. Phan, R. M. Lim, S. A. Wank, N. P. Restifo, P. F. Robbins, C. M. Laurencot and S. A. Rosenberg (2011). "T Cells Targeting Carcinoembryonic Antigen Can Mediate Regression of Metastatic Colorectal Cancer but Induce Severe Transient Colitis." Mol Ther 19(3): 620-626.
- Perica, K., J. C. Varela, M. Oelke and J. Schneck (2015). "Adoptive T cell immunotherapy for cancer." Rambam Maimonides Med J 6(1): e0004.
- Qi, S. Y., M. Krogsgaard, M. M. Davis and A. K. Chakraborty (2006). "Molecular flexibility can influence the stimulatory ability of receptor-ligand interactions at cell-cell junctions." Proc Natl Acad Sci U S A 103(12): 4416-4421.
- Rabinowitz, J. D., C. Beeson, D. S. Lyons, M. M. Davis and H. M. McConnell (1996). "Kinetic discrimination in T-cell activation." Proc Natl Acad Sci U S A 93(4): 1401-1405.
- Restifo, N. P., M. E. Dudley and S. A. Rosenberg (2012). "Adoptive immunotherapy for cancer: harnessing the T cell response." Nat Rev Immunol 12(4): 269-281.
- Riddell, S. R., D. Sommermeyer, C. Berger, L. S. Liu, A. Balakrishnan, A. Salter, M. Hudecek, D. G. Maloney and C. J. Turtle (2014). "Adoptive therapy with chimeric antigen receptor-modified T cells of defined subset composition." Cancer J 20(2): 141-144.
- Robbins, P. F., R. A. Morgan, S. A. Feldman, J. C. Yang, R. M. Sherry, M. E. Dudley, J. R. Wunderlich, A. V. Nahvi, L. J. Helman, C. L. Mackall, U. S. Kammula, M. S. Hughes, N. P. Restifo, M. Raffeld, C. C. Lee, C. L. Levy, Y. F. Li, M. El-Gamil, S. L. Schwarz, C. Laurencot and S. A. Rosenberg (2011). "Tumor regression in patients with metastatic synovial cell sarcoma and melanoma using genetically engineered lymphocytes reactive with NY-ESO-1." J Clin Oncol 29(7): 917-924.

- Rosenberg, S. A., B. S. Packard, P. M. Aebbersold, D. Solomon, S. L. Topalian, S. T. Toy, P. Simon, M. T. Lotze, J. C. Yang, C. A. Seipp, C. Simpson, C. Carter, S. Bock, D. Schwartzentruber, J. P. Wei and D. E. White (1988). "Use of Tumor-Infiltrating Lymphocytes and Interleukin-2 in the Immunotherapy of Patients with Metastatic Melanoma - a Preliminary-Report." New England Journal of Medicine 319(25): 1676-1680.
- Rosenberg, S. A., N. P. Restifo, J. C. Yang, R. A. Morgan and M. E. Dudley (2008). "Adoptive cell transfer: a clinical path to effective cancer immunotherapy." Nat Rev Cancer 8(4): 299-308.
- Rosenberg, S. A., J. C. Yang, R. M. Sherry, U. S. Kammula, M. S. Hughes, G. Q. Phan, D. E. Citrin, N. P. Restifo, P. F. Robbins, J. R. Wunderlich, K. E. Morton, C. M. Laurencot, S. M. Steinberg, D. E. White and M. E. Dudley (2011). "Durable complete responses in heavily pretreated patients with metastatic melanoma using T-cell transfer immunotherapy." Clin Cancer Res 17(13): 4550-4557.
- Rosenberg, S. A., J. R. Yannelli, J. C. Yang, S. L. Topalian, D. J. Schwartzentruber, J. S. Weber, D. R. Parkinson, C. A. Seipp, J. H. Einhorn and D. E. White (1994). "Treatment of patients with metastatic melanoma with autologous tumor-infiltrating lymphocytes and interleukin 2." J Natl Cancer Inst 86(15): 1159-1166.
- Rosette, C., G. Werlen, M. A. Daniels, P. O. Holman, S. M. Alam, P. J. Travers, N. R. Gascoigne, E. Palmer and S. C. Jameson (2001). "The impact of duration versus extent of TCR occupancy on T cell activation: a revision of the kinetic proofreading model." Immunity 15(1): 59-70.
- Rubio, V., T. B. Stuge, N. Singh, M. R. Betts, J. S. Weber, M. Roederer and P. P. Lee (2003). "Ex vivo identification, isolation and analysis of tumor-cytolytic T cells." Nat Med 9(11): 1377-1382.
- Sanchez, E., M. J. Li, A. Kitto, J. Li, C. S. Wang, D. Rauch, K. Delijani, K. DeCorso, A. Prajogi, H. M. Chen and J. R. Berenson (2012). "Serum Levels of B-Cell Maturation Antigen Are Elevated in Multiple Myeloma Patients and Correlate with Disease Status and Overall Survival." Blood 120(21).
- Savage, P., M. Millrain, S. Dimakou, J. Stebbing and J. Dyson (2007). "Expansion of CD8+ cytotoxic T cells in vitro and in vivo using MHC class I tetramers." Tumour Biol 28(2): 70-76.

- Skokos, D., G. Shakhar, R. Varma, J. C. Waite, T. O. Cameron, R. L. Lindquist, T. Schwickert, M. C. Nussenzweig and M. L. Dustin (2007). "Peptide-MHC potency governs dynamic interactions between T cells and dendritic cells in lymph nodes." Nat Immunol 8(8): 835-844.
- Smith, E. L., D. Zamarin and A. M. Lesokhin (2014). "Harnessing the immune system for cancer therapy." Curr Opin Oncol 26(6): 600-607.
- Snyder, J. E., W. J. Bowers, A. M. Livingstone, F. E. H. Lee, H. J. Federoff and T. R. Mosmann (2003). "Measuring the frequency of mouse and human cytotoxic T cells by the LysisSpot assay: independent regulation of cytokine secretion and short-term killing." Nat Med 9(2): 231-235.
- Stevanovic, S., L. M. Draper, M. M. Langhan, T. E. Campbell, M. L. Kwong, J. R. Wunderlich, M. E. Dudley, J. C. Yang, R. M. Sherry, U. S. Kammula, N. P. Restifo, S. A. Rosenberg and C. S. Hinrichs (2015). "Complete regression of metastatic cervical cancer after treatment with human papillomavirus-targeted tumor-infiltrating T cells." J Clin Oncol 33(14): 1543-1550.
- Till, B. G., M. C. Jensen, J. J. Wang, E. Y. Chen, B. L. Wood, H. A. Greisman, X. J. Qian, S. E. James, A. Raubitschek, S. J. Forman, A. K. Gopal, J. M. Pagel, C. G. Lindgren, P. D. Greenberg, S. R. Riddell and O. W. Press (2008). "Adoptive immunotherapy for indolent non-Hodgkin lymphoma and mantle cell lymphoma using genetically modified autologous CD20-specific T cells." Blood 112(6): 2261-2271.
- Tran, E., S. Turcotte, A. Gros, P. F. Robbins, Y. C. Lu, M. E. Dudley, J. R. Wunderlich, R. P. Somerville, K. Hogan, C. S. Hinrichs, M. R. Parkhurst, J. C. Yang and S. A. Rosenberg (2014). "Cancer immunotherapy based on mutation-specific CD4+ T cells in a patient with epithelial cancer." Science 344(6184): 641-645.
- Turtle, C. J., L. A. Hanafi, C. Berger, T. A. Gooley, S. Cherian, M. Hudecek, D. Sommermeyer, K. Melville, B. Pender, T. M. Budiarto, E. Robinson, N. N. Steevens, C. Chaney, L. Soma, X. Chen, C. Yeung, B. Wood, D. Li, J. Cao, S. Heimfeld, M. C. Jensen, S. R. Riddell and D. G. Maloney (2016). "CD19 CAR-T cells of defined CD4+:CD8+ composition in adult B cell ALL patients." J Clin Invest 126(6): 2123-2138.
- Turtle, C. J., M. Hudecek, M. C. Jensen and S. R. Riddell (2012). "Engineered T cells for anti-cancer therapy." Curr Opin Immunol 24(5): 633-639.

- van der Merwe, P. A. (2001). "The TCR triggering puzzle." Immunity 14(6): 665-668.
- van der Stegen, S. J. C., M. Hamieh and M. Sadelain (2015). "The pharmacology of second-generation chimeric antigen receptors." Nature Reviews Drug Discovery 14(7): 499-509.
- Wang, X., W. C. Chang, C. W. Wong, D. Colcher, M. Sherman, J. R. Ostberg, S. J. Forman, S. R. Riddell and M. C. Jensen (2011). "A transgene-encoded cell surface polypeptide for selection, in vivo tracking, and ablation of engineered cells." Blood 118(5): 1255-1263.
- Welniak, L. A., B. R. Blazar and W. J. Murphy (2007). "Immunobiology of allogeneic hematopoietic stem cell transplantation." Annu Rev Immunol 25: 139-170.
- Wooldridge, L., A. Lissina, D. K. Cole, H. A. van den Berg, D. A. Price and A. K. Sewell (2009). "Tricks with tetramers: how to get the most from multimeric peptide-MHC." Immunology 126(2): 147-164.
- Zhou, G. and H. Levitsky (2012). "Towards curative cancer immunotherapy: overcoming posttherapy tumor escape." Clin Dev Immunol 2012: 124187.
- Zou, L. H., B. Barnett, H. Safah, V. F. LaRussa, M. Evdemon-Hogan, P. Mottram, S. N. Wei, O. David, T. J. Curiel and W. P. Zou (2004). "Bone marrow is a reservoir for CD4(+)CD25(+) regulatory T cells that traffic through CXCL12/CXCR4 signals." Cancer Res 64(22): 8451-8455.

CURRICULUM VITAE

PERSONAL INFORMATION

Family Name: García Guerrero

First Name: Estefanía

Date of Birth: 13/07/1987

ID: 53342158Y

Address: Schiesshausstr. 7a, 97072, Würzburg, Germany

Phone: +49 15163122224

Email: egarcia-ibis@us.es

Garcia_E@ukw.de

EDUCATION

- | | |
|-----------------|---|
| 08/2015-present | PhD student, Department of Medizinische Klinik und Poliklinik II, Universitätsklinikum Würzburg, Germany

PhD thesis: "Strategies to Obtain Tumor-reactive Cells for Cancer Immunotherapy by Cell Sorting and Genetic Modifications of T Lymphocytes" |
| 09/2011-09/2015 | PhD student, Department of Hematology, Cell Therapy and New Therapeutics Targets in Oncohematology Laboratory

Institute of Biomedicine of Seville (IBIS), Spain

PhD thesis: "Strategies to Obtain Tumor-reactive Cells for Cancer Immunotherapy by Cell Sorting and Genetic Modifications of T Lymphocytes" |

09/2005-07/2010 Bachelor Degree of Biotechnology, Pablo de Olavide
University, Seville

09/2010-09/2011 Master Degree of Biomedical Investigation, Seville
University, Seville

RESEARCH AND PROFESSIONAL EXPERIENCE

2007/2008 Demonstrator in Practical Lessons. Pablo de Olavide University

2008/2009 Student Fellow. Consejo Superior de Investigaciones Científicas

2012-2016 Research grant. The Spanish Ministry of Health

FELLOWSHIPS AND AWARDS

Pre-doctoral fellowship from the Spanish Ministry of Health, program “Beca pre-doctoral de Formación en Investigación en Salud, PFIS” (2012/2016)

ACREDITATIONS

“Laboratory Animal Science” researcher level B

PARTICIPATION IN RESEARCH PROJECTS

Title: Tratamiento de EICH refractaria a primera línea de tratamiento con infusión secuencial de células mesenquimales alogénicas expandidas in vitro

Funding organisation: CONSEJERIA DE SALUD Y BIENESTAR SOCIAL, JUNTA DE ANDALUCIA (2012/2015)

Principal Investigator: Teresa Caballero Velázquez

Title: Recuperación inmune celular T específica como guía para el tratamiento de la infección por citomegalovirus en receptores de trasplante hematopoyético

Funding organisation: INSTITUTO DE SALUD CARLOS III (2012/2015)

Principal Investigator: Ildelfonso Espigado Tocino

Title: Nuevas estrategias terapeuticas en pacientes con leucemia aguda mieloblastica: cannabinoides y terapia celular

Funding organisation: Ministerio de Ciencia e Innovación, Fondo de Investigación Sanitaria: INSTITUTO DE SALUD CARLOS III, 2014

Principal Investigator: José Antonio Pérez Simón

PUBLICATIONS

García-Guerrero E, Gogishvili T, Danhof S, Schreder M, Pallaud C, Pérez-Simón JA, Einsele H, Hudecek M. Panobinostat induces CD38 upregulation and augments the anti-myeloma efficacy of daratumumab. *Blood*. 2017 May 5. pii: blood-2017-03-770776. doi: 10.1182/blood-2017-03-770776. [Epub ahead of print]

Barbado MV, Medrano M, Caballero-Velázquez T, Álvarez-Laderas I, Sánchez-Abarca LI, García-Guerrero E, Martín-Sánchez J, Rosado IV, Piruat JI, Gonzalez-Naranjo P, Campillo NE, Páez JA, Pérez-Simón JA. Cannabinoid derivatives exert a potent anti-myeloma activity both in vitro and in vivo. *Int J Cancer*. 2017 Feb 1;140(3):674-685. doi: 10.1002/ijc.30483. Epub 2016 Nov 10.

García-Guerrero E, Pérez-Simón JA, Sánchez-Abarca LI, Díaz-Moreno I, De la Rosa MA, Díaz-Quintana A. *Antigen-dependent Changes in the Major Histocompatibility Complex Head Domain and their Implications for Immune Recognition*. *PLoS One*. 2016 Apr 28;11(4):e0154219. doi: 10.1371/journal.pone.0154219. **(Directly originating from the thesis)**

Báez A, Piruat JI, Caballero-Velázquez T, Sánchez-Abarca LI, Álvarez-Laderas I, Barbado MV, García-Guerrero E, Millán-Uclés Á, Martín-Sánchez J, Medrano M, Pérez-Simón JA. *Myelomatous plasma cells display an aberrant gene expression pattern similar to that observed in normal memory B cells*. *Am J Cancer Res*. 2014 Dec 15;5(1):386-95. eCollection 2015.

Báez A, Alvarez-Laderas I, Piruat JI, Caballero-Velázquez T, Barbado MV, Millán-Uclés A, Medrano M, García-Guerrero E, Sánchez-Abarca L, Pérez-Simón JA. Title: *The CD27+ memory B cells display changes in the gene expression pattern in elderly individuals*. *Immunology*. 2014 Sep 6. doi: 10.1111/imm.12381.

Sánchez-Abarca LI, Alvarez-Laderas I, Díez Campelo M, Caballero-Velázquez T, Herrero C, Muntión S, Calderón C, García-Guerrero E, Sánchez-Guijo F, Del Cañizo C, San Miguel J, Pérez-Simón JA. *Uptake and delivery of antigens by mesenchymal stromal cells*. Cytotherapy. 2013 Jun;15(6):673-8

PATENTS

Procedimiento para la selección de linfocitos T antígeno-específicos mediante la identificación de dobletes.

Procedure for the selection of antigen-specific T lymphocytes by the identification of doublets.

Ref: 153 178 CHB

Número solicitud: P201231848

Inventors: Jose Antonio Pérez Simón, L. Ignacio Sanchez-Abarca, Estefanía García Guerrero

CONGRESSES AND MEETINGS

Estefanía García-Guerrero, Antonio Díaz Quintana, LI Sánchez-Abarca, Teresa Caballero-Velázquez, José I. Piruat, Isabel Álvarez-Laderas, Alicia Báez, África Millán-Uclés, M.V Barbado y José Antonio Pérez-Simón

Oral presentation: La Dinámica Molecular como herramienta computacional para estudiar la aloreactividad linfocitaria en pacientes sometidos a trasplante hematopoyético

Nacional Congress SETH -Seville 2013

Estefanía García-Guerrero, Irene Díaz Moreno, Miguel A. De la Rosa, José Antonio Pérez-Simón and Antonio Díaz Quintana

Poster presentation: Molecular Dynamics as a Computational Tool to Analyze Lymphocyte Alloreactivity in Hematopoietic Transplant Recipients

ASH Annual Meeting - American Society of Hematology (New Orleans) 2013

E García-Guerrero; A Díaz Quintana; LI Sánchez-Abarca; JI Piruat; T Caballero-Velázquez; MV Barbado; I Álvarez-Laderas; M Medrano, A Millán-Uclés y JA Pérez-Simón

Oral presentation: La dinámica molecular como herramienta computacional para estudiar la reactividad inmune: Identificación de cambios conformacionales en el complejo mayor de histocompatibilidad

Nacional Congress SETH -Madrid 2014

Estefanía García-Guerrero, José Antonio Pérez-Simón, Luis Ignacio Sánchez-Abarca, Irene Díaz Moreno, Miguel A. De la Rosa, and Antonio Díaz Quintana

Poster presentation: Molecular Dynamics as a Computational Tool to Study the Immune Reactivity: Identification of Conformational Changes in the Major Histocompatibility Complex

ASH Annual Meeting - American Society of Hematology -San Francisco 2014

Estefania Garcia-Guerrero, Sophia Danhof, Jose-Antonio Perez-Simon, Hermann Einsele, Michael Hudecek, Tea Gogishvili.

Oral presentation: Engineering of chimeric antigen receptor (CAR)-modified T cells targeting B-cell maturation antigen (BCMA) for immunotherapy of multiple myeloma

II Seville Molecular Medicine Workshop "Cell Therapy, Molecular Mechanisms and Clinical Translation"-Seville 2016

Estefanía García-Guerrero, Tea Gogishvili, Sophia Danhof, Martin Schreder, Celine Pallaud, Jose Antonio Pérez-Simón, Hermann Einsele and Michael Hudecek

Poster presentation: Panobinostat Induces Upregulation of CD38 and Augments the Anti-Myeloma Efficacy of Daratumumab in Pre-Clinical Models

ASH Annual Meeting - American Society of Hematology -San Diego 2016

Estefanía García-Guerrero, Tea Gogishvili, Sophia Danhof, Martin Schreder, Celine Pallaud, Jose Antonio Pérez-Simón, Hermann Einsele and Michael Hudecek

Poster presentation: Panobinostat Induces Upregulation of CD38 and Augments the Anti-Myeloma Efficacy of Daratumumab

EHA Annual Meeting - European Hematology Association- Madrid 2017

